Grey-box PK/PD Modelling of Insulin

Christoffer Wenzel Tornøe

LYNGBY 2002
MASTER'S THESIS

IMM

Christoffer@tornoe.dk

Typeset with LaTeX 2$_\varepsilon$ and printed by IMM, DTU

Preface

This master's thesis serves as part of the requirements for acquiring the civil engineer degree at the Technical University of Denmark (DTU). The thesis is written at Informatics and Mathematical Modelling (IMM) in collaboration with Department of Biostatistics at Novo Nordisk A/S in the period from the 1st of February to the 1st of July 2002.

I wish to thank my advisors, Ph.D. Judith L. Jacobsen (Novo Nordisk A/S), Professor Henrik Madsen (IMM, DTU), and Professor Sten Bay-Jørgensen (KT, DTU), along with Aage Vølund (Novo Nordisk A/S) and Ph.D students Lasse Engbo Christiansen and Niels Rode Kristensen for help and support with this thesis.

Furthermore, I am grateful to Novo Nordisk A/S and M.D. Ph.D. Torben Hansen for providing the data for the clamp study and the glucose tolerance studies, respectively.

Finally, the help of Christian Wenzel Tornøe with proofreading this thesis along with the patience and support from Trine Lykke Frederiksen is greatly appreciated.

Christoffer Wenzel Tornøe
IMM,DTU,Lyngby
June 28, 2002

Abstract

Grey-box PK/PD modelling is presented as a new and promising way of modelling the pharmacokinetics and pharmacodynamics of the *in vivo* system of insulin and glucose and to estimate model and derived PK/PD parameters. The concept behind grey-box modelling consists of using *a priori* physical knowledge along with information from data in the estimation of model parameters.

The grey-box PK/PD modelling principle is applied to two different insulin studies.

The PK/PD properties of two types of insulin are investigated in an euglycaemic clamp study where a single bolus of insulin is injection subcutaneously. The effect of insulin on the glucose disappearance is investigated by artificially maintaining a blood glucose concentration close to the normal fasting level. The infused glucose needed to maintain the clamped blood glucose concentration can therefore be used as a measure for the glucose utilization. The PK and PD parameters are successfully estimated simultaneously thereby describing the uptake, distribution, and effect of two different types of insulin.

The glucose tolerance tests are used for assessing the glucose tolerance of possible diabetic patients. The intravenous glucose tolerance test (IVGTT) is modelled using Bergman's 'Minimal Model' from where metabolic indices are estimated and compared for normal glucose tolerant and impaired glucose tolerant subjects. The

grey-box estimates of the system noise parameters using CTSM indicate that the minimal model of glucose kinetics is too simple and should preferably be revised. The estimated metabolic indices from the IVGTT are compared with previously published results using MinMod and further compared with those from an oral glucose tolerance test (OGTT). The derived OGTT models are inaccurate and not suitable for predicting the indices from an IVGTT.

KEYWORDS: Insulin, grey-box PK/PD modelling, stochastic differential equations, maximum likelihood estimation, extended Kalman filter, euglycaemic clamp study, IVGTT, and OGTT.

Resumé

Dette eksamensprojekt omhandler alternative måder til at modellere insulin farmakokinetikken og farmakodynamikken (PK/PD). Grey-box modellering er en ny måde at modellere *in vivo* dynamikken mellem insulin og glucose samt til at estimere model- og afledte PK/PD parametre. Konceptet bag grey-box modellering består i at anvende *a priori* fysisk kendskab til systemet samt information fra data til estimation af modelparametre.

Grey-box PK/PD modelleringsprincippet er anvendt på to forskellige studier af insulin.

PK/PD egenskaberne for to typer insulin er undersøgt i et euglycaemisk clamp studie, hvor en enkelt dosis af insulin injiceres subkutant for at undersøge insulinens effekt på glucose optaget ved kunstigt at holde blodglukoseniveauet tæt på det normale faste niveau. Det indførte glukose, som er nødvendigt for at opretholde et konstant blodglukoseniveau, kan derved anvendes som et mål for det metaboliserede glukose. Det er lykkedes at estimere PK og PD parametrene simultant og derved beskrive optaget, distributionen og effekten af to forskellige typer insulin.

Glukosetolerance-test er anvendt til at bestemme glukosetolerancen for mulige diabetikere. Det intravenøse glukosetolerance-test (IVGTT) er modelleret ved hjælp af Bergman's 'Minimal Model', hvorfra metabolske indices er estimeret og sammenlignet for normale

og forringede glukose tolerante patienter. Grey-box estimaterne af systemstøjen fra CTSM indikerer, at minimal modellen for glukosekinetikken er for simpel og skal revideres. De estimerede metabolske indices fra IVGTT er sammenlignet med tidligere publiserede resultater ved brug af MinMod samt med estimater fra en oral glukosetolerance-test (OGTT). De anvendte OGTT modeller er unøjagtige og er ikke passende til at prædiktere de metabolske indices fra et IVGTT.

NØGLEORD: Insulin, grey-box PK/PD modellering, stokastiske differential ligninger, maximum likelihood estimation, extended Kalman filter, euglycaemisk clamp studie, IVGTT og OGTT.

Symbols & Abbreviations

This chapter gives a quick overview of the symbols and abbreviations used in this thesis. The first time a parameter or abbreviation is used, it is explained and the abbreviation is given in parentheses.

Notation

The symbols and abbreviations in the following are listed alphabetically starting with the Greek letters and followed by the Roman letters. A short description of each symbol is given along with the units used. A bold face symbol in the text is either a vector or matrix of the symbol explained in the following table.

List of Symbols

Greek Letters

Symbol	Description	Unit
$\delta(t)$	Dirac delta function	[-]
ϵ	White noise	[-]
ε	Residuals	[-]
γ	Sigmoidicity/response factor	[-]
γ	Proportionality factor between the glucose and the rate of change of insulin	[nmol min^{-2}]
Λ	Likelihood ratio test-score	[-]
μ	Mean	[-]
ϕ	Partial autocorrelation function	[-]
ϕ_1	First-phase pancreatic responsivity index	[nM min^{-1}]
ϕ_2	Second-phase pancreatic responsivity index	[10^4·nmol min^{-2}]
ρ	Autocorrelation function	[-]
σ	Standard deviation	[-]
Σ	Dispersion matrix	[-]
τ	Time	[min]
θ	Parameter	[-]

Roman Letters

Symbol	Description	Unit
AUC_0^t	Area under insulin curve	[U L^{-1} min]
		[pM min]
B	Hepatic glucose	[mM]
BG	Blood glucose concentration	[mM]
C	Concentration	[-]
C_c	Central compartment concentration	[pM]
C_e	Effect concentration	[pM]
C_{G_b}	Basal glucose concentration	[mM]
C_I	Insulin plasma concentration	[U L^{-1}]
		[pM]
C_{I_b}	Basal insulin concentration	[pM]
C_{max}	Maximum insulin concentration	[U L^{-1}]
		[pM]
D	Dose	[U]
D^2	Mahalanobis' distance	[-]
e_k	Measurement error	[-]

Continued on the following page

Roman Letters continued from the previous page

Symbol	Description	Unit
E	Effect	[-]
E_{max}	Intrinsic activity of the drug	[mmol/min]
EC_{50}	Potency of the drug	[nM]
F	Bioavailability factor	[-]
$\mathcal{F}$	Objective function	[-]
G	Glucose	[mM]
GIR_0^t	Area under GIR curve	[mol]
h	Threshold level	[mM]
I	Inhibiting effect	[-]
I_c	Plasma insulin	[U] [pmol]
I_e	Effect compartment insulin	[pmol]
I_D	Dimeric insulin	[U]
I_H	Hexameric insulin	[U]
I_p	Peripheral insulin	[U]
I_r	Remote insulin concentration	[pM]
I_{sc}	Subcutaneous insulin	[U] [pmol]
k_a	Absorbtion rate constant	[min^{-1}]
k_{cp}	Rate constant for transfer from central to peripheral compartment	[min^{-1}]
k_e	Elimination rate constant	[min^{-1}]
k_{1-6}	Rate constants in the MM	[-]
k_{ce}	Elimination rate constant from the central compartment	[min^{-1}]
k_{e0}	Elimination rate constant from the effect compartment	[min^{-1}]
K_{e0}	Equilibrium constant	[min^{-1}]
k_{in}	Response formation rate constant	[min^{-1}]
K_M	Michaelis constant	[U/L]
k_{out}	Degradation rate constant	[min^{-1}]
k_{pc}	Rate constant for transfer from peripheral to central compartment	[min^{-1}]
L	Likelihood function	[-]
n	Rate constant for insulin disappearance	[min^{-1}]
P	Rate constant for the transfer from hexamer to dimer	[min^{-1}]
$\mathcal{P}$	Penalty function	[-]
p_1	Insulin-independent rate constant of glucose uptake	[min^{-1}]

Continued on the following page

Roman Letters continued from the previous page

Symbol	Description	Unit
p_2	Spontaneous decrease of tissue glucose uptake ability	$[\text{min}^{-1}]$
p_3	Insulin-dependent increase in tissue glucose uptake ability	$[\text{min}^{-2}\text{pM}^{-1}]$
Q	Equilibrium constant between hexamer and dimer	$[\text{mL}^2\text{U}^{-2}]$
R	Response	[-]
R_{in}	Intravenous insulin	$[\text{U min}^{-1}]$ $[\text{pmol min}^{-1}]$
R_{max}	Maximum response	$[\text{mmol min}^{-1}]$
S_I	Insulin sensitivity index	$[\text{min}^{-1}\text{pM}^{-1}]$
S_G	Glucose effectiveness	$[\text{min}^{-1}]$
S_{max}	Maximal stimulating effect	[-]
SC_{50}	Potency of insulin	[nM]
t, T	Time	[min]
$t_{1/2}$	Half-life	[min]
t_{max}	Time to maximum insulin concentration	[min]
TR_{max}	Time to maximum response	[min]
U_p	Glucose utilization into the peripheral tissue	[mM]
V_d	Apparent volume of distribution	[L]
V_e	Effect compartment volume	[L]
V_G	Glucose compartment volume	[L]
V_{max}	Maximal rate of elimination	$[\text{U (L min)}^{-1}]$
V_{sc}	Subcutaneous volume	[L]
w_t	Wiener process	[-]
X	Insulin action	$[\text{min}^{-1}]$

1 mU is equivalent to 6.56 pmol of insulin. The unit M is the SI unit for concentration and is short for mol/L.

Abbreviations

Abbreviation	Description
ACF	Autocorrelation Function
AIC	Akaike's Information Criterion
AIR	Acute Insulin Response
ARMA	Autoregressive Moving Average
AUC	Area Under Curve
BG	Blood Glucose
BIC	Bayesian Information Criterion
BMI	Body Mass Index
BW	Body Weight
C-peptide	Connecting-peptide
CTSM	Continuous Time Stochastic Modelling
EKF	Extended Kalman Filter
GIR	Glucose Infusion Rate
IDDM	Insulin-Dependent Diabetes Mellitus
IGT	Impaired Glucose Tolerance
IV	Intravenous/Intravenously
IVGTT	Intravenous Glucose Tolerance Test
KF	Kalman Filter
LDF	Lag-Dependency Function
LRT	Likelihood Ratio Test
LTI	Linear Time Invariant
MAP	Maximum *a Posteriori*
ML	Maximum Likelihood
MM	Minimal Model
NGT	Normal Glucose Tolerance
NIDDM	Non-Insulin-Dependent Diabetes Mellitus
NL	Non-linear
OGTT	Oral Glucose Tolerance Test
PACF	Partial Autocorrelation Function
PD	Pharmacodynamics
PK	Pharmacokinetics
PK/PD	Pharmacokinetics/Pharmacodynamics
PLDF	Partial Lag-Dependency Function
SC	Subcutaneous/Subcutaneously
SDE	Stochastic Differential Equation

Contents

Chapter 1

Introduction

In this chapter, the background and motivation behind this thesis are presented along with a description of the two insulin studies which are modelled. A detailed outline of the organization of the rest of this thesis is given at the end of the chapter.

1.1 Background

The objective of clinical drug development is to provide relevant information on safety and efficacy of the drug to enable physicians to treat patients optimally. Clinical drug development is a costly and time consuming process which on average costs 600 million US dollars over a 6-12 year period before the authorities clear the product for distribution.

To ensure faster and a more effective development of new pharmaceutical products, a pharmacokinetic and pharmacodynamic (PK/PD) approach to drug development has been shown to be a very helpful tool in determining which drug candidates to select for further testing and whether a project should be discontinued or moved to the next phase of the clinical trials.

PK/PD models can be used for simulation and prediction of uninvestigated doses along with predictions of the effects after long time exposure. The estimated and derived parameters from PK/PD models can thereby give valuable information about e.g. the dose needed to obtain a clinical observable effect and possible side effects.

In the short term, the perspectives of PK/PD modelling is to use all the available data from the clinical trials in statistical analysis of new drug candidates. In the long term, it will perhaps be possible to build so good models that considerable fewer and shorter clinical trials will be necessary. At the same time, an optimization of the experimental design will lead to a reduction in the number of animals and humans used for testing. In the end, this will lead to faster development of more effective pharmaceutical products which will improve the possibilities for optimal treatment of the individual patient.

1.2 Project Description

The purpose of this thesis is to model the dynamical system of insulin and glucose using grey-box PK/PD modelling. The two types of insulin studies which are considered are briefly introduced in the following along with the purposes of this thesis.

1.2.1 Clamp Study

The clamp study is used to determine the characteristics of different types of insulin, their absorption, distribution, and elimination kinetics along with its pharmacodynamic characteristics. The information obtained from clamp studies is usually used in phase I clinical trials where the insulin is tested in healthy volunteers to verify that it has the intended properties without too many side effects and to determine the insulin dose needed to produce an observable effect.

The main focus of this thesis is centered on the clamp study. Several different PK/PD models are derived to investigate the dynamical system of insulin and glucose using compartment modelling. The models are estimated and validated using the principles of grey-box modelling where a plausible model structure is combined with a stochastic term representing disturbances and unmodelled dynamics of the system. Traditionally, the PK and PD of insulin are described and estimated separately even though the two are very interdependent. The purpose is therefore also to investigate whether it is possible to estimate the PK and PD of insulin simultaneously.

1.2.2 Glucose Tolerance Tests

Glucose tolerance tests are used for assessing the glucose tolerance of possible diabetic patients. Since impaired insulin action is an underlying feature of commonly encountered clinical disorders, there has been a widespread interest in the development of techniques to determine metabolic indices for the patient's ability to react to his/her own insulin. These measures give an indication whether the patient has normal glucose tolerance, impaired glucose tolerance or is diabetic.

The two glucose tolerance studies in this thesis are an intravenous glucose tolerance test (IVGTT) and an oral glucose tolerance test (OGTT). The IVGTT is usually modelled using the 'Minimal Model' initially proposed by Bergman *et al.* [7] from where two metabolic indices for the insulin-dependent and insulin-independent glucose uptake are derived. The purpose of modelling the IVGTT is to compare the grey-box estimates of the minimal model with previously published results. The estimated metabolic indices derived from the IVGTT are further compared with those from the OGTT to investigate the correlations between them.

1.3 Outline of Thesis

In **Chapter 2**, the physiological aspects of the insulin/glucose system are introduced along with a description of the two types of diabetes.

Chapter 3 is concerned with the concepts of pharmacokinetics and pharmacodynamics. Three different approaches to pharmacokinetic modelling are mentioned along with the aspects of effect, link and response models in pharmacodynamic modelling.

The principles of grey-box modelling are mentioned in **Chapter 4**. This includes an introduction to stochastic differential equations, maximum likelihood estimation, and state filtering. The issues of model validation are also discussed in this chapter.

In **Chapter 5**, the experimental procedures and data from the clamp and glucose tolerance studies are described.

The derived PK and PK/PD models for the clamp study are discussed in **Chapter 6**. Four different PK models are presented to investigate the SC absorption, distribution, and elimination of insulin along with two different PK/PD models using a direct and indirect response model, respectively.

The results and analysis of the clamp models are shown in **Chapter 7**. The four PK models and two PK/PD models are validated and compared for a representative subject from the study while the most suitable PK and PK/PD models are used for parameter estimation for all twenty subjects.

Chapter 8 deals with the glucose tolerance models. The minimal model for an intravenous glucose tolerance test (IVGTT) is derived and explained along with different metabolic indices used for assessing the glucose tolerance of possible diabetics. The chapter also includes some of the most commonly used regression models for an oral glucose tolerance test (OGTT).

In **Chapter 9**, the results and analysis of the glucose tolerance models are discussed and compared with previously published results. The metabolic indices from the IVGTT are compared with those from the OGTT to investigate possible correlations between the two.

The obtained results from the two insulin studies and the usefulness of grey-box PK/PD modelling of insulin are discussed in **Chapter 10**. The chapter also includes suggestions for future work.

The conclusion reached for the modelling of the two insulin studies is given in **Chapter 11**.

In **Appendix A**, the anthropometric measurements from the clamp study are presented and the identifiability of the linear PK models is investigated. The equations for the effect-compartment model are derived using Laplace transformation and the input and output files from CTSM are shown for the estimation of the effect-compartment model.

Appendix B includes the anthropometric measurements of the glucose tolerance studies, the minimal model equation for plasma glucose, the obtained minimal model grey-box estimates, and the input and output files from CTSM for the estimation of the minimal model of glucose kinetics.

Chapter 2

Physiological Aspects

This chapter gives an overview of the physiological aspects concerned with the insulin/glucose dynamical system of the human body. First, the pancreas is mentioned along with a description of the insulin/glucose feedback system. Thereafter, the insulin molecule and receptor are introduced. Finally, a quick description of the two types of diabetes and the difference between them is given at the end of the chapter.

2.1 The Pancreas

The pancreas consists of two very different tissues, exocrine and endocrine tissue[1], where the bulk of its mass consists of exocrine tissue. Scattered throughout the exocrine tissue are thousands of small clusters of endocrine glands. These clusters, called the islets of Langerhans, make up only about 2 % of the weight of the pancreas and consist mainly of three types of cells: α-, β-, and δ-cells, which secrete glucagon, insulin, and somatostatin, respectively [56, p. 321].

[1] Endocrine glands are ductless organized structures of cells specialized to secrete hormones directly into the blood. Exocrine glands are drained with ducts.

Insulin is an anabolic hormone that facilitates glycogen[2] synthesis (glucogenesis) and increases the storage of carbohydrates, fatty acids and amino acids. Glucagon is a catabolic hormone that mobilizes glucose by facilitating the breakdown of glycogen (glucogenolysis), fatty acids and amino acids from the tissue to the blood. Somatostatin inhibits both insulin and glucagon [56, p. 322]. Insulin and glucagon serve as regulators of blood glucose concentration [18, p. 246] and the connection between plasma glucose concentration and insulin and glucagon secretion is illustrated in Figure 2.1.

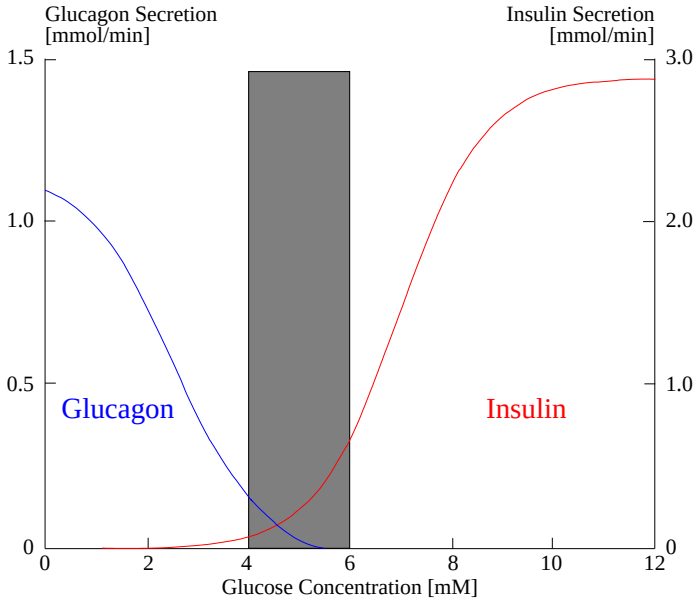

Figure 2.1: Illustration of the connection between glucose concentration and the secretion of insulin and glucagon [56, p. 324].

The grey area in the figure above is the normal physiological range of glucose concentration. Under conditions with smooth changes in the

[2]Glycogen is a polysaccharid consisting of glucose units which serves as fuel depots.

glucose concentration, a sigmoidal functional relationship between glucose concentration and insulin/glucagon secretion is observed [51, p. 28].

2.2 Insulin/Glucose Feedback

The hormone/substrate pair insulin/glucose makes up an important and very complicated feedback system that regulates the blood sugar concentration [56, 21]. The feedback mechanism is summarized in Figure 2.2.

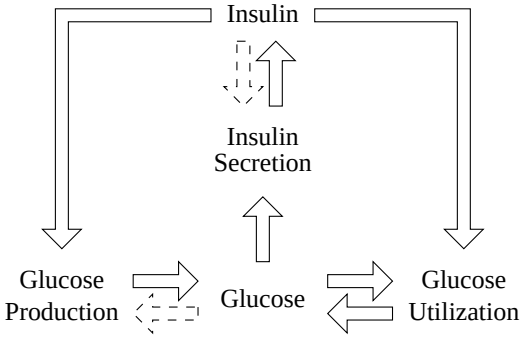

Figure 2.2: Causal loop diagram of dominant feedback in the insulin/glucose system. Stimulation and inhibition are illustrated with solid arrows while the dashed arrows describe inhibition of insulin/glucose upon its own secretion which is considered to be insignificant [51, p. 26].

The primary stimulus for insulin secretion is glucose. At the same time, insulin stimulates glucose storage as glycogen in the liver and as triglycerides in fat. Furthermore, insulin increases the glucose utilization as the primary source of energy in muscle and inhibits degradation of triglycerides and glycogen. Under normal conditions, glucose is produced at a rate of about 2 mg/kg/min but with the stimulating effect of insulin the production of glucose is close to zero

and the uptake is around 10 mg/kg/min [54]. Finally, insulin secretion is inhibited by insulin itself, but the glucose stimulation is considered to be much greater than the inhibition in the normal physiological range [51, pp. 25-26].

2.3 The Insulin Molecule

The amino acid sequence (the primary structure) of insulin was discovered in 1953 by Frederick Sanger [49, p. 25]. Insulin is a protein hormone consisting of 51 L-amino acids with amide linkages between the α-amino and α-carboxyl groups.[3] It consists of two peptide chains, α and β, connected by two disulfide bonds and is produced through biosynthesis of pre-proinsulin [49, p. 25]. First, pre-proinsulin is converted to proinsulin by elimination of a signal sequence consisting of 24 amino acids. Secondly, proinsulin decomposes to connecting-peptide (C-peptide) and insulin [56, p. 238]. The final insulin molecule has a molecular weight of approximately 6,000 and is illustrated along with proinsulin in Figure 2.3.

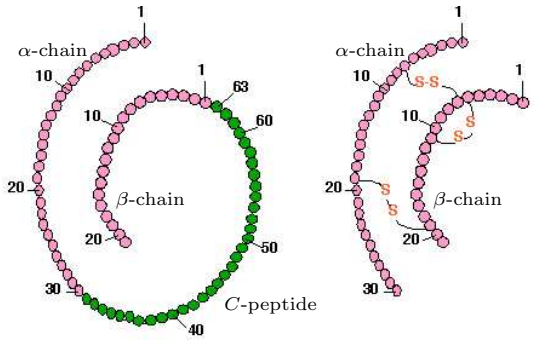

Figure 2.3: Illustration of a proinsulin and insulin molecule [24].

[3] Amino acids with four different substituents on the α-carbon atom are optical active and consist of two isomers: L and R isomer which are mirror images of each other.

The insulin molecule is mainly degraded in the liver and kidneys while C-peptide only is degraded in the kidneys. Since the half-life ($t_{1/2}$) for plasma insulin is approx. 6 min. while that of C-peptide is larger, the C-peptide concentration can be used as a better measure for the human secretion of insulin [56, p. 325].

Insulin can be produced outside the human body by gene-manipulated yeast that expresses the insulin extracellularly and is later purified and modified to resemble the characteristics of human insulin. Other types of insulin are also produced, each with their special use. The two main types of insulin, besides human insulin, are a fast and short acting insulin analogue consisting of mainly dimers or monomers, and a slow and long lasting insulin analogue where the hexamer form is stabilized.

Human insulin exists as monomers in solution near neutral pH and physiological concentrations (1 ng/mL). At higher concentrations, and at acidic or neutral pH, it self-associates to form dimeric units, while in the presence of zinc, hexamer units are formed. The uptake of different association states of insulin from the subcutaneous (SC) tissue, and at which concentrations they exist, are shown in Figure 2.4.

The activity of injected insulin has been shown to depend on the different association states of the SC injected insulin. It is only the monomer that has a mono-exponential decay from the time of injection whereas the dimer has an initial slower phase (exponential decay with a larger, i.e. less negative, time constant) followed by a phase that is similar to that of monomer. It is not clear whether human insulin, mainly consisting of hexamer units at therapeutic concentrations, is absorbed as both hexamers and dimers, or as dimers only. The early delay in absorption of human insulin is due to the breakdown of hexameric units into dimers and monomers. Human insulin shows three phases: 1) An early slow phase, 2) a middle phase where the absorption rate is equal to the initial phase of dimer absorption, and 3) a late phase in which the absorption rate approaches that of monomer [28].

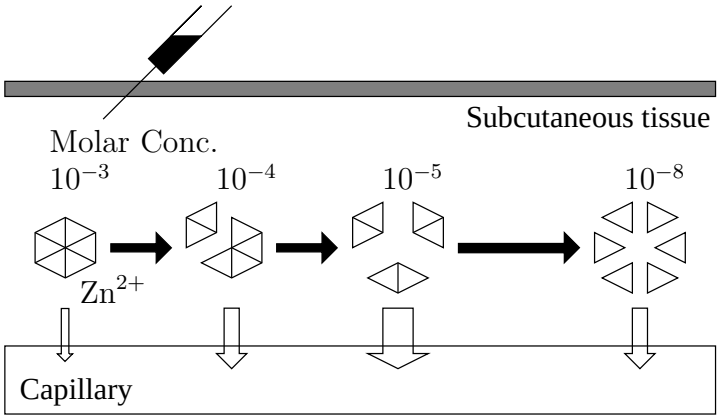

Figure 2.4: Illustration of the uptake of different association states of insulin from the SC tissue [28].

2.4 Insulin Receptor

The insulin receptor is a tetramer consisting of two regulatory α-chains exposed to the extracellular fluids and two regulatory β-chains embedded into the cell across the lipid bilayer cell membrane. The subunits are held together by disulfide bonds [4]. The insulin receptor is illustrated in Figure 2.5.

The receptor is an allosteric enzyme[4] where the binding of insulin on the α-subunits induces tyrosine kinase activity on the β-subunits by rapid autophosphorylation. The binding of insulin leads to an increase in the activity of glucose transporters which facilitate the absorption of glucose, thereby lowering the extracellular glucose levels [56, p. 326].

[4] An allosteric enzyme is an enzyme where binding of substrate to one active site alters the properties of other active sites in the same molecule.

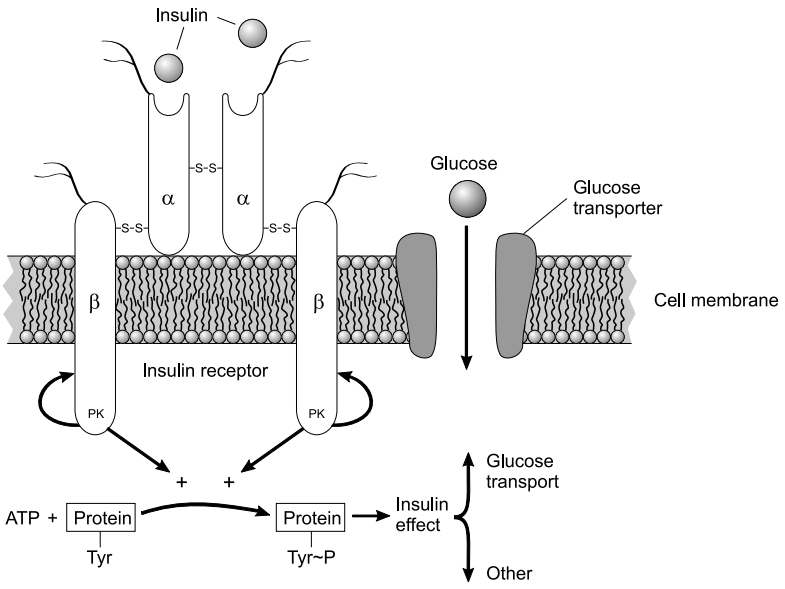

Figure 2.5: Illustration of the insulin receptor [56, p. 326].

2.5 Diabetes

Diabetes is the most common metabolic disease in the world. The early symptoms of diabetes are extreme thirst and hunger since an excess amount of water and glucose is excreted in abnormal amounts of urine. If the disease is not treated, the symptoms can lead to more severe complications or death.

One distinguishes between two types of diabetes: Type I and II. The difference between the two is explained in the following.

Type I diabetes (insulin-dependent diabetes mellitus, IDDM) is caused by autoimmune destruction[5] of the insulin-secreting β-cells in the pancreas. Since a sufficient amount of insulin is not produced, the entry of glucose into the cells is impaired. Furthermore, the

[5]Destruction caused by the organism's own antibodies.

high ratio between glucagon and insulin promotes the breakdown of glycogen resulting in an excessive amount of glucose being produced in the liver and released into the blood [49, pp. 779-780].

The treatment for type I diabetes is insulin injections to maintain a normal level of insulin in the body. Different types of insulin are used depending on whether a short or long lasting effect is needed [56, pp. 332-334]. The insulin is normally given SC since it breaks down in the stomach and gut when given orally. By giving the injection SC, the insulin bypasses the epidermal and dermal skin layers resulting in a slow rise and decline of plasma insulin after the injection. The primary absorption membrane in the SC tissue is the capillary wall which has a low capillary density. The drug absorption is therefore generally slow but effective [58, pp. 11-12].

Type II diabetes (non-insulin-dependent diabetes mellitus, NIDDM) is a heterogeneous disorder which is characterized by a progressive functional β-cell defect where the capacity of the β-cells to secrete insulin is deteriorated and/or an impaired insulin action (insulin resistance) is observed on the peripheral tissue which does not respond to the hormone. This type of diabetes occurs predominantly (but not only) at a later age than type I diabetes and among people with severe obesity. In countries with high living standards, this type of diabetes is affecting hundreds of millions and the number is growing. Typical predictors for type II diabetes are hyperinsulinemia and hyperglycemia (elevated insulin and glucose levels) which are risk factors for cardiovascular diseases. Type II diabetes is normally treated through diet, exercise, and sometimes insulin injections [56, pp. 332-334].

Chapter 3

Pharmacokinetics/ Pharmacodynamics

After having discussed the physiological aspects of the insulin/glucose system, the basic concepts of pharmacokinetic/pharmacodynamic (PK/PD) modelling are introduced in this chapter. The main purposes of PK/PD modelling is listed below with increasing importance [52].

- Conceptualize the system
- Test competing hypotheses/models
- Estimate system variables/parameters (model robustness)
- Identify controlling factors and variability
- Assess system response predictability under new conditions

Several different types of models are presented in the following which are supposed to give an overview of the available PK/PD modelling techniques.

3.1 Pharmacokinetics

Pharmacokinetics (PK) is the study of the rate of change of drug concentrations in the body. PK modelling is aimed at a mathematical description of the concentration of drug and metabolites in areas of the body, e.g. blood, tissue, urine, etc. This includes a description of the rates of drug absorption, distribution, metabolism, and excretion following various types of administration, e.g. IV, SC, oral, etc.

PK modelling has diverged into the following three major approaches [58, p. 4].

The model-independent approach is based purely on a mathematical description of e.g. plasma profiles of a drug without making any assumptions about a particular model. Thereby, the use of kinetic parameters which cannot readily be validated is avoided. This approach can be seen as a 'curve fitting method' to data.

In compartment modelling , the body is assumed to consist of one or more compartments which are either spacial or chemical in nature. Generally, the compartments represent a volume or group of similar tissues/fluids into which a drug is distributed. The drug movement between compartments is mainly based on reversible or irreversible first-order processes or by use of Michaelis-Menten kinetics[1]. The mathematical functions or differential equations are employed without regard to any mechanistic aspects of the system.

The physiological approach implies certain mechanisms or entities that have physiological, biochemical or physical significance. Contrary to compartmental models, physiological modelling uses flow rates (fluxes) through particular organs or tissues along with experimentally determined ratios, e.g. the ratio

[1] Michaelis-Menten kinetics describe the properties of many enzyme-catalyzed reactions and are often used to describe the elimination of a drug from the body.

between the blood and tissue concentration. The advantage of the physiological approach is that events such as fever or heart failure can be taken into account. The disadvantage is that the mathematics then become very complex.

The range of compartments in physiological modelling is normally from 4 to 20 whereas the number of compartments is from 1 to 3 in compartmental modelling and zero in the model-independent approach.

Compartmental modelling is chosen as the modelling approach in this thesis because of its simplicity and widespread use in insulin studies.

3.2 Pharmacodynamics

While the concentration-time relationship is studied in PK, pharmacodynamics (PD) deals with drug-target (receptor) interaction and how the PK of a drug, control the time course of the PD response. A major goal of PD is to relate different types of concentration-effect relationships through coupling with the PK. Furthermore, the objective in establishing PK/PD relationships is to be able to design an optimal dosage regimen that maximizes the effect elicited by the drug pr. unit dose. This is done through concentration-effect correlation, since it is the rate of availability (dose/time) at the receptor which is of importance to the therapeutic outcome. PK/PD modelling has become an integral part of drug development and plays a significant role in drug therapy.

Three basic aspects of PD models will be considered next. These aspects are effect, link, and response.

3.2.1 Effect Models

A drug effect can be defined as any drug-induced change in a physiological parameter when compared to the respective pre-dose or baseline values. A more relevant term in PK/PD modelling than effect is efficacy which is the sum of all therapeutically beneficial drug effects. Efficacy is however difficult to quantify and thus effect models are used instead [37].

Either polynomial or logistic models can be used when modelling the effect. A polynomial can be fitted to a logistic curve, which is why the difference between the two types of models can become virtually indistinguishable within a certain interval. However, the drawbacks of using polynomials are that the parameters do not have any physical interpretation unlike those of logistic models and that the predictions outside the observed range of effect are less reliable than logistic models. Furthermore, logistic models generally use fewer parameters than polynomials to obtain the same fit, thereby giving a more parsimonious description of the effect [43, p. 274]. Therefore, polynomials will not be considered in the following where the five most commonly used logistic effect models are presented.

Fixed Effect Model: A fixed effect model (quantal effect model) is a statistical approach based on logistic regression analysis. The simplest type of fixed effect models are threshold models where the effect occurs after a certain effect E_{fixed} is reached:

$$E = E_{fixed} \qquad C \geq C_{threshold} \tag{3.1}$$

where E and C are the measured effect and concentration, respectively.

The problem with the fixed effect model is that it often falls short at predicting complete effect-time profiles.

Linear Effect Model: In the linear effect model, the observed effect is considered to be proportional to the drug concentration [42]:

$$E = S \cdot C + E_0 \tag{3.2}$$

where S and E_0 represent the effect induced by one unit of C and the baseline effect in the absence of drug, respectively.

This model is preferable to measured effects with physiological baselines such as blood glucose and the parameters are easily estimated using linear regression. A similar model to the linear model is the log-linear model where C is replaced by $\log C$.

Even though the linear and log-linear models seem intuitively right, they rarely fit PD data very well. The explanation is that a threshold concentration must be attained before any response is elicited and because there usually exists a maximum effect which is independent of the drug concentration.

Hyperbolic E_{max} Model: Another possibility is to have a hyperbolic relation (E_{max} model) between the drug concentration and the observed effect [40]:

$$E = \frac{E_{max} \cdot C}{EC_{50} + C} + E_0 \tag{3.3}$$

where EC_{50} (the potency of the drug) is the drug concentration producing 50 % of the maximum effect E_{max} (the intrinsic activity of the drug).

This model becomes equivalent with the linear model when $C \ll EC_{50}$ and is consistent with the log-linear model in the range between 20 % and 80 % of E_{max}.

The model is based on the theory of drug-receptor interaction and is derived for the equilibrium interaction of a drug with its receptor.

It is widely used to describe pharmacologic effects under both competitive and non-competitive agonist and antagonist interactions[2] at the response system [37].

Sigmoidal E_{max} Model: Finally, the relation between the drug concentration and the observed effect can be described by the Hill response equation (sigmoidal E_{max} model) [42]:

$$E = \frac{E_{max} \cdot C^{\gamma}}{EC_{50}^{\gamma} + C^{\gamma}} + E_0 \tag{3.4}$$

where γ represents the sigmoidicity/response factor (steepness of the curve).

The sigmoidal E_{max} model is a generalization of the hyperbolic E_{max} model ($\gamma = 1$). For $\gamma < 1$, a smoother and for $\gamma > 1$, a steeper curve is obtained. The parameter γ allows more different types of PK/PD data to be modelled. Theoretically, the sigmoidal E_{max} model is derived from the interaction between γ drug molecules and one receptor [37].

The five effect models are illustrated in Figure 3.1.

3.2.2 Link Models

Ideally, the insulin concentration should be measured at the effect site (extracellular space) where the interaction with the biological receptor system takes place [42]. Since this is not possible in most cases, the concentration in the more accessible plasma is measured instead and related to the effect site under the assumption that the pharmacologically active and unbound concentration at the effect site is directly related to the more accessible plasma concentration

[2] An agonist is a drug responsible for triggering a response while an antagonist interferes or prevents the action of a drug [32, p. 18+36].

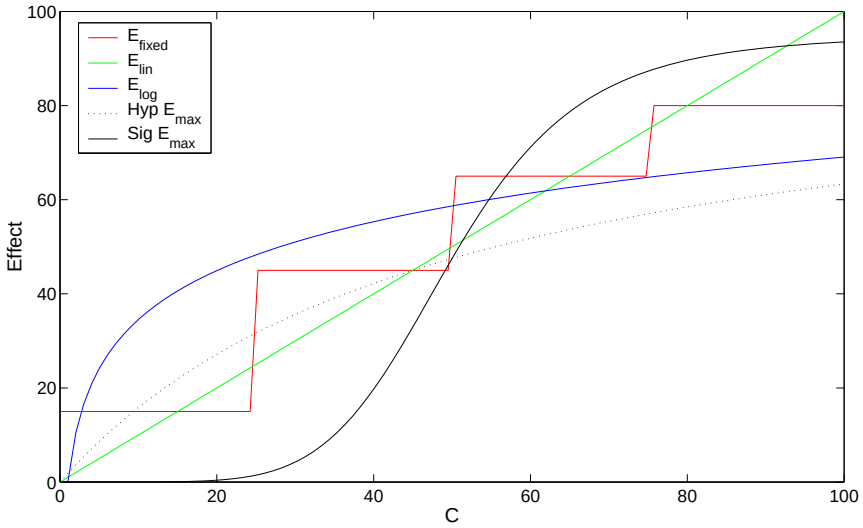

Figure 3.1: Illustration of five effect models. The parameters used are: $E_0 = 0$, $S = 1$ and 15 for the linear and log-linear model, respectively. $E_{max} = 95$, $EC_{50} = 50$, and $\gamma = 6$.

or other body fluids. Furthermore, the concentration at the effect site is assumed to be in PK equilibrium (steady-state) [37].

There exist two ways of linking the drug concentration and the effect, i.e. direct and indirect link models. When the measured plasma concentration is assumed to be equivalent to the concentration at the effect site, direct link models are used. If a drug does not distribute instantaneously to all the body tissues (including the effect site), the pharmacological response will not always parallel the drug concentrations in the plasma and an indirect link model is needed. One way to determine if a direct or indirect link model should be used is through the shape of a phase-plot where the drug effect is plotted against the drug concentration and the data points are connected in chronological order.

Direct Link Models

At steady-state conditions, a phase-plot of effect vs. plasma concentration typically results in a sigmoid-shaped curve. Direct link models, where the effect site (the receptor) is placed in the central or peripheral compartment in the PK model, can be used under such conditions.

Indirect Link Models

At non steady-state, a counter-clockwise hysteresis loop is observed in the phase-plot, the size of which depends on the delay between maximum drug concentration C_{max} and maximum effect E_{max}. The phenomenon can be explained by the effect rising slowly, reaching a peak, and is more sustained than the plasma drug concentration [42]. Therefore, there exists two different effects for any drug concentration depending on the time after drug administration, also referred to as 'kinetic-dynamic dissociation' [26].

An indirect link model is then needed to circumvent the dissociation problem. If the hysteresis loop is related to a distributional delay and not an indirect response mechanism, a hypothetical effect compartment containing the drug receptor can be added to the PK model, receiving only a negligible amount of drug. The concentration and effect are thereby aligned (in time) and steady-state conditions are achieved [59]. The drawbacks of the indirect link model is that the link between measured drug concentration and observed effect is based on an unknown mechanism (black box) [37].

Soft and Hard Link Models

The link between the PK and PD data can also be established in two different ways, i.e. soft and hard link models. In soft link models, both the PK and PD data are used to determine the link between

them, i.e. the flow of used information is bidirectional. The link thereby serves as a buffer accounting for a misfit between the PK and PD relationships, e.g. the temporal delay of the effect compartment described above.

In hard link models, the PD data is not used in characterizing the model. The PK data is instead combined with information such as receptor affinity obtained from *in vitro*[3] studies. The flow of information is thereby unidirectional, where the additional *in vitro* information determines the link between the PK and PD data. The prediction of the PD data is thereby thought of as 'truly predictive' since the PD data is not used in the determination of the link. Hard link models are by definition also direct link models [37].

3.2.3 Response Models

This leads to the next issue of choosing between a direct or indirect response model to describe the relationship between drug concentration and pharmacological effect. A direct response is when the interaction of the drug with a response structure at the effect site *directly* results in the observed effect. When a physiological factor that governs the observed effect is modulated, it is thought of as an *indirect* response.

Unfortunately, plasma concentration and effect measurements are usually insufficient to distinguish whether the apparent delay between the two are related to a distribution delay (tissue equilibration) or an indirect response mechanism (delays downstream from the receptor) [46].

[3] *In vitro* means isolated from the living organism opposed to *in vivo* meaning within the living organism.

Direct Response

Direct response models are characterized by a direct correlation between the effect site concentration of the drug and the observed effect without time lag. The indirect link model like the effect model presented in Section 3.2.2 is thus a direct response model where the observed hysteresis loop is related to a distributional delay and closed by adding a steady-state effect compartment to the model. If the apparent delay between plasma concentration and effect is related to an indirect response mechanism, an indirect response model must be used instead [37].

Indirect Response

Indirect response models are used under non steady-state conditions when the drug inhibits or stimulates the observed effect *indirectly*. The indirect response model can be understood as a black-box, which exposed to an input k_{in}, yields a pharmacological response R as an output as illustrated in Figure 3.2 [30, 46].

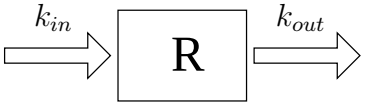

Figure 3.2: Indirect response model.

The change in response is described by the following equation [37, 45]:

$$\frac{dR}{dt} = k_{in} - k_{out} \cdot R \tag{3.5}$$

where k_{in} and k_{out} are the response formation and degradation rate constants, respectively.

The drug can either inhibit or stimulate k_{in} or k_{out} resulting in the following four indirect response models [42]:

$$\frac{dR}{dt} = k_{in} \cdot S - k_{out} \cdot R \tag{3.6a}$$

$$\frac{dR}{dt} = k_{in} \cdot I - k_{out} \cdot R \tag{3.6b}$$

$$\frac{dR}{dt} = k_{in} - k_{out} \cdot S \cdot R \tag{3.6c}$$

$$\frac{dR}{dt} = k_{in} - k_{out} \cdot I \cdot R \tag{3.6d}$$

where S and I are the stimulating/inhibiting effect described by one of the effect models mentioned in Section 3.2.1.

Chapter 4

Modelling & Estimation Methods

The modelling and estimation methods used in grey-box PK/PD modelling of insulin in this thesis are presented in the following sections.

First, three types of modelling principles for dynamical systems are introduced. Thereafter, stochastic differential equations (SDE) which are used in grey-box models, are deduced. Next, continuous-discrete time state space models based on SDE are suggested as a suitable way to describe the relationship between input and output signals in dynamical systems. The issues of identifiability and distinguishability are discussed before maximum likelihood estimation is introduced along with state filtering. Finally, different methods of validating a proposed grey-box model are mentioned to address the issue of model control.

4.1 Modelling Principles

Dynamical systems in continuous time are often described by differential equations. The three most used methods for modelling such systems are white-box, black-box, and grey-box modelling. The connection between the three methods is illustrated in Figure 4.1.

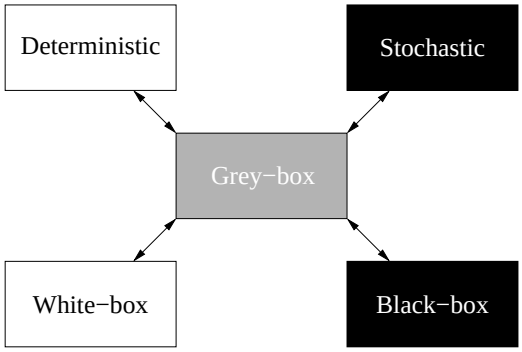

Figure 4.1: Illustration of different modelling principles.

The three methods are further explained in the following sections.

White-box Modelling: White-box models, also referred to as deterministic models, are based on deterministic equations and prior knowledge only. The future evolution of the system can be predicted exactly with knowledge about the initial state and future inputs. The limitation of white-box modelling is that differential equations rarely describe the uncertainties and measurement errors in a true physiological system such as the insulin/glucose system.

Black-box Modelling: The black-box model is identified from the use of data and statistics only and not by any prior knowledge. The parameters are estimated so that the model describes the data in a predefined best possible way. Therefore, the parameters have no

direct physical meaning and are not very helpful in understanding the dynamics of e.g. the insulin/glucose system. An example of a black-box model is the well known ARMA (autoregressive moving average) model.

Grey-box Modelling: Grey-box modelling is a hybrid of the two previously mentioned modelling methods. A grey-box model consist of a known or proposed model structure including a stochastic term which represents disturbances, inputs to the system which are not measured, and unmodelled dynamics of the system. It is therefore possible to use prior physical knowledge and at the same time describe the noise in the system by combining a deterministic part with a stochastic part. This makes grey-box modelling a very attractive tool for modelling the insulin/glucose dynamics since it is not yet fully understood or cannot be explicitly modelled. The advantage of using grey-box models is that the physiological knowledge is combined with information from data. Thereby the parameters in the models have physical meaning and may readily be interpreted. Furthermore, it is possible to treat missing data and to model non-linear (NL) and time-varying systems.

4.2 Stochastic Differential Equations

The equations used in grey-box models are stochastic differential equations and can be defined from the following stochastic difference equation of finite differences [33, pp. 167-169]:

$$\boldsymbol{x}_{t+h} - \boldsymbol{x}_t = h\boldsymbol{f}(\boldsymbol{x}_t, \boldsymbol{u}_t, \boldsymbol{\theta}, t) + \boldsymbol{G}(\boldsymbol{x}_t, \boldsymbol{u}_t, \boldsymbol{\theta}, t)(\boldsymbol{w}_{t+h} - \boldsymbol{w}_t) \qquad (4.1)$$

where $\boldsymbol{x}_t$ is the state vector, $\boldsymbol{u}_t$ is the input vector, $\boldsymbol{\theta}$ is the parameter vector, h is the time step, $\boldsymbol{f}$ is a deterministic function called the drift coefficient, $\boldsymbol{G}$ is the diffusion coefficient, and $\boldsymbol{w}_t$ is a Wiener process with the following mathematical properties.

The Wiener process is a non-stationary stochastic process that starts in 0 and has mutually independent (orthogonal) increments which are normally distributed with mean and covariance [33, p. 167]:

$$E[\boldsymbol{w}_t - \boldsymbol{w}_s] = 0 \tag{4.2a}$$
$$V[\boldsymbol{w}_t - \boldsymbol{w}_s] = \sigma^2|t-s| \tag{4.2b}$$

The derivative of the Wiener process has a constant spectral density for all frequencies and thus has infinite variance. This makes it the closest to the concept 'continuous white noise' [33, p. 168].

The stochastic differential equation is obtained by letting the time step h tend to zero in (4.1):

$$d\boldsymbol{x}_t = \boldsymbol{f}(\boldsymbol{x}_t, \boldsymbol{u}_t, \boldsymbol{\theta}, t)\, dt + \boldsymbol{G}(\boldsymbol{x}_t, \boldsymbol{u}_t, \boldsymbol{\theta}, t)\, d\boldsymbol{w}_t \tag{4.3}$$

The solution to (4.3) can formally be written as:

$$\boldsymbol{x}_t = \boldsymbol{x}_0 + \int_0^t \boldsymbol{f}(\boldsymbol{x}_s, \boldsymbol{u}_s, \boldsymbol{\theta}, s)\, ds + \int_0^t \boldsymbol{G}(\boldsymbol{x}_s, \boldsymbol{u}_s, \boldsymbol{\theta}, s)\, d\boldsymbol{w}_s \tag{4.4}$$

with the first integral being a standard Riemann integral, while the last integral is a stochastic integral[1]. A suitable way to represent the relationship between input and output signals in a dynamical system is by a state space formulation which is introduced in the following section.

4.3 State Space Models

A state space model is an internal parametric representation between input and output which in a continuous time formulation enables a direct physical meaning of the parameters. Since the structural information of the physical system is formulated in continuous time

[1] In this thesis, the stochastic integral is an Itô integral.

and the data is observed at discrete time instants, the following continuous-discrete time state space model, consisting of a continuous time system equation and a discrete time observation equation, is used.

$$d\boldsymbol{x}_t = \boldsymbol{f}(\boldsymbol{x}_t, \boldsymbol{u}_t, \boldsymbol{\theta}, t)\, dt + \boldsymbol{G}(\boldsymbol{x}_t, \boldsymbol{u}_t, \boldsymbol{\theta}, t)\, d\boldsymbol{w}_t \tag{4.5a}$$

$$\boldsymbol{y}_k = \boldsymbol{h}(\boldsymbol{x}_k, \boldsymbol{u}_k, \boldsymbol{\theta}, t_k) + \boldsymbol{e}_k \tag{4.5b}$$

The state $\boldsymbol{x}_t$ is not directly measurable in the system equation (4.5a). The observation equation (4.5b) describes what is actually measured at discrete time instants t_k, and is a function of the state contaminated with Gaussian distributed white noise. The system noise $\boldsymbol{w}_t$ and observation noise $\boldsymbol{e}_k$ are assumed mutually independent.

4.4 Identifiability & Distinguishability

The analysis of the two related topics, identifiability and distinguishability, are *a priori* in nature, meaning that it assumes perfect input-output data and can be performed before the data is collected. The issue about identifiability with respect to the experimental conditions is briefly mentioned in Chapter 5 and will not be discussed in this section.

Structural identifiability is concerned with whether the unknown parameters within a model such as the state space model in (4.5) can be identified uniquely from the experiment considered given that the set of data is informative (persistently excited) enough. The state space representation is in general not a unique representation because any given model can be written in a continuum of ways. This makes the concept of structural identifiability an important and necessary one since the estimation of a non-identifiable model will not converge to a single set of parameters [33, p. 182]. An example of determining the structural identifiability of a linear model is illustrated in Appendix A.2 using Laplace transformation. Several different approaches such

as linearization [13] and differential algebra [6] has been suggested for investigating the identifiability of NL models. Structural identifiability is far more complicated for NL than linear models and will therefore not be considered in this thesis.

Another important issue when constructing the model structure is *distinguishability* – the ability to distinguish between models. The model parameters in compartmental models often have diagnostic significance which makes it important to validate the correctness of the chosen model. Some techniques for testing for distinguishability are the phase-plane method [19], the local state isomorphism theorem [12] along with several other numerical algorithms which can be applied to distinguish what type of e.g. absorption and elimination kinetics is present.

4.5 Estimation Methods

The two most used methods for parameter estimation in continuous state space models are: Maximum likelihood (ML) and maximum *a posteriori* (MAP) estimation. The major difference between these two approaches is that MAP estimation uses not only the experimental data, but also the *a priori* available statistical information on the parameter vector (Baysian approach), e.g. mean and covariance matrix in the gaussian case, while ML is a Fisherian approach, where only experimental measurements are used by the estimator.

In [48], it is shown that MAP estimation of insulin secretion, always leads to higher precision estimates than ML with the possibility of a slightly worse fit. Since the *a priori* information from population studies of insulin is not available for the studies mentioned in this thesis, only ML estimation is considered.

4.5.1 Maximum Likelihood

Maximum likelihood estimation is based on maximizing the likelihood function of the observations $\mathcal{Y}_N = [\boldsymbol{y}_N, \boldsymbol{y}_{N-1}, \ldots, \boldsymbol{y}_0]$ given the parameter vector $\boldsymbol{\theta}$ [29].

The likelihood function is given by [33, pp. 186-188]:

$$\begin{aligned} L(\mathcal{Y}_N|\theta) = p(\mathcal{Y}_N|\boldsymbol{\theta}) &= p(\boldsymbol{y}_N \cap \mathcal{Y}_{N-1}|\boldsymbol{\theta}) \\ &= p(\boldsymbol{y}_N|\mathcal{Y}_{N-1}, \boldsymbol{\theta}) p(\mathcal{Y}_{N-1}|\boldsymbol{\theta}) \\ &= \Big(\prod_{k=1}^{N} p(\boldsymbol{y}_k|\mathcal{Y}_{k-1}, \boldsymbol{\theta}) \Big) p(\boldsymbol{y}_0|\boldsymbol{\theta}) \end{aligned} \tag{4.6}$$

where Bayes rule $P(A \cap B) = P(A|B)P(B)$ is used to obtain the likelihood function as a product of conditional probability densities. Under the assumption that the conditional density function is Gaussian, which is only valid for linear models, the following equations describe the one-step conditional density in (4.6):

$$\hat{\boldsymbol{y}}_{k|k-1} = E\{\boldsymbol{y}_k|\mathcal{Y}_{k-1}, \boldsymbol{\theta}\} \tag{4.7}$$

$$\boldsymbol{R}_{k|k-1} = V\{\boldsymbol{y}_k|\mathcal{Y}_{k-1}, \boldsymbol{\theta}\} \tag{4.8}$$

$$\boldsymbol{\epsilon}_k = \boldsymbol{y}_k - \hat{\boldsymbol{y}}_{k|k-1} \tag{4.9}$$

Under the assumption that the data is normally distributed, the conditional likelihood for the output $\mathcal{Y}$ is completely characterized by equation (4.7) and (4.8), its first and second moments in the conditional densities, respectively. The likelihood function can then be written as:

$$L(\mathcal{Y}_N, \boldsymbol{\theta}) = \left(\prod_{k=1}^{N} \frac{\exp\big(-\frac{1}{2}\boldsymbol{\epsilon}_k^T \boldsymbol{R}_{k|k-1}^{-1} \boldsymbol{\epsilon}_k\big)}{\sqrt{\det(\boldsymbol{R}_{k|k-1})}\big(\sqrt{2\pi}\big)^l} \right) p(\boldsymbol{y}_0|\boldsymbol{\theta}) \tag{4.10}$$

where l is the dimension of $\boldsymbol{y}_k$.

If the likelihood function is further conditioned on $\boldsymbol{y}_0$ and by taking the negative logarithm of (4.10), the following equation appears:

$$-\ln\Big(L(\mathcal{Y}_N|\boldsymbol{\theta},\boldsymbol{y}_0)\Big) = \frac{1}{2}Nl\ln\big(2\pi\big) + \frac{1}{2}\sum_{k=1}^{N}\Big(\ln\big(\det(\boldsymbol{R}_{k|k-1})\big) + \boldsymbol{\epsilon}_k^T\boldsymbol{R}_{k|k-1}^{-1}\boldsymbol{\epsilon}_k\Big) \quad (4.11)$$

The innovation $\boldsymbol{\epsilon}_k$ and the conditional variance $\boldsymbol{R}_{k|k-1}$ can be calculated for given parameters $\boldsymbol{\theta}$ and initial conditions $\boldsymbol{x}_0$ by the use of the Kalman Filter (see Section 4.6.1) or the Extended Kalman Filter (section 4.6.2) for linear and NL systems, respectively. To find the estimate of the parameters $\boldsymbol{\theta}$, the following argument must be minimized with respect to $\boldsymbol{\theta}$:

$$\hat{\boldsymbol{\theta}} = \arg\min_{\boldsymbol{\theta}\in\boldsymbol{\Theta}}\{-\ln\big(L(\mathcal{Y}_N|\boldsymbol{\theta},\boldsymbol{y}_0)\big)\} \quad (4.12)$$

The optimization of the likelihood function is implemented in the program CTSM (Continuous Time Stochastic Modelling) by using a quasi-Newton step for numerical NL optimization [29].

The maximum likelihood estimates are asymptotically normally distributed with mean $\boldsymbol{\theta}$ and covariance matrix $\boldsymbol{D}$. An approximation of the uncertainty $\boldsymbol{D}$ can be found by:

$$\boldsymbol{D}(\hat{\boldsymbol{\theta}}) \simeq \boldsymbol{H}^{-1} \quad (4.13)$$

where $\boldsymbol{H}$ is the Hessian calculated as the second derivative of the negative log-likelihood function (4.11) at the obtained parameter estimate.

4.6 State Filtering

Since the system equation of the state space model is continuous while the observation equation is discrete, state filtering is introduced as a tool for estimating the underlying states such as the SC

insulin concentration or the concentration in a non-measurable compartment at time t based on the measurements until time t_k.

The two types of models considered in this section are linear time-invariant (LTI) and NL models. The Kalman Filter (KF) is an exact solution to the state filtering problem for linear dynamical systems while the Extended Kalman Filter (EKF) is used in case of NL systems.

4.6.1 Kalman Filter

The KF is a set of mathematical equations that provides an efficient and exact recursive solution to the state filtering problem for linear systems. In the following, the KF will be derived for the LTI system below [33, pp. 172-174]:

$$d\boldsymbol{x}_t = \Big(\boldsymbol{A}(\boldsymbol{\theta})\boldsymbol{x}_t + \boldsymbol{B}(\boldsymbol{\theta})\boldsymbol{u}_t\Big)\,dt + \boldsymbol{\sigma}(\boldsymbol{\theta})\,d\boldsymbol{w}_t \tag{4.14a}$$

$$\boldsymbol{y}_k = \boldsymbol{C}(\boldsymbol{\theta})\boldsymbol{x}_k + \boldsymbol{D}(\boldsymbol{\theta})\boldsymbol{u}_k + \boldsymbol{e}_k \tag{4.14b}$$

where $\boldsymbol{A}$, $\boldsymbol{B}$, $\boldsymbol{C}$, and $\boldsymbol{D}$ are constant coefficient matrices, $\boldsymbol{w}_t$ is a standard Wiener process assumed to be independent of $\boldsymbol{e}_k$, which is a Gaussian white noise process with zero mean and covariance $\boldsymbol{S}(\boldsymbol{\theta}, t_k)$.

For linear models, the covariance $\boldsymbol{R}_{k|k-1}$ and the innovation $\boldsymbol{\epsilon}_k$, i.e. equation (4.8) and (4.9), can be computed for a given set of parameters $\boldsymbol{\theta}$ and initial states $\boldsymbol{x}_0$ by means of the KF.

The update equations are:

$$\hat{\boldsymbol{x}}_{k|k} = \hat{\boldsymbol{x}}_{k|k-1} + \boldsymbol{K}_k\big(\boldsymbol{y}_k - \hat{\boldsymbol{y}}_{k|k-1}\big) \tag{4.15}$$

$$\boldsymbol{P}_{k|k} = \boldsymbol{P}_{k|k-1} - \boldsymbol{K}_k\boldsymbol{R}_{k|k-1}\boldsymbol{K}_k^T \tag{4.16}$$

where the initial conditions are $\hat{\boldsymbol{x}}_{1|0} = \boldsymbol{\mu}_0$ and $\boldsymbol{P}_{1|0} = \boldsymbol{V}_0$. $\hat{\boldsymbol{x}}_{k|k}$ is the update of the state, $\boldsymbol{P}_{k|k}$ is the update of the covariance, and $\boldsymbol{K}_k$ is

the Kalman gain which can be calculated by the Kalman equation, i.e.:

$$\boldsymbol{K}_k = \boldsymbol{P}_{k|k-1}\boldsymbol{C}^T\boldsymbol{R}_{k|k-1}^{-1} \tag{4.17}$$

Next, the state prediction equations which are the optimal (minimum variance) linear prediction of the mean and covariance can be calculated as:

$$d\hat{\boldsymbol{x}}_{t|k}/dt = \boldsymbol{A}\hat{\boldsymbol{x}}_{t|k} + \boldsymbol{B}\boldsymbol{u}_t \tag{4.18}$$

$$d\boldsymbol{P}_{t|k}/dt = \boldsymbol{A}\boldsymbol{P}_{t|k} + \boldsymbol{P}_{t|k}\boldsymbol{A}^T + \boldsymbol{\sigma}\boldsymbol{\sigma}^T \tag{4.19}$$

Finally, the output prediction equations of the observation $\hat{\boldsymbol{y}}_{k+1|k}$ along with the covariance $\boldsymbol{R}_{k+1|k}$ are shown below:

$$\hat{\boldsymbol{y}}_{k+1|k} = \boldsymbol{C}\hat{\boldsymbol{x}}_{k+1|k} + \boldsymbol{D}\boldsymbol{u}_{k+1} \tag{4.20}$$

$$\boldsymbol{R}_{k+1|k} = \boldsymbol{C}\boldsymbol{P}_{k+1|k}\boldsymbol{C}^T + \boldsymbol{S} \tag{4.21}$$

where $\boldsymbol{S}$ is the covariance matrix of the measurement error.

Since it is necessary to estimate the systems' evolution between discrete time instants, the integration of (4.14a) through the sample interval $[t_k, t_{k+1}]$ is shown below [33, pp. 185-186]:

$$\begin{aligned}\boldsymbol{x}_{t_{k+1}} = e^{\boldsymbol{A}(t_{k+1}-t_k)}\boldsymbol{x}_{t_k} &+ \int_{t_k}^{t_{k+1}} e^{\boldsymbol{A}(t_{k+1}-s)}\boldsymbol{B}\boldsymbol{u}_s\, ds \\ &+ \int_{t_k}^{t_{k+1}} e^{\boldsymbol{A}(t_{k+1}-s)}\boldsymbol{\sigma} d\boldsymbol{w}_s\end{aligned} \tag{4.22}$$

The two first terms in (4.22) are the deterministic parts while the last integral is a stochastic Itô integral. Using the assumption that $\boldsymbol{w}_t$ is a Wiener process, the integral $\int_{t_k}^{t_{k+1}} e^{\boldsymbol{A}(t_{k+1}-s)}\boldsymbol{\sigma} d\boldsymbol{w}_s$ is normally distributed white noise with zero mean and covariance $\boldsymbol{P}_{k+1|k}$, i.e.:

$$\boldsymbol{P}_{k+1|k} = e^{\boldsymbol{A}\tau_s}\boldsymbol{P}_{k|k}\left(e^{\boldsymbol{A}\tau_s}\right)^T + \int_0^{\tau_s} e^{\boldsymbol{A}s}\boldsymbol{\sigma}\boldsymbol{\sigma}^T\left(e^{\boldsymbol{A}s}\right)^T ds \tag{4.23}$$

where $\tau_s = t_{k+1} - t_k$ is the sampling time.

If $\boldsymbol{u}_t$ is constant in the sample interval, the sampled version of (4.22) can be written as:

$$\hat{\boldsymbol{x}}_{k+1|k} = e^{\boldsymbol{A}\tau_s}\boldsymbol{x}_k + \int_0^{\tau_s} e^{\boldsymbol{A}s}\, ds\, \boldsymbol{B}\boldsymbol{u} \tag{4.24}$$

The Kalman procedure is visualized in Figure 4.2.

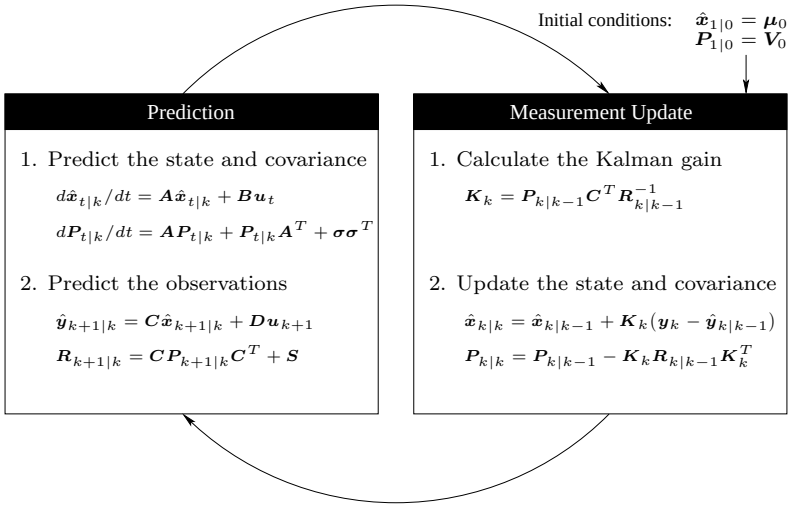

Figure 4.2: Kalman procedure [57].

4.6.2 Extended Kalman Filter

In case of NL models like the one shown in (4.25), it is necessary to use the extended Kalman filter (EKF) to get the optimal NL estimation of the state.

$$d\boldsymbol{x}_t = \boldsymbol{f}(\boldsymbol{x}_t, \boldsymbol{u}_t, \boldsymbol{\theta}, t)\, dt + \boldsymbol{\sigma}(\boldsymbol{u}_t, \boldsymbol{\theta}, t)\, d\boldsymbol{w}_t \tag{4.25a}$$

$$\boldsymbol{y}_k = \boldsymbol{h}(\boldsymbol{x}_k, \boldsymbol{u}_k, \boldsymbol{\theta}, t_k) + \boldsymbol{e}_k \tag{4.25b}$$

where the functions $\boldsymbol{f}(\cdot)$ and $\boldsymbol{h}(\cdot)$ are NL functions of the state vector $\boldsymbol{x}_t$ while $\boldsymbol{e}_k$ is a Gaussian white noise process mutually independent of $\boldsymbol{w}_t$.

The EKF uses a local linear approximation of the functions $\boldsymbol{f}(\cdot)$ and $\boldsymbol{h}(\cdot)$ by Taylor expansion at each sampling time to describe the dynamics in the system [33, pp. 199-200], i.e.:

$$\boldsymbol{A}(\hat{\boldsymbol{x}}_t, \hat{\boldsymbol{u}}_t, \boldsymbol{\theta}, t) = \left.\frac{\partial \boldsymbol{f}}{\partial \boldsymbol{x}}\right|_{\boldsymbol{x}=\hat{\boldsymbol{x}}} \tag{4.26a}$$

$$\boldsymbol{C}(\hat{\boldsymbol{x}}_{k|k-1}, \hat{\boldsymbol{u}}_k, \boldsymbol{\theta}, t_k) = \left.\frac{\partial \boldsymbol{h}}{\partial \boldsymbol{x}}\right|_{\boldsymbol{x}=\hat{\boldsymbol{x}}_{k|k-1}} \tag{4.26b}$$

The prediction of the output $\hat{\boldsymbol{y}}_{k+1|k}$ in the NL case using EKF is:

$$\hat{\boldsymbol{y}}_{k+1|k} = \boldsymbol{h}(\hat{\boldsymbol{x}}_{k+1|k}, \boldsymbol{u}_{k+1}, \boldsymbol{\theta}, t_{k+1}) \tag{4.27}$$

while the formulas for prediction of the mean and covariance of the state-vector are:

$$d\hat{\boldsymbol{x}}_{t|k}/dt = \boldsymbol{f}(\hat{\boldsymbol{x}}_{t|k}, \boldsymbol{u}_t, \boldsymbol{\theta}, t) \tag{4.28a}$$

$$d\boldsymbol{P}_{t|k}/dt = \boldsymbol{A}\boldsymbol{P}_{t|k} + \boldsymbol{P}_{t|k}\boldsymbol{A}^T + \boldsymbol{\sigma}\boldsymbol{\sigma}^T \tag{4.28b}$$

where $\boldsymbol{A} = \boldsymbol{A}(\hat{\boldsymbol{x}}_{t|k}, \boldsymbol{u}_t, \boldsymbol{\theta}, t)$ which is calculated as in (4.26a) and $t \in [t_k, t_{k+1}]$.

An iterated EKF is used to avoid numerical integration of the state-prediction equations (4.28) where the time interval $[t_k, t_{k+1}]$ is sub-sampled and the equations are linearized at each subsample.

A fundamental problem with EKF and the iterated EKF is that the assumption of the random variables being normal no longer is valid after the linearization. The state estimator is therefore only an approximative solution and not exact like the KF [57].

4.7 Model Validation

After having determined the model structure and estimated the parameters in the model, the next step is to validate the results. The

purpose of model validation is to test whether the model assumptions are valid. Furthermore, the ability of the estimated model to predict/simulate the observed dynamics of the modelled system is tested.

The models in this thesis are validated using visual inspection along with statistical analysis of the model structure, the parameter estimates, and the residuals, i.e. the difference between the observed data and the 1-step prediction. This is done to get an indication whether the models are able to capture the relevant features of the dynamics of the modelled system. If the proposed model is accepted in these tests, it should preferably be followed by cross validation where the results from a model identified from one set of data is tested on another set of data.

4.7.1 Test for Model Structure

The tests for model structure mentioned in this section serve as a tool for comparing alternative model structures, to reveal possible over-fitting, and to test whether a model reduction is relevant.

Likelihood Ratio Test

The likelihood ratio test (LRT) is a way to test if it is reasonable to reduce a previously proposed model to a submodel. This is done by testing whether or not the value of the negative log-likelihood function for the reduced model is significant compared to the original model. The hypothesis to test is $H_0 : \boldsymbol{\theta} \in \mathcal{M}_0$ against the alternative $H_1 : \boldsymbol{\theta} \in \mathcal{M}_1$ with $\boldsymbol{\theta}$ being the parameter vector and where $\mathcal{M}_0$ and $\mathcal{M}_1$ are the two models to test for which $\mathcal{M}_0 \subset \mathcal{M}_1$. The likelihood-ratio is [33, pp. 104-105]:

$$\Lambda = \frac{\mathcal{L}(\hat{\boldsymbol{\theta}}_0)}{\mathcal{L}(\hat{\boldsymbol{\theta}}_1)} \tag{4.29}$$

where $\mathcal{L}(\hat{\boldsymbol{\theta}}_i)$ $(i = 0, 1)$ is the maximized likelihood function under H_0 and H_1, respectively.

A test for accept of H_0 against H_1 is:

$$-2\log\Lambda \in_{a.s.} \chi^2(s-r) \tag{4.30}$$

where r and s denote the dimensions of $\mathcal{M}_0$ and $\mathcal{M}_1$.

In the output from CTSM, the value of the objective function $\mathcal{F}$ is calculated along with the value of the penalty function $\mathcal{P}$. The objective function is the negative log-likelihood function corrected with the penalty function [29], i.e.:

$$\mathcal{F}(\boldsymbol{\theta}) = -\log\left(L(\mathcal{Y}|\boldsymbol{\theta}, y_0)\right) + \mathcal{P} \tag{4.31}$$

Equation (4.29) can be rewritten using (4.31):

$$\begin{aligned} -2\log\Lambda &= 2\big(-\log L_0 - (-\log L_1)\big) \\ &= 2\Big(\big(\mathcal{F}_0 - \mathcal{P}_0\big) - \big(\mathcal{F}_1 - \mathcal{P}_1\big)\Big) \end{aligned} \tag{4.32}$$

which can be calculated readily using the output from CTSM.

Information Criteria

The LRT is limited to comparison of two nested models and does therefore not apply when one wishes to test a model which is not a true subset of a larger model. Furthermore, it is not possible to choose between models by comparing the value of the likelihood function as a measure for the optimal model since models with more parameters tend to fit a data set better than models with fewer parameters. A penalty on the model complexity is therefore needed.

Instead, several information criteria has been proposed for order selection where the optimal order $p = \dim(\boldsymbol{\theta})$ is found through minimizing a specified cost function. First, the data is fitted using ML

and the model complexity is thereafter penalized. The two most common information criteria are AIC (Akaike's Information Criterion) and BIC (Bayesian Information Criterion) where the model order can be found through minimizing the following expressions for AIC and BIC, respectively [33, p. 106]:

$$AIC = 2p - 2\log L(\boldsymbol{\theta}, \mathcal{Y}_N) \tag{4.33}$$

$$BIC = p\log N - 2\log L(\boldsymbol{\theta}, \mathcal{Y}_N) \tag{4.34}$$

AIC is not a consistent estimator since it has a tendency to overestimate the model order for large data sets, i.e. large N. Opposed to AIC, BIC generally gives a consistent estimate of the model order by penalizing with $p\log N$ instead of $2p$.

4.7.2 Residual Analysis

The principle of residual analysis is to check whether the information obtained from the model contradicts with the model assumptions. Plots of the residuals along with tests in the sample autocorrelation and lag-dependency functions, will be considered to test for independence of the residuals in this thesis.

Plot of Residuals

By plotting the residuals between the observed data y_k and the 1-step prediction $\hat{y}_{k|k-1}$, it is possible to spot trends and inhomogeneity of the variance, outliers and poor data. This often gives a quick indication whether something is missing in the model and may also provide hints for an alternative model structure.

Autocorrelation Functions

The autocorrelation function (ACF) $\rho(k)$ is a measure for the correlation between observations with time lag k. Provided that the

residuals ε_t are white noise, then:

$$\hat{\rho}(k) \in_{approx.} N(0, \frac{1}{N}) \tag{4.35}$$

where N is the number of observations.

The variance of $\hat{\rho}(k)$ for lags k greater than some value q is computed using Bartlett's approximation [9, pp. 34-36]:

$$V[\hat{\rho}(k)] \simeq \frac{1}{N}\Big\{1 + 2\sum_{v=1}^{q}\rho_v^2\Big\}, \qquad k > q \tag{4.36}$$

An approximate 95 % confidence interval to test whether the prediction errors are significantly different from white noise can be found as $\pm 2\sqrt{V[\hat{\rho}(k)]}$.

The partial autocorrelation function (PACF) $\phi_{kk}(k)$ is a measure of the correlation between the observations at time t and $t+k$ given all the observations in between. An approximative 95 % confidence interval is calculated as $\pm\frac{2}{\sqrt{N}}$ where N is the number of observations [9, p. 65].

These two types of tests for whiteness of the residuals are only valid for linear systems since it is only the linear dependencies which are taken into account.

Lag-Dependency Functions

To identify lag-dependencies in the residuals for NL models, it is not sufficient to carry out tests in the autocorrelation functions as mentioned above. Instead, a lag-dependency (LDF) and partial lag-dependency function (PLDF) is introduced in [39] where the NL dependency is taken into account.

LDF(k) and PLDF(k) are calculated as:

$$LDF(k) = sign\Big(\hat{f}_k(b) - \hat{f}_k(a)\Big)\sqrt{(\tilde{R}^2_{0(k)})_+} \tag{4.37}$$

$$PLDF(k) = sign\Big(\hat{f}_{kk}(b) - \hat{f}_{kk}(a)\Big)\sqrt{(\tilde{R}^2_{(0k)|(1\ldots k-1)})_+} \tag{4.38}$$

where $f_k(x) = E[X_t|X_{t-k} = x]$ and $f_{kk}(x)$ is a partial dependence function in lag k when the effect of lag $1, \ldots, k-1$ is accounted for while a and b are the minimum and maximum of the observations. R^2 is the coefficient of determination while the '+' indicates that only non-negative values are used [39].

LDF(k) can be interpreted as the part of the totale variation in x_t which can be explained by x_{t-k} while PLDF(k) is the relative decrease in the variance of the 1-step prediction, when lag k is included as an extra predictor [33, pp. 76-77].

4.7.3 Validation of Parameter Estimates

Hotelling's T^2 test can be used to test whether the estimated parameter vectors $\hat{\boldsymbol{\theta}}_i$, $i = 1 \ldots n$, for n subjects can be assumed to come from the same normal distribution, i.e.:

$$\hat{\boldsymbol{\theta}}_i \in N_p(\boldsymbol{\mu}, \boldsymbol{\Sigma}) \tag{4.39}$$

where p is the dimension of $\hat{\boldsymbol{\theta}}_i$, $\boldsymbol{\mu}$ is the mean vector, and $\boldsymbol{\Sigma}$ is the dispersion matrix.

The hypothesis to test is $H_0 : \boldsymbol{\mu} = \boldsymbol{\mu}_0$ against the alternative $H_1 : \boldsymbol{\mu} \neq \boldsymbol{\mu}_0$ where $\boldsymbol{\mu}_0$ is a given vector. The test can be written as [15, pp. 273-275]:

$$\frac{n-p}{(n-1)p} T^2 \in F(p, n-p) \tag{4.40}$$

where T^2 is calculated as:

$$T^2 = n\big(\bar{\boldsymbol{\theta}} - \boldsymbol{\mu}_0\big)^T \boldsymbol{S}^{-1} \big(\bar{\boldsymbol{\theta}} - \boldsymbol{\mu}_0\big) \tag{4.41}$$

where $\bar{\boldsymbol{\theta}}$ and $\boldsymbol{S}$ are the empirical mean parameter vector and the empirical dispersion matrix, respectively.

Each parameter can further be tested individually to see if it is significantly different from a given parameter value θ_0. The hypothesis

can formally be written as [14, p. 337]:

$$\frac{\hat{\theta} - \theta_0}{\hat{\sigma}} \in t(N - 1 - p) \tag{4.42}$$

where $\hat{\theta}$ and $\hat{\sigma}$ are the estimated parameter value and variance, respectively, while N is the number of observations and p is the number of estimated parameters in the model. This test is automatically generated in the output from CTSM for $\theta_0 = 0$.

Chapter 5

Experimental Procedures and Data

When clinical studies are carried out, the number of measurements should be as large as possible to ensure the greatest precision in parameter estimation by maximizing the information in the data. Furthermore, the measurements should cover a wide range of insulin and effect concentrations to describe the shape of the PK/PD relationship optimally. However, the constraints are many in human clinical studies, which is why issues like identifiability cannot always be taken into account. The frequency of data collection is therefore not always optimal for distinguishing what type of PK/PD model is needed.

In the following, the two different experiments considered in this thesis are explained.

5.1 Euglycaemic Clamp Study

The euglycaemic clamp study performed at Steno Diabetic Center is used to determine the characteristics of two different types of insulin

and to verify that the insulin has the intended properties without too many side effects [27]. The information obtained from the clamp study is further used to determine the insulin dose needed to obtain a clinically observable effect in human patients.

5.1.1 Subjects

The euglycaemic clamp study is performed on twenty healthy non-smoking Caucasian males between 18 and 40 years of age with a body mass index $< 27\,\mathrm{kg/m^2}$. The anthropometric measurements of each subject can be seen in Appendix A.1.

5.1.2 Trial and Procedure Information

The experimental design is a single center two-period randomized double blind crossover experiment as illustrated in Figure 5.1. Each patient receives a bolus dose of either insulin A or B[1] on the first day of the study and the opposite type of insulin at the next visit which is one or two weeks later to prevent carry-over effects from the first treatment to the next.

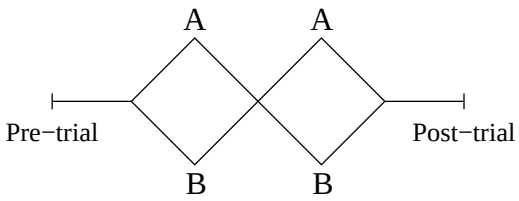

Figure 5.1: Experiment diagram.

The insulin and C-peptide levels are measured by inserting a catheter into an antecubital vein in the patient's arm. The glucose concen-

[1]The difference between insulin A and B is not known and of no importance since it is the modelling and estimation methods which are the primary interests of this thesis.

tration is measured through a glucose sensor in the hand of the same arm. To suppress the secretion of insulin from the pancreas, the patient continuously receives an IV infusion of regular human insulin (0.15 mU/kg BW/min) during the whole experiment in the opposite arm along with an IV infusion of glucose (GIR) to maintain a constant blood glucose (BG) concentration. The experiment can be thought of as some sort of titration where the amount of infused glucose needed to maintain euglycemia (constant glucose concentration) can be assumed to be equal to the amount of glucose utilized in the body.

After 90 min. of monitoring the insulin and the BG, the patient receives a single dose of either insulin type A or B (0.2 U/kg BW) which is injected SC and the insulin, GIR, BG, and C-peptide concentration are observed during the next 10 hours.

The plasma insulin concentration is sampled at non-equidistant time instants. Each patient is monitored 90 min. before the injection with samples every 30 min. until the time of injection. The patients are thereafter monitored for 10 hours with samples every 10 min. during the first hour, every 15 min. the next hour, and every 20 min. the last 8 hours. The GIR, BG, and C-peptide concentration are sampled every minute throughout the entire study.

The C-peptide concentration is used as a measure for the human secretion of insulin (see Section 2.3) and may be used to correct the measured insulin concentration for endogenous insulin by use of the following equation [27]:

$$I_{exo} = I_{meas} - \frac{I_{ini}}{C_{ini}} \cdot C_{meas} \tag{5.1}$$

where I_{exo} is the exogenous insulin, I_{meas} and C_{meas} are the measured insulin and C-peptide concentrations, respectively, I_{ini} is the initial insulin concentration, and C_{ini} is the initial C-peptide concentration. I_{ini} and C_{ini} are computed as the average of the measurements up to the time of injection at $t = 0$.

5.1.3 Experimental Data

The plasma insulin concentration, GIR, and BG concentration are shown in Figure 5.2 for a representative subject from the study.

A sudden drop in the insulin concentration at high concentrations resulting in two apparent peaks for each type of insulin is observed in Figure 5.2. It can be explained as insulin crystallizing in the high insulin concentration blood samples resulting in a lower measured insulin concentration than the actual plasma insulin concentration. The crystallization of insulin does not only appear at high concentration but is a known phenomena at all concentrations.

5.2 Glucose Tolerance Studies

The glucose tolerance studies are used for assessing the insulin sensitivity/resistance for normal (NGT) and impaired glucose tolerant (IGT) subjects. The two tests used in the glucose tolerance studies are an intravenous glucose tolerance test (IVGTT) and a less invasive oral glucose tolerance test (OGTT). The studies were performed at Steno Diabetic Center [23].

The IVGTT experiment consists of injecting a bolus of glucose into the bloodstream thus inducing an increase of the insulin plasma concentration secreted by the pancreas. The difference between the IVGTT and the OGTT is that the glucose is given orally in the OGTT.

5.2.1 Subjects

The glucose tolerance studies were performed on 70 verified type II diabetes mellitus subjects with four or more offspring and a spouse without known diabetes (288 subjects).

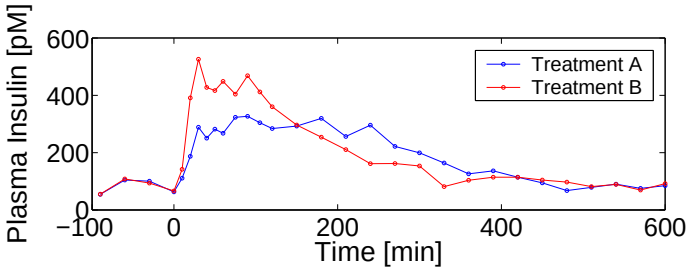

(a) Insulin

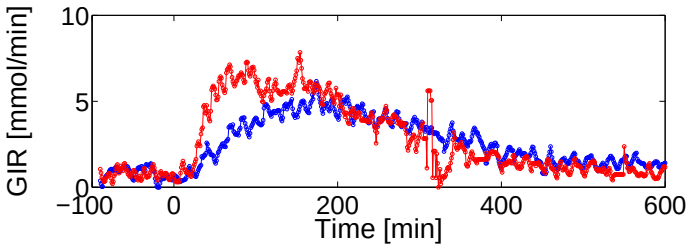

(b) GIR

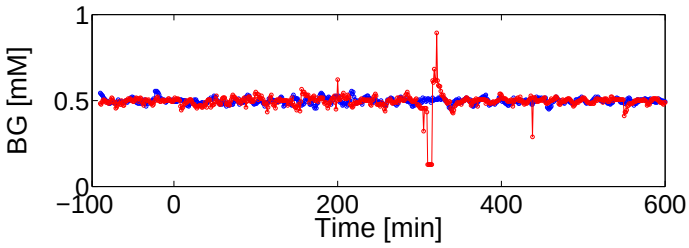

(c) BG

Figure 5.2: Insulin concentration, GIR, and BG concentration for a representative subject for treatment with insulin A (Blue) and insulin B (Red).

5.2.2 Trial and Procedure Information

The NGT and IGT subjects from the study underwent an IVGTT and OGTT while the type II diabetic subjects only underwent an OGTT. The focus in the study is on the NGT and IGT subjects where detailed information from the IVGTT and OGTT performed on the same subject are used to predict the sensitivity to insulin.

IVGTT

All non-diabetic subjects underwent a tolbutamide modified, frequently sampled IVGTT. After 12 hours of fasting, veneous blood samples were drawn in triplicate at -10, -5, and 0 min. before the IVGTT and at 2, 3, 4, 5, 6, 7, 8, 10, 12, 14, 16, 19, 22, 23, 24, 25, 27, 30, 35, 40, 50, 60, 70, 80, 90, 100, 120, 140, 160, and 180 min. for analysis of serum insulin, plasma glucose, and C-peptide concentrations. At $t = 0$ min., glucose was injected IV in the contralateral antecubital vein over a period of 1 min. (0.3 g/(kg BW) of 50 % glucose).

At $t = 20$ min., a bolus of 3 mg tolbutamide/(kg BW) was injected during 5 seconds to elicit a secondary pancreatic beta-cell response. The injected tolbutamide causes an insulin burst. This ensures that as much of the dynamics of the insulin/glucose system is present in the measured data. For IGT subjects, it is especially necessary to inject tolbutamide since it raises the plasma insulin level above the insulin baseline.

OGTT

All subjects underwent a 75 g frequently sampled OGTT within 1-4 weeks prior to the IVGTT. After a 12 hour overnight fasting, veneous blood samples were drawn in triplicate at -10, -5, and 0 min. before the OGTT and at 10, 20, 30, 40, 50, 60, 75, 90, 105, 120, 140, 160,

210, and 240 min. from the start of the glucose load for analysis of serum insulin, plasma glucose, and C-peptide concentrations.

5.2.3 Experimental Data

In both studies, anthropometric measurements including age, height, weight, waist, hip, and BMI was recorded. The sample mean and standard deviation of these measurements are shown in Table B.1 in Appendix B.1.

The plasma insulin, BG, and C-peptide concentrations are plotted in Figure 5.3 and Figure 5.4 for a representative NGT and IGT subject, respectively, from the IVGTT and OGTT.

The fasting and stimulated glucose concentrations are clearly higher in the NGT than the IGT subjects whereas the fasting plasma insulin are more alike for the NGT and IGT subject.

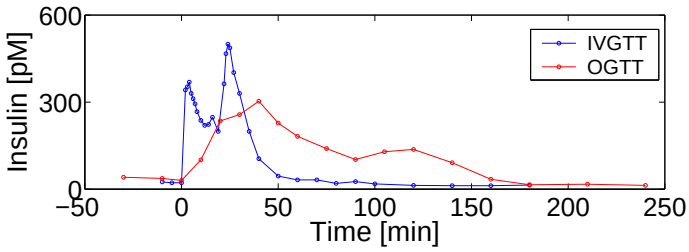

(a) Plasma Insulin

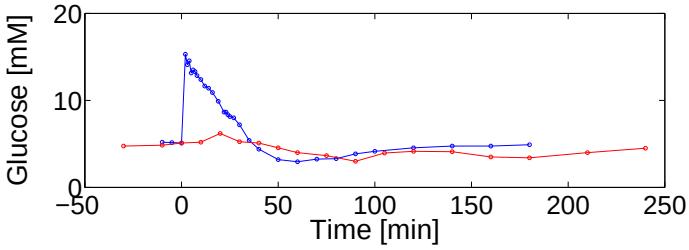

(b) Blood Glucose

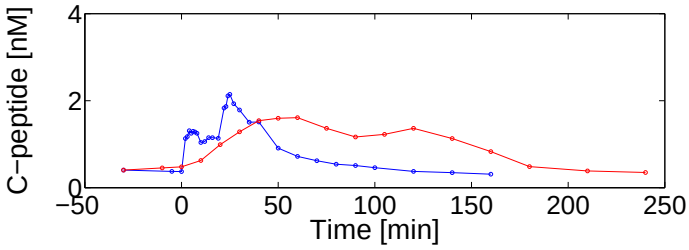

(c) C-peptide

Figure 5.3: Plasma insulin, BG, and C-peptide concentrations for a representative NGT subject from IVGTT (Blue) and OGTT (Red).

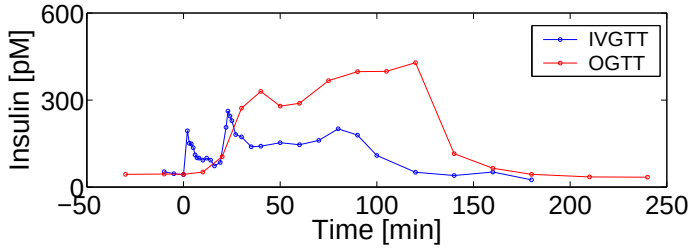

(a) Plasma Insulin

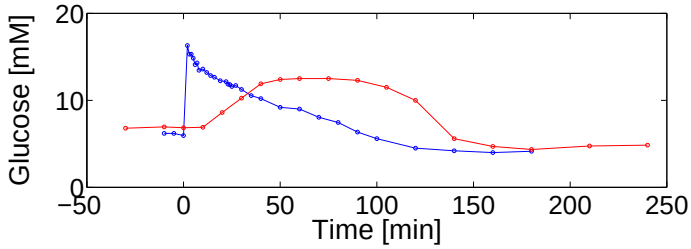

(b) Blood Glucose

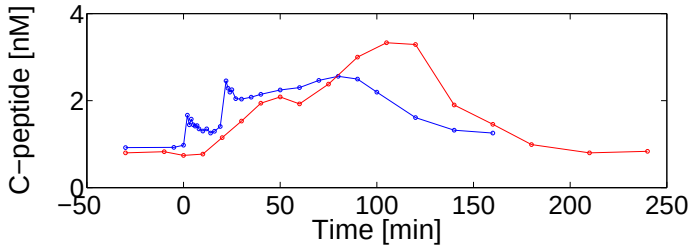

(c) C-peptide

Figure 5.4: Plasma insulin, BG, and C-peptide concentrations for a representative IGT subject from IVGTT (Blue) and OGTT (Red).

Chapter 6

Clamp Models

The purpose of the PK/PD models for the clamp study is to determine the characteristics of two different types of insulin which can be used for reliable glycaemic predictions and eventually for therapeutic control.

This chapter reflects the model building process and a discussion hereof. In the following sections, different PK and PK/PD models for the clamp study are derived and described along with an introduction to important PK and PD parameters. The PK models considered in this chapter are purely empirical compartmental models, meaning descriptive and not explanatory mechanistic models [1]. The logistic sigmoidal E_{max} effect model used in the PK/PD models is derived empirically by incorporating known, theoretical characteristics of the data and can therefore be considered as a semi-mechanistic model. The information needed to build truly mechanistic models is substantially larger compared to empirical models. They are very time consuming and will therefore not be considered in this thesis.

The compartments of interest are illustrated using boxes while the arrows represent the absorption, distribution, and elimination of insulin. The black arrows represent inputs to the system while the

white arrows describe the distribution and elimination of insulin. When a rate constant is written above an arrow it means that it follows first-order kinetics while an arrow without a rate constant above symbolizes zero-order kinetics.

6.1 PK Models

Four different PK models are presented in the following, starting with the simplest model consisting of only one compartment. Next, the model is expanded with compartments for the SC depot in two different ways. Thereafter, the single-compartment model is expanded with a peripheral compartment representing the insulin equilibration with the tissue. Finally, the four models are summarized and compared.

6.1.1 Single-Compartment Model

The single-compartment model is a very simplified model where the plasma is assumed to consist of a single-compartment with first-order absorption and elimination and is illustrated in Figure 6.1.

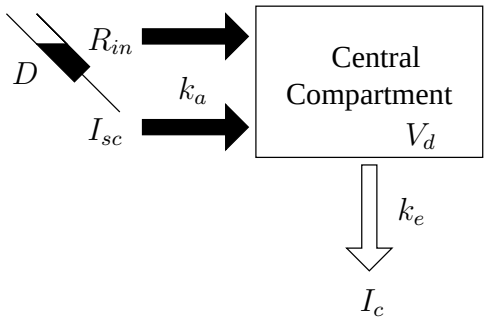

Figure 6.1: Single-compartment model. The symbols in the model are explained in the text.

The two states in the model are I_{sc} and I_c. I_{sc} describes the amount of insulin remaining to be absorbed from the SC tissue and I_c represents the amount of insulin in the central compartment.

The parameters k_a and k_e are the rate constants for the irreversible absorption to and elimination from the central compartment, respectively. The parameter V_d is the volume of the central compartment. V_d should not be mistaken with the plasma volume but can be thought of as the *apparent* volume of distribution in the body.

The two inputs to the system are D and R_{in}. D describes the SC injected insulin dose of either type A or B while R_{in} is the IV infusion of regular human insulin given throughout the study to suppress the secretion of insulin from the pancreas.

Assumptions

The model assumptions are:

`A1:` The insulin is mixed instantaneously in the plasma. The actual time taken for mixing is approx. a few minutes and is therefore insignificant compared with the sampling time.

`A2:` The insulin absorption and elimination is assumed to follow first-order kinetics meaning that the rate of change of insulin concentration is directly proportional to the remaining concentration of insulin. This assumption leads to a linear model.

`A3:` The amount of insulin removed from the SC tissue is equal to the amount absorbed in the central compartment. This assumption is made because the break down of SC insulin is not modelled.

`A4:` No insulin is secreted from the pancreas because the IV infusion of regular human insulin suppresses the production. The small amount of insulin that actually is secreted in the pancreas is corrected by using C-peptide measurements. It

is therefore reasonable not to include any feedback mechanisms in the model since they have been disrupted.

Model equations

The difference equation of finite differences Δt for the amount of insulin is shown in Table 6.1 where t is the time from SC injection of insulin A/B.

Table 6.1: Integral mol balance for insulin.

Accumulated	=	In	−	Out
$I_{sc}(t+\Delta t) - I_{sc}(t)$	=	D	−	$k_a I_{sc} \Delta t$
$I_c(t+\Delta t) - I_c(t)$	=	$(k_a F I_{sc} + R_{in})\Delta t$	−	$k_e I_c \Delta t$

The parameter F is the bioavailability factor which is included to describe the fraction of the injected dose D which is available in the SC depot.

The differential equation is obtained by dividing with Δt and letting the time step tend to zero in the difference equation, i.e.:

$$\frac{dI_{sc}}{dt} = D \cdot \delta(t) - k_a I_{sc} \tag{6.1a}$$

$$\frac{dI_c}{dt} = k_a F I_{sc} + R_{in} - k_e I_c \tag{6.1b}$$

where $\delta(t)$ is a Dirac delta function.

The specified model in (6.1) is structural unidentifiable (see Appendix A.2) but can be made identifiable by setting the bioavailability factor F equal 1, thereby assuming that all the SC injected insulin is available.

Analytical solution

The amount of insulin remaining to be absorbed from the SC depot can be found by solving (6.1a), i.e.:

$$I_{sc} = D \cdot e^{-k_a t} \tag{6.2}$$

with the initial condition $I_{sc} = D$ for $t = 0$.

By substituting (6.2) into (6.1b), the change in the amount of insulin in the central compartment can be written as:

$$\frac{dI_c}{dt} = k_a F D e^{-k_a t} + R_{in} - k_e I_c \tag{6.3}$$

The deterministic equation (6.3) is split into two domains:

$$\frac{dI_{c,1}}{dt} = R_{in} - k_e I_{c,1} \qquad -90 < t < 0 \tag{6.4}$$

$$\frac{dI_{c,2}}{dt} = k_a F D e^{-k_a t} + R_{in} - k_e I_{c,2} \qquad 0 < t \tag{6.5}$$

since IV infusion of regular human insulin is given throughout the study ($t \in [-90, 600]$) while the SC injection of insulin A/B is given at $t = 0$.

The solution to (6.4) is:

$$I_{c,1} = \frac{R_{in}}{k_e}\Big(1 - e^{-k_e \tau}\Big) + I_{c,0} e^{-k_e \tau} \tag{6.6}$$

with the initial condition $I_c = I_{c,0}$ for $\tau = t + 90 = 0$.

The solution to (6.5) can be found using the Panzer equation, i.e.:

$$\begin{aligned} I_{c,2} &= e^{-k_e t}\Big[\int e^{k_e t}\Big(k_a F D e^{-k_a t} + R_{in}\Big)\, dt + C\Big] \\ &= FD\frac{k_a}{k_a - k_e}\Big(e^{-k_e t} - e^{-k_a t}\Big) + I_{c,1} \end{aligned} \tag{6.7}$$

Thereby, the analytical solution for the insulin concentration $C_c = \frac{I_c}{V_d}$ becomes:

$$C_{c,1} = \frac{R_{in}}{V_d k_e}\left(1 - e^{-k_e \tau}\right) + \frac{I_{c,0}}{V_d} e^{-k_e \tau} \qquad -90 < t < 0 \quad (6.8)$$

$$C_{c,2} = \frac{FD}{V_d} \frac{k_a}{k_a - k_e}\left(e^{-k_e t} - e^{-k_a t}\right) + C_{c,1} \qquad 0 < t \quad (6.9)$$

The analytical solution (6.8) and (6.9) can be expressed as a linear combination of exponential terms and a constant term K, i.e.:

$$C_c = (\phi_1 + \phi_2) \cdot e^{-\phi_3 \tau} + \phi_4 \cdot e^{-\phi_3 t} + \phi_5 \cdot e^{-\phi_6 t} + K \quad (6.10)$$

where $k_e = \phi_3 > 0$, and $k_a = \phi_6 > 0$.

The sum of the parameters ϕ_1 and ϕ_2 can be identified from (6.10) but not the individual parameters since they cannot be distinguished from one another. The biexponential terms $\phi_4 \cdot e^{-\phi_3 t}$ and $\phi_5 \cdot e^{-\phi_6 t}$ for SC insulin are not identifiable in the sense of having a unique vector of parameters associated with a given set of predictions since the parameters ϕ_3 and ϕ_6 may be exchanged without changing the predictions. Identifiability of the biexponential terms is ensured by requiring that $\phi_3 > \phi_6$ so that the first exponential term determines the initial absorption phase of insulin while the terminal elimination phase primarily is determined by the second exponential term.

Fundamental PK Parameters

Three fundamental pharmacokinetic parameters, that frequently are used to characterize the insulin profile in the plasma, are the time to maximum insulin concentration (t_{max}), the maximum insulin concentration (C_{max}), and the area under the insulin concentration profile (AUC). These parameters are derived from the single-compartment model presented above.

Time to Maximum Insulin Concentration: The maximum insulin concentration C_{max}, occurs at time t_{max}. At this time, the insulin profile is at its peak and the slope is zero. t_{max} can be found by setting the first derivative of (6.9) equal to zero and solving for t_{max} [58, p. 171]:

$$\begin{aligned}\frac{dC_c}{dt} = \frac{FD}{V_d}\frac{k_a}{k_a - k_e}\Big(- k_e e^{-k_e t_{max}} + k_a e^{-k_a t_{max}}\Big) \\ + \frac{\big(R_{in} - I_{c,0}k_e\big)}{V_d} e^{-k_e(t_{max}+90)} = 0\end{aligned} \tag{6.11}$$

Maximum Insulin Concentration: The maximum insulin concentration C_{max} can be found by inserting the time t_{max} which solves (6.11) into (6.9):

$$\begin{aligned}C_{max} = \frac{FD}{V_d}\frac{k_a}{k_a - k_e}\Big(e^{-k_e t_{max}} - e^{-k_a t_{max}}\Big) \\ + \frac{R_{in}}{k_e V_d}\Big(1 - e^{-k_e(t_{max}+90)}\Big) + \frac{I_{c,0}}{V_d} e^{-k_e(t_{max}+90)}\end{aligned} \tag{6.12}$$

Area Under Curve: The area under the insulin concentration profile (AUC) describes how much of the insulin is absorbed. AUC_0^T is found by integrating (6.9) from $t = 0$ to T:

$$\begin{aligned}\text{AUC}_0^T = &\frac{FD}{V_d}\frac{k_a}{k_a - k_e}\int_0^T \Big(e^{-k_e t} - e^{-k_a t}\Big)\, dt \\ &+ \frac{R_{in}}{V_d k_e}\int_0^T \Big(1 - e^{-k_e \tau}\Big)\, dt \\ &+ \frac{I_{c,0}}{V_d}\int_0^T e^{-k_e \tau}\, dt\end{aligned} \tag{6.13}$$

The expression in (6.13) for AUC depends on a good estimation of the rate constants and of a possible lag-time [44, p. 30]. Therefore,

the Trapezoidal-method is used to determine the AUC, i.e.:

$$AUC_0^T = \sum_{i=0}^{N} \frac{C_{c,i+1} + C_{c,i}}{2}\left(t_{i+1} - t_i\right) \tag{6.14}$$

where N is the number of measurements.

6.1.2 SC Uptake Models

Several models for SC insulin kinetics are proposed in the literature [41, 55]. The two most prominent models are:

- The hexamer/dimer SC uptake model proposed in [55] where the SC depot consists of two compartments for hexamer and dimer insulin, respectively.
- The two-compartment SC uptake model proposed in [41] is an expansion of the single-compartment model where an extra SC compartment is added to account for the delay between the SC injection of insulin and the absorption into the plasma along with degradation from the SC depot.

Hexamer/Dimer SC Uptake Model

The hexamer/dimer SC uptake model describes the diffusion in the SC depot and the equilibration between different association states of insulin. The model is illustrated in Figure 6.2.

The model proposed in [55] also included a compartment for binding of insulin in the tissue and has previously only been used for simulation. The compartment for binding of insulin is made superfluous by assuming that the binding in the SC depot is negligible at therapeutic concentrations. Thereby, the model is more suitable for estimation since the number of parameters in the model are reduced considerably.

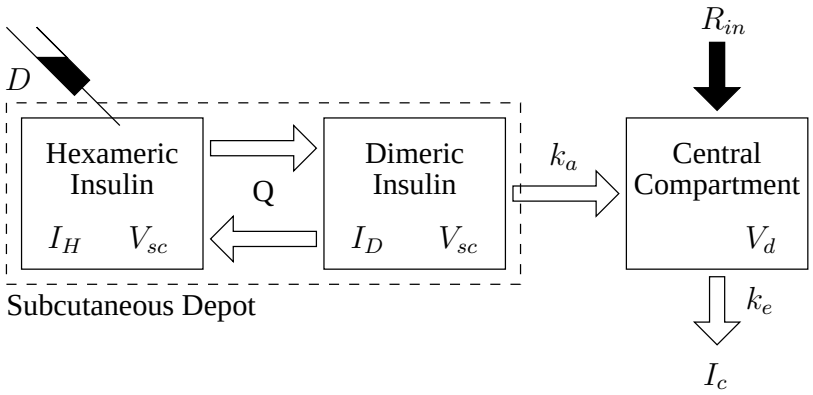

Figure 6.2: Hexamer/dimer SC uptake model.

Assumptions

The following assumptions are made about the hexamer/dimer SC uptake model along with assumption `A1`, `A3`, and `A4` from the single-compartment model to obtain a model suitable for estimation:

`A1:` Insulin A mainly consists of hexamer units while insulin B is an analogue where the dimer structure is stabilized. The insulin in the SC depot is therefore assumed to be of those two forms only. If a monomer stabilized insulin had been used, it would be necessary to include a compartment for monomer insulin.

`A2:` Since therapeutic concentrations and doses[1] are much higher than 10^{-8} M, the binding of insulin in the SC tissue is clinically not relevant and therefore not modelled. Because of the high concentration in the syringe, the SC injected dose is assumed to be in the hexamer form for both types of insulin.

[1]The actual concentration in the syringe is 100 U/mL, which is equal to 0.66 mM.

`A3:` Only dimeric insulin is assumed to be absorbed since the hexameric molecule is too large to pass through the capillary wall. The insulin is therefore only removed from the dimer compartment in the SC depot. When the insulin is absorbed into the plasma, the insulin is assumed to be in the monomeric form.

`A4:` The spherical geometry of the SC injected dose is not modelled, as e.g. in [55], to circumvent the use of partial differential equations. The influence of different injection volumes are therefore not modelled.

`A5:` The spread of insulin in the SC depot is assumed to be negligible. The volume of the SC depot is thereby assumed to be constant and equal to the volume of the SC injected insulin which is around 0.1 mL.

Model equations

With the assumptions mentioned above, the equations for the hexamer/dimer SC uptake model becomes:

$$\frac{1}{V_{sc}}\frac{dI_H}{dt} = -P\Big(\frac{I_H}{V_{sc}} - Q\Big(\frac{I_D}{V_{sc}}\Big)^3\Big) + \frac{1}{6}\frac{D\cdot\delta(t)}{V_{sc}} \tag{6.15a}$$

$$\frac{1}{V_{sc}}\frac{dI_D}{dt} = P\Big(\frac{I_H}{V_{sc}} - Q\Big(\frac{I_D}{V_{sc}}\Big)^3\Big) - k_a\frac{I_D}{V_{sc}} \tag{6.15b}$$

$$\frac{dI_c}{dt} = 2\cdot k_a I_D + R_{in} - k_e I_c \tag{6.15c}$$

where $Q = I_H/I_D^3$ is the equilibrium constant and P is the rate constant describing the transfer from hexamer to dimer. D is divided by $6\cdot V_{sc}$ since D is the injected amount of monomer insulin while the compartment in which it is injected is modelled using the hexamer concentration, i.e. consisting of 6 monomers. The same argument is used for the transfer of dimer insulin from the dimer SC compartment to the central compartment where the insulin is assumed to be in the monomeric form, hence it is multiplied by 2.

Two-Compartment SC Uptake Model

The two-compartment SC uptake model is a combination of two of the models proposed in [41] in which the rate constant k_e and the volume V_d are estimated from an intravenous experiment and subsequently considered as fixed variables in the SC injection experiment.

The modelling approach of the two-compartment SC uptake model is quite different from the hexamer/dimer model. The delay from injection to absorption is modelled by adding an extra SC compartment and not due to hexamer/dimer equilibration. Furthermore, the degradation of insulin in the SC compartment is also modelled. The two-compartment SC uptake model is illustrated in Figure 6.3.

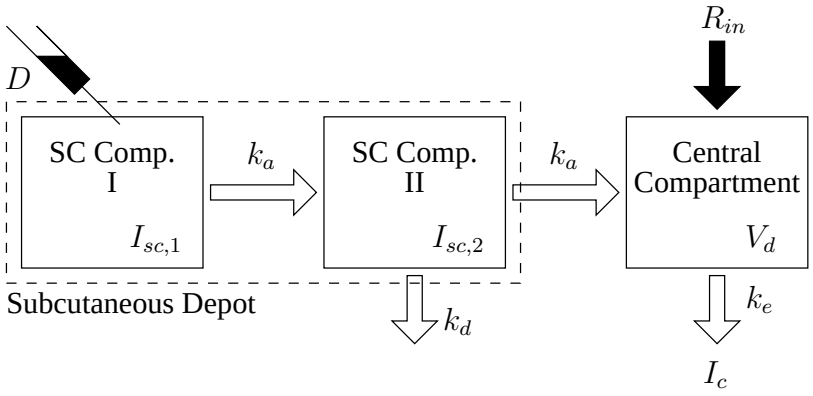

Figure 6.3: Two-compartment SC uptake model.

The SC compartment I in Figure 6.3 can be thought of as the injection site while SC compartment II is the SC tissue from where some of the insulin is degraded while the rest is absorbed into the central compartment.

Assumptions

The assumptions about the two-compartment SC uptake model are summarized below:

`A1:` The degradation of SC insulin is only present in SC compartment II since the degradation is assumed to occur in the SC tissue and not at the injection site.

`A2:` The rate constant describing the transfer from the SC compartment I to II is the same as the rate constant for absorption into the central compartment. This assumption is made to circumvent the estimation of an extra parameter.

Assumption `A1`, `A2`, and `A4` from the single-compartment model also apply to the two-compartment SC uptake model.

Model equations

The differential equations for the two-compartment SC uptake model are:

$$\frac{dI_{sc,1}}{dt} = D \cdot \delta(t) - k_a I_{sc,1} \tag{6.16a}$$

$$\frac{dI_{sc,2}}{dt} = k_a I_{sc,1} - \big(k_a + k_d\big) I_{sc,2} \tag{6.16b}$$

$$\frac{dI_c}{dt} = k_a I_{sc,2} + R_{in} - k_e I_c \tag{6.16c}$$

where $I_{sc,1}$ and $I_{sc,2}$ are the amounts of insulin in SC compartment I and II, respectively. k_d is the rate constant for insulin degradation in SC compartment II. The rest of the parameters are the same as in the single-compartment model.

The system of equations (6.16) are a priori non-identifiable, but identifiability is obtained by fixing the parameter k_d (see Appendix A.3).

6.1.3 Peripheral-Compartment Model

The last PK model to be investigated is the peripheral-compartment model with Michaelis-Menten elimination kinetics. The reason for including a peripheral compartment is to try and model the plasma insulin equilibration with tissue. The Michaelis-Menten kinetics used to describe the elimination from the central compartment is a generally accepted expression for the elimination from the organism, especially when the capacity of the metabolism is exceeded by the therapeutic concentration. The peripheral-compartment model is illustrated in Figure 6.4 and consists of: 1) a central compartment where the IV and SC injected insulin is absorbed and eliminated and 2) a peripheral compartment in equilibrium with the central compartment.

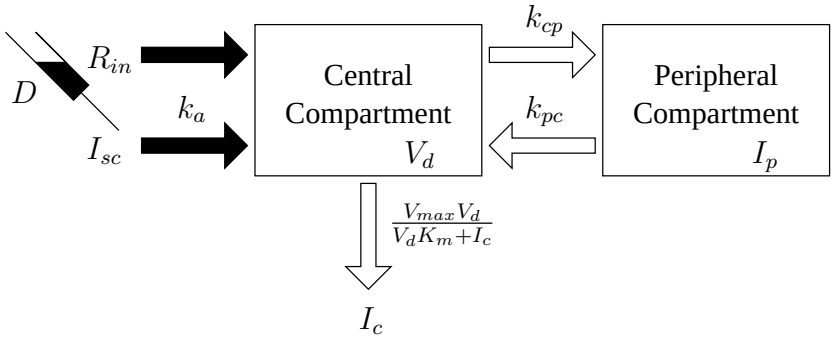

Figure 6.4: Peripheral-compartment model with Michaelis-Menten elimination kinetics.

The parameter K_M is the Michaelis constant. It represents the insulin concentration at which the rate of elimination is half its maximal value V_{max}.

The Michaelis-Menten kinetics used for the elimination of insulin from the central compartment is a mixture between zero- and first-order kinetics and is very similar to the hyperbolic effect model men-

tioned in Section 3.2.1. At low concentrations, the rate of elimination is almost linearly proportional to the insulin concentration C_c in the central compartment while the elimination is almost independent of C_c at high concentrations. Mathematically, this translates into the following equation for the rate of elimination V_{MM} following Michaelis-Menten kinetics:

$$V_{MM} = \frac{V_{max}}{K_M + C_c} C_c$$

When $C_c \ll K_M$, the expression for V_{MM} reduces to $\frac{V_{max}}{K_M} C_c$ while the rate of elimination is equal to the maximal rate of elimination V_{max} in situations where $C_c \gg K_M$.

Assumptions

Assumption `A1`, `A3`, and `A4` mentioned in the section about the single-compartment model also apply to the peripheral-compartment model. Furthermore, no insulin is assumed to be degraded or eliminated from the peripheral compartment. This assumption is made to reduce the number of parameters to be estimated.

Model equations

The three differential equations for SC (I_{sc}), central (I_c) and peripheral insulin (I_p) for the peripheral-compartment model can thereby be written as:

$$\frac{dI_{sc}}{dt} = D \cdot \delta(t) - k_a I_{sc} \tag{6.17a}$$

$$\frac{dI_c}{dt} = k_a I_{sc} - \Big(\frac{V_{max} V_d}{V_d K_m + I_c} + k_{cp}\Big) I_c + k_{pc} I_p + R_{in} \tag{6.17b}$$

$$\frac{dI_p}{dt} = k_{cp} I_c - k_{pc} I_p \tag{6.17c}$$

where the rate constants k_{cp} and k_{pc} describe the transfer between the central and peripheral compartments. The remaining parameters are otherwise the same as those used in the single-compartment model.

6.1.4 Summary of PK Models

The presented PK models are briefly summarized in Table 6.2 to show the differences between them before moving on to the PK/PD models.

Table 6.2: Summary of the PK models for the clamp study.

Model	**Single-Compartment**	**Hexamer/Dimer SC Uptake**
Focus	Plasma insulin	SC distribution and equilibration
States	2	3
Parameters	2	4
Strengths	Simple, few parameters	Different association states of SC insulin
Weaknesses	All SC insulin is absorbed Many simplifying assumptions	SC injected insulin is assumed to be hexameric for both types of insulin
Model	**Two-Comp. SC Uptake**	**Peripheral-Compartment**
Focus	SC distribution and elimination	Tissue equilibration Michaelis-Menten elimination
States	3	3
Parameters	3	6
Strengths	Delay from injection to absorption	Saturable elimination kinetics
Weaknesses	Same rate constant k_a for SC and plasma absorption	No degradation from the peripheral compartment
	Only degradation from SC comp. II	Unmeasurable insulin equilibration with tissue

6.2 PK/PD Models

After having considered the PK models, the insulin concentration is coupled to the effect through PK/PD models. To determine which type of PK/PD model is needed to model the dynamics between insulin and glucose, a phase-plot of GIR vs. the plasma insulin concentration, where data points are connected in chronological order, is plotted in Figure 6.5 for a representative subject from the study.

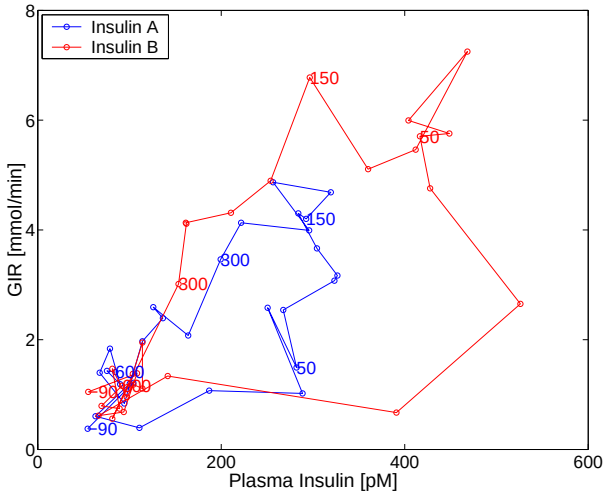

Figure 6.5: Phase-plot of GIR vs. plasma insulin.

A counter-clockwise hysteresis loop is observed in the phase-plot above since there exists two different values of GIR for any plasma insulin concentration depending on the time after the insulin administration. The delay for insulin A is smaller than that for insulin B since the hysteresis loop is smaller for insulin A. Had there been no hysteresis loop, a basic PK/PD model such as the single-compartment model expanded with a direct link model could have been used. Instead, two PK/PD models with different assumptions about the nature of the response are presented in the following. The

single-compartment model is used as the PK part of the following PK/PD models for simplicity but can easily be replaced by any of the PK models in Section 6.1.

6.2.1 Effect-Compartment Model

The effect-compartment model was initially proposed by Sheiner *et al.* in [47] concerning its application to *d*-tubocurarine. The single-compartment model is expanded with a hypothetical effect compartment since the time course of insulin effect does not parallel the time course of drug computed to reside in the central compartment. The effect site can be thought of as the extracellular space where the interaction with the biological receptor system takes place [42]. Modelling the kinetics of the effect site by adding an effect compartment is a simple way to correct non steady-state data to the equivalent of steady-state data so that a concentration-response curve can be discerned, unobscured by a hysteresis loop as seen in Figure 6.5 [46].

The effect-compartment model is shown in Figure 6.6.

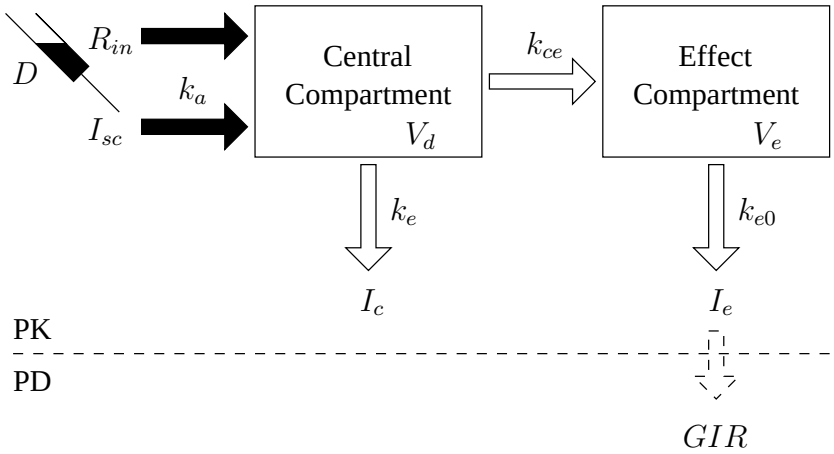

Figure 6.6: Effect-compartment model.

Assumptions

The assumptions from the single-compartment model also apply to the effect-compartment model along with the following three assumptions [17, 26, 42]:

`A1:` It is assumed that the effect compartment receives a negligible mass from the central compartment, thereby not affecting the equations for the insulin in the central compartment.

`A2:` The PD effect of insulin is assumed to be proportional to C_e. Consequently, the time-dependent aspects of the equilibrium between the plasma and effect concentrations are only controlled by the equilibrium constant K_{e0}.

`A3:` Because of the nature of the experimental procedure in the clamp study and since the endogenous production of insulin is ignored, the amount of infused glucose (GIR) needed to maintain euglycemia can be assumed to be equal to the amount of glucose utilized in the body. The GIR can thereby be used as the response to the injected insulin.

Model Equations

The PK model for the effect-compartment model in Figure 6.6 is described by the following differential equations:

$$\frac{dI_{sc}}{dt} = D \cdot \delta(t) - k_a I_{sc} \tag{6.18a}$$

$$\frac{dI_c}{dt} = k_a I_{sc} + R_{in} - k_e I_c \tag{6.18b}$$

$$\frac{dI_e}{dt} = k_{ce} I_c - k_{e0} I_e \tag{6.18c}$$

where the rate constants k_a and k_e are the same as in the single-compartment model described in Section 6.1.1, while k_{ce} and k_{e0} are

the rate constants for the irreversible elimination from the central and effect compartment, respectively.

At steady-state, the concentration in the effect compartment $C_{e,ss}$ is equal to the concentration in the central compartment $C_{c,ss}$. The rate of input will therefore equal that of output, i.e. $k_{ce} \cdot I_c = k_{e0} \cdot I_e$ [17]. This assumption allows for the calculation of the volume V_e for the effect compartment by the following equation [31]:

$$V_d \cdot k_{ce} \cdot C_{c,ss} = V_e \cdot k_{e0} \cdot C_{e,ss} \tag{6.19}$$

The concentration in the effect compartment can then be calculated by dividing I_e with V_e. When doing so, the rate constant for the irreversible elimination from the central compartment to the effect compartment k_{ce} cancels out as shown in Appendix A.4. The following system of equations thereby describes the PK part of the effect-compartment model:

$$\frac{dI_{sc}}{dt} = D \cdot \delta(t) - k_a I_{sc} \tag{6.20a}$$

$$\frac{dI_c}{dt} = k_a I_{sc} + R_{in} - k_e I_c \tag{6.20b}$$

$$\frac{1}{V_e}\frac{dI_e}{dt} = K_{e0}\Big(\frac{I_c}{V_d} - \frac{I_e}{V_e}\Big) \tag{6.20c}$$

where K_{e0} is the equilibrium constant for the passive diffusion between the central and effect compartment. The remaining parameters are otherwise the same as the ones from the single-compartment model.

Since the BG level is clamped, the GIR is used as the response variable to the insulin injection. The PD are therefore modelled by combining the GIR with the insulin concentration in the effect compartment using the sigmoidal E_{max} model presented in Section 3.2.1, i.e.:

$$GIR = \frac{E_{max}}{EC_{50}^{\gamma} + \left(\frac{I_e}{V_e}\right)^{\gamma}} \cdot \left(\frac{I_e}{V_e}\right)^{\gamma} \tag{6.21}$$

where EC_{50} is the insulin concentration producing 50 % of the maximum effect E_{max} while γ is the sigmoidicity/response factor.

Analytic Solution

The analytic solution for the insulin concentration C_c is the same as the one found in the single-compartment model while the analytic solution for the concentration in the effect compartment C_e is derived and shown in Appendix A.4.

6.2.2 Indirect Response Model

The last model in this chapter is the indirect response model where the delay between plasma insulin and BG is assumed to be related to an indirect response mechanism downstream from the insulin receptor. Since insulin stimulates glucose storage and utilization, this model seem intuitively as a physiological more likely description of the PK/PD of the insulin/glucose system than the effect-compartment model.

The PK part of the indirect response model is the same as the single-compartment model. The PD indirect response model is used to describe the rate of change of glucose G which is stimulated by the insulin concentration in the central compartment. The indirect response model is illustrated in Figure 6.7.

Assumptions

The assumptions for the indirect response model besides those of the single-compartment model are mentioned below [21]:

`A1:` The delay between the glucose is injected and later observed in the blood is insignificant compared to the sampling time since it is injected IV.

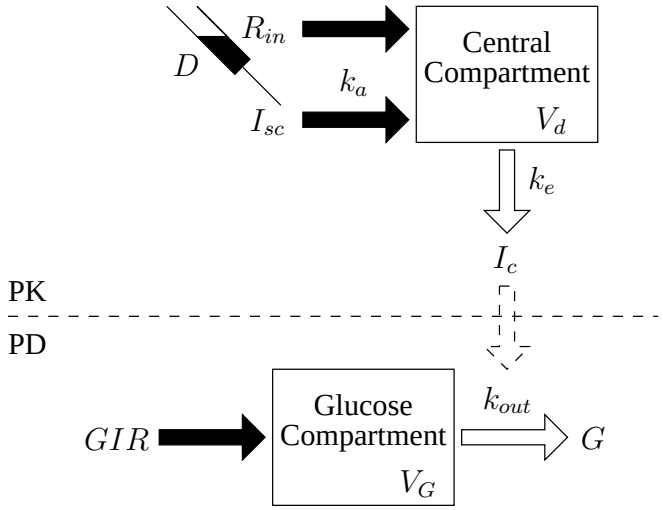

Figure 6.7: Illustration of the indirect response model. The insulin stimulation of glucose utilization is illustrated using a dashed arrow.

`A2:` The GIR is assumed to be mixed instantaneously with the BG. The GIR can thereby be used as a direct input to the differential equation governing the rate of change of glucose.

`A3:` The glucose is eliminated in a first-order manner (k_{out}) plus a stimulating effect of insulin modelled using the Hill response equation.

`A4:` The insulin in the central compartment stimulates the utilization of glucose indirectly. Ideally, it should be the concentration at the receptor but since this is not measured, the central compartment concentration is used instead.

Model equations

The differential equations for the indirect response model are:

$$\frac{dI_{sc}}{dt} = D \cdot \delta(t) - k_a I_{sc} \tag{6.22a}$$

$$\frac{dI_c}{dt} = k_a I_{sc} + R_{in} - k_e I_c \tag{6.22b}$$

$$\frac{dG}{dt} = GIR - k_{out}\Big(1 + \frac{S_{max} \cdot \big(\frac{I_c}{V_d}\big)^{\gamma}}{SC_{50}^{\gamma} + \big(\frac{I_c}{V_d}\big)^{\gamma}}\Big)G \tag{6.22c}$$

where k_{out} is a first-order rate constant for elimination of G and the GIR is used as a zero-order input. The Hill response equation is used to describe the stimulating effect of insulin on the utilization of G where the parameter SC_{50} is the insulin concentration producing 50% of the maximum stimulating effect S_{max}.

6.2.3 Summary of PK/PD Models

The two PK/PD models presented above are different in the sense of how the physiological response to the injected insulin is thought of, i.e.:

- In the effect-compartment model, the PK and PD are coupled using a soft indirect link model. The GIR is assumed to be a direct response to the insulin concentration in a hypothetical effect compartment which is added to the single-compartment model to ensure steady-state conditions.
- In the indirect response model, the response is assumed to be indirect and the PK and PD are coupled using a hard direct link model. The BG concentration is used as the PD response to the insulin concentration in the central compartment.

From a physiological point of view, the injected insulin stimulates the utilization of glucose *indirectly* by activating the transport of glucose into the cells. The indirect response model therefore seem to be the

choice of model for the insulin/glucose system but because of the experimental procedure of the clamp study, the effect-compartment model, where a direct response mechanism is assumed, is more likely to be able to capture the dynamics of the insulin/glucose system since the GIR is used as a measure of the utilized glucose.

Chapter 7

Results from Clamp Models

In this chapter, the results and statistical analysis of the clamp models in Chapter 6 are shown.

The following grey-box models are all implemented in CTSM 2.1 [29] and estimated using ML. The derived PK and PD parameters t_{max}, c_{max}, AUC_0^∞, TR_{max}, R_{max} and GIR_0^∞ are determined from the pure simulation using the grey-box estimates from CTSM.

The PK models from the clamp study are modelled using the insulin concentration in U/L while the PK/PD models are modelled using the insulin concentration in pM to be able to compare with estimates from the literature. The values of the estimated model parameters and derived PK/PD parameters are shown along with the concentration and response profiles of a representative subject, i.e. subject 3 in Table A.1. Furthermore, the models are validated and compared and the residuals are tested whether or not they can be considered to be white noise. Since only one set of data is available for each treatment with insulin A and B for each subject, it has not been possible to cross validate the estimated models on a set of data

which has not been used in the estimation of the model parameters.

After comparing the different PK models, one is chosen as the most suitable. Thereafter, the parameter estimates for all twenty subjects in the study are shown for that particular model. This model is then used as the PK part in the PK/PD model where both the PK and PD parameters are estimated simultaneously. Finally, the two PK/PD models in Section 6.2 are estimated and compared at the end of this chapter.

7.1 PK Models

The four PK models presented in Section 6.1 are estimated, validated, and compared in the following section.

7.1.1 Single-Compartment model

Two different ways of estimating the parameters are presented in this section concerning the single-compartment model.

- A white-box model without system or observation noise where the parameters are estimated using unconstrained NL optimization. The set of algebraic equations for the analytical solution for the single-compartment model are used in the estimation procedure, i.e. equation (6.8) and (6.9).
- Two grey-box models for the single-compartment model with and without the bioavailability factor F. The parameters are estimated using ML and implemented in CTSM 2.1.

Grey-box Model

The LTI state space model for the single-compartment model using the derived differential equation (6.1) in Section 6.1.1, consists of two

continuous time system equations and a discrete time observation equation, i.e.:

$$\begin{aligned}\begin{bmatrix} dI_{sc} \\ dI_c \end{bmatrix} &= \left(\begin{bmatrix} -k_a & 0 \\ k_a F & -k_e \end{bmatrix} \begin{bmatrix} I_{sc} \\ I_c \end{bmatrix} + \begin{bmatrix} 1 & 0 \\ 0 & 1 \end{bmatrix} \begin{bmatrix} D \\ R_{in} \end{bmatrix} \right) dt + \boldsymbol{\sigma}\, dw_t \\ C_I &= \frac{I_c}{V_d} + e_k \end{aligned}$$

where D and R_{in} are input variables, w_t is a standard Wiener process with covariance matrix $\boldsymbol{\sigma}$ with σ_{sc} and σ_c in the diagonal, and $e_k \in N(0, S^2)$ is a white noise process mutually independent of w_t.

The two different types of insulin are injected subcutaneously at $t = 0$. Therefore, the input variable D assumes the value of $0.2 \frac{U}{kgBW\,L}$ at $t = 0$ and zero otherwise. The injection of SC insulin is assumed to last 1 minute and since the insulin concentration is not measured at $t = 1$, a missing observation for plasma insulin is entered into the data files used for estimation. The other input variable in the model is R_{in} which is equal to $0.15 \frac{mU}{kgBW\,L}$ throughout the experiment. Since it is the insulin concentration in the central compartment that is measured, the state I_c is divided by V_d, the apparent volume of distribution of the central compartment, in the observation equation.

Parameter Estimates

Three different estimates of the parameters of the single-compartment model are shown in Table 7.1 for treatment with insulin A and B. The column 'White' refers to the parameter estimation in the deterministic algebraic equations (6.8) and (6.9) implemented in *Matlab*, using unconstrained NL optimization with the estimates from the grey-box model used as the initial guesses. The next two columns, 'Grey' and 'Grey(F=1)', contain the grey-box parameter estimates of the single-compartment model with the parameter F estimated using ML and where it is fixed at the value 1, respectively.

Table 7.1: Single-compartment model PK parameter estimates for insulin A and B.

		Insulin A				Insulin B			
		White	Grey	Grey (F=1)		White	Grey	Grey (F=1)	
Parameter	Unit	$\hat{\theta}$	$\hat{\theta}$	$\hat{\theta}$	Std. dev.	$\hat{\theta}$	$\hat{\theta}$	$\hat{\theta}$	Std. dev.
$I_{c,0}$	[U]	6.4490	2.3709	2.4154	0.8442	0.3266	0.3266	0.3676	0.5315
k_a	[min^{-1}]	0.0143	0.0107	0.0108	0.0040	0.0091	0.0090	0.0073	0.0086
k_e	[min^{-1}]	0.0053	0.0079	0.0078	0.0026	0.0320	0.0331	0.0394	0.0069
F	[-]	2.0433	0.9898			0.6728	0.6766		
V_d	[L]	457.6149	174.5839	177.5967	59.5071	32.5001	31.5793	34.0248	10.4146
σ_{sc}	[-]		0.0000	0.0000	0.0016		0.0000	0.0000	0.0001
σ_c	[-]		0.0000	0.0000	0.0034		0.0000	0.0000	0.0066
S^2	[-]		0.0000	0.0000	0.0000		0.0000	0.0000	0.0000
t_{max}	[min]	105.00	105.00	105.00		55.00	50.00	50.00	
c_{max}	[U/L]	0.05	0.05	0.05		0.07	0.07	0.07	
AUC_0^∞	[U/L min]	18.03	18.05	18.05		18.47	18.30	18.30	

The parameter estimates of the three different models in Table 7.1 are very different but they describe the observed insulin concentration-time profiles equally well. It is clearly seen that there does not exist one true set of parameters in the three models. In Appendix A.2, it is shown that the parameters in the single-compartment model are *a priori* non-identifiable when the parameter F is not fixed and the identifiability of the white-box model is discussed in Section 6.1.1. In the following, only the the grey-box estimates with $F = 1$ are considered.

The limiting rate constant in the model is k_a for insulin B since $k_a < k_e$ while the two rate constants are more equal for insulin A. When comparing the rate constants for absorption and elimination for the two types of insulin, k_a seems to be the same while k_e is about twice as large for insulin B than A. The change in the primary structure of insulin B compared to insulin A[1] seems to alter the kinetics for elimination rather than that of absorption. This observation does not fit very well to the fact that it is k_a which is attempted enlarged in insulin B to speed up the absorption while no attempt is made to alter k_e. This phenomena is referred to as the 'flip-flop' effect and is further discussed in Chapter 10.

The significantly different V_d for the two types of insulin can partially be explained by the two types of insulin occupy a different volume in the body. The large value of V_d for insulin A is probably due to some of the insulin is bound in the tissue resulting in less insulin in the plasma. The volume is thereby over-estimated since the model does not include a compartment for bound insulin or a bioavailability factor F that compensates for non-available insulin since F was eliminated from the model to make it *a priori* identifiable.

The system noise (σ_{SC}, σ_c) and measurement error (S^2) in the model are all estimated to zero. This gives an indication that the measured data does not deviate from the model approximations. Furthermore, the correlation between the noise parameters is high since the data

[1]The primary structure of the insulin molecule is the amino acid sequence.

probably is not persistently excited enough and the model is linear which makes it difficult for CTSM to determine where to add the noise. The noise parameters are the only parameters in the model which are not significantly different from zero on a 95 % confidence level.

Statistical Analysis

A way to distinguish between the two grey-box models, with and without F, is by using the likelihood ratio test (LRT) (see Section 4.7.1). The test score for the LRT between the single-compartment grey-box model with and without the parameter F for insulin B is:

$$\begin{aligned} -2\log\Lambda &= 2\big(-\log\mathcal{L}_0 - (-\log\mathcal{L}_1)\big) \\ &= 2\big(-113.97 - 1.40\cdot 10^{-5} - (-114.60 - 2.34\cdot 10^{-4})\big) \\ &= 1.2696 < \chi^2(1)_{0.95} = 3.84 \end{aligned}$$

which is why the hypothesis $H_0 : \boldsymbol{\theta} \in \mathcal{M}_0$ cannot be rejected since the single-compartment model without the parameter F is not significantly worse than the model with F. The hypothesis is neither rejected for insulin A since the LRT score is $-2\log\Lambda = -0.0097$. Therefore, the grey-box model without the bioavailability factor F is the only model considered in the model validation.

Model Validation

The 1-step prediction and pure simulation are plotted along with the observed plasma insulin concentration for both types of insulin in Figure 7.1(a). The residuals are shown in Figure 7.1(b) along with the ACF in Figure 7.1(c) and PACF in Figure 7.1(d).

The estimated noise parameters in the system equations (σ_{SC} and σ_c) are estimated to zero as mentioned previously, which is why the 1-step prediction and the pure simulation are identical in Figure 7.1(a).

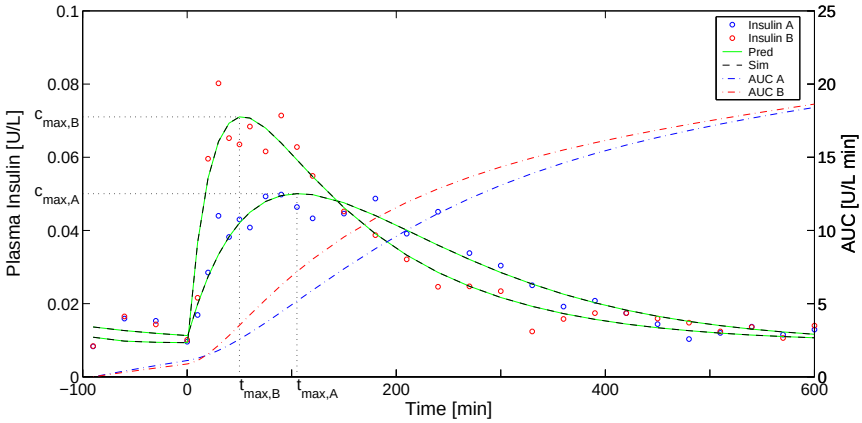

(a) Insulin concentration-time profiles

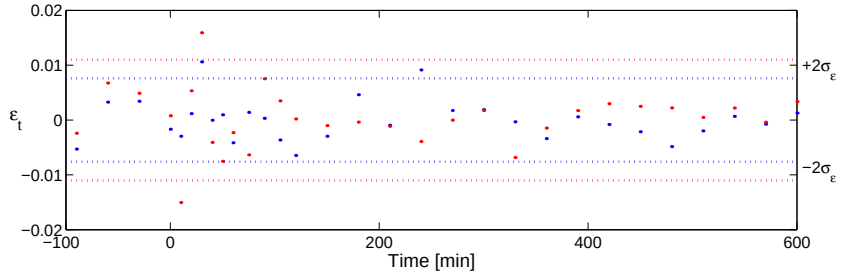

(b) Residuals

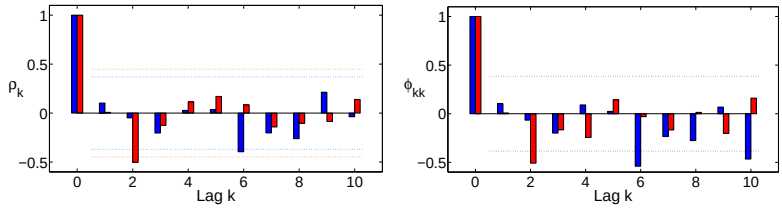

(c) ACF **(d)** PACF

Figure 7.1: Insulin concentration-time profiles, residuals, ACF, and PACF for insulin A (Blue) and insulin B (Red).

From the concentration-time profile of the two types of insulin, it is seen that k_a and k_e are more alike for treatment with insulin A than treatment with insulin B since the profile of insulin A is more 'bell-shaped' than that of insulin B.

After a visual inspection, it seems like the 1-step prediction and simulation capture the PK of the system quite well with only few exceptions. In the insulin residual plot (see Figure 7.1(b)), it is seen that the residuals close to c_{max} are outside the approximative 95 % confidence interval plotted as $\pm 2\sigma_\varepsilon$. All the observed insulin concentrations close to c_{max} are somewhat lower than the 1-step predicted/simulated. This could be because the insulin crystalizes in the drawn blood samples taken at high insulin concentrations. The measured insulin concentrations close to c_{max} are therefore perhaps a bit lower than the actual plasma concentration.

The residuals are further tested by plotting ACF and PACF with an approximative 95 % confidence interval in Figure 7.1(c) and Figure 7.1(d). Lag(k) is significant for $k = 2$ for insulin A and $k = 6, 10$ for insulin B but the residuals are otherwise close to being white noise.

Derived PK Parameters

The three derived PK parameters t_{max}, c_{max}, and AUC are also plotted in Figure 7.1(a). The time to maximum insulin concentration t_{max} for insulin B is almost half of that of insulin A while the maximum insulin concentration c_{max} is about 40 % larger for insulin B than insulin A. The AUC is not very different for the two types of insulin and can therefore not be used to assess the difference in the treatment with insulin A and B. By comparing the three derived PK parameters it can be concluded that insulin B is a faster and shorter acting insulin compared to that of insulin A, while the amount of insulin absorbed throughout the study is almost the same for both types of insulin.

7.1.2 SC Uptake PK Models

The single-compartment model is next expanded with compartments for the SC depot to investigate the different absorption characteristics of the two types of insulin and to see whether this expansion results in physiological more reasonable parameter estimates. The grey-box models of the hexamer/dimer and two-compartment SC uptake models are presented along with a short description of the model parameters (See Section 6.1.2 for a more detailed description). The results from the estimation are shown along with plots of the 1-step prediction and pure simulation of the model and the ability of the two models to estimate the time course of SC insulin is compared.

Grey-box Models

The NL state space model for the hexamer/dimer SC uptake model described by the differential equations in (6.15) in Section 6.1.2, consisting of three continuous time system equations and a discrete time observation equation, is shown below:

$$\begin{pmatrix} dC_H \\ dC_D \\ dI_c \end{pmatrix} = \begin{pmatrix} -P\Big(C_H - Q \cdot C_D^3\Big) + D/(6 \cdot V_{sc}) \\ P\Big(C_H - Q \cdot C_D^3\Big) - k_a C_D \\ 2 \cdot V_{sc} \cdot k_a \cdot C_D + R_{in} - k_e I_c \end{pmatrix} dt + \boldsymbol{\sigma}\, dw_t$$

$$C_I = \frac{I_c}{V_d} + e_k$$

where $C_H = I_H/V_{sc}$ and $C_D = I_D/V_{sc}$ represent the hexamer and dimer concentrations in the SC compartments, respectively, while the state variable I_c describes the amount of insulin in the central compartment as in the single-compartment model. The volume of the SC compartment is assumed to be 0.1 mL and fixed at that value in the estimation of model parameters. $Q = C_H/C_D^3$ is the equilibrium constant between hexamer and dimer and P is the rate constant describing the transfer from hexamer to dimer. The rest of

the parameters are otherwise the same as in the grey-box model for the single-compartment model.

The LTI state space model for the two-compartment SC uptake model using the deterministic differential equations in (6.16), consisting of three continuous time system equations and a discrete time observation equation, can be written as:

$$\begin{aligned}
\begin{bmatrix} dI_{sc,1} \\ dI_{sc,2} \\ dI_c \end{bmatrix} &= \left(\begin{bmatrix} -k_a & 0 & 0 \\ k_a & -(k_a + k_d) & 0 \\ 0 & k_a & -k_e \end{bmatrix} \begin{bmatrix} I_{sc,1} \\ I_{sc,2} \\ I_c \end{bmatrix} + \begin{bmatrix} 1 & 0 \\ 0 & 0 \\ 0 & 1 \end{bmatrix} \begin{bmatrix} D \\ R_{in} \end{bmatrix} \right) dt \\
&\quad + \boldsymbol{\sigma}\, dw_t \\
C_I &= \frac{I_c}{V_d} + e_k
\end{aligned}$$

where the rate constant k_a describing the transfer from SC compartment I to II is assumed to be the same as the rate constant for absorption to the central compartment. The rate constant for degradation k_d in SC compartment II is fixed at $0.015\,\mathrm{min}^{-1}$ for the model to be *a priori* identifiable (see Appendix A.3). The value of $k_d = 0.015\,\mathrm{min}^{-1}$ is chosen since it gives the best estimation results.

The plasma insulin concentration is measured in both SC uptake models which is why the state I_c is divided by V_d in the observation equations.

Parameter Estimates

The obtained estimates from the two grey-box models, the hexamer/dimer (Hex/Dim) and two-compartment (Two-Comp.) SC uptake models, are shown in Table 7.2.

The estimated volume V_d is physiological more likely than the ones obtained from the single-compartment model. The differences in the estimated volumes for treatment with insulin A and B are much larger for the hexamer/dimer model than the two-compartment SC

Table 7.2: PK model parameter estimates for the SC uptake models for treatment with insulin A and B.

		Insulin A				Insulin B			
		Hex/Dim		Two-Comp.		Hex/Dim		Two-Comp.	
Parameter	Unit	$\hat{\theta}$	Std. dev.	$\hat{\theta}$	Std. dev.	$\hat{\theta}$	Std. dev.	$\hat{\theta}$	Std. dev.
$I_{c,0}$	[U]	0.2459	0.1031	0.0244	0.0202	0.0664	0.0470	0.2181	0.0181
k_a	[min^{-1}]	0.0475	0.0098	0.0077	0.0008	0.0292	0.0150	0.0125	0.0007
k_e	[min^{-1}]	0.0269	0.0053	0.2648	0.1955	0.0896	0.0338	0.3244	0.1777
P	[min^{-1}]	0.2900	0.9500			0.0292	0.0150		
Q	[mL^2U^{-2}]	0.9601	0.5496			0.0292	0.0467		
V_d	[L]	27.0070	5.5457	2.8261	2.1610	7.9391	3.0453	2.5969	1.4512
$\sigma_{sc,1}$	[-]			0.2297	0.0629			0.0000	0.0003
$\sigma_{sc,2}$	[-]			0.0000	0.0000			0.0000	0.0000
σ_H	[-]	0.0000	0.0000			0.0549	0.1155		
σ_D	[-]	0.1162	0.0492			0.0000	0.0000		
σ_c	[-]	0.0000	0.0001	0.0026	0.0356	0.0000	0.0000	0.0109	0.0035
S^2	[-]	0.0000	0.0000	0.0000	0.0000	0.0000	0.0000	0.0000	0.0000
t_{max}	[min]	105.00		75.00		40.00		60.00	
c_{max}	[U/L]	0.05		0.05		0.07		0.07	
AUC_0^∞	[U/L min]	18.58		18.05		19.19		18.61	

uptake model. This is not to say that the estimates of the hexamer/dimer model are unreliable since the volume of distribution of the two types of insulin are not necessarily the same.

The limiting rate constant is k_a for insulin B in both SC uptake models as in the single-compartment model. For insulin A, the limiting rate constant is k_e for the hexamer/dimer model and k_a for the two-compartment model.

Unlike the single-compartment model, the parameters for the system noise in the SC equations (σ_H, σ_D, and $\sigma_{sc,1}$) are not estimated to zero in the two SC models. However, the standard deviations of the system noise parameters are quite large why most of them are not significantly different from zero on a 95 % confidence level.

There is quite a difference between the derived parameters for the two models. The difference between the time to maximum insulin concentration is 30 min. for insulin A and 20 min. for insulin B while the parameters c_{max} and AUC_0^∞ are almost the same for the two models.

Statistical Analysis

The two SC models are compared by means of the BIC to reveal possible over-fitting. The LRT cannot be used since the two models are not nested. The columns in Table 7.3 from left to right are the model, the number of model parameters p, the value of the objective function $\mathcal{F}$, penalty function $\mathcal{P}$, log-likelihood function $\log L$, and the BIC.

Table 7.3: Test for model structure for hexamer/dimer and two-compartment SC uptake models.

Model	p	$\mathcal{F}$	$\mathcal{P}$	$\log L(\boldsymbol{\theta}, \mathcal{Y}_N)$	BIC
Hexamer/dimer					
Insulin A	10	−125.0527	0.0026	125.0553	−216.0986
Insulin B	10	−115.1348	0.0001	115.1349	−196.2578
Two-compartment					
Insulin A	8	−122.1274	0.0001	122.1275	−217.0454
Insulin B	8	−114.7022	0.0001	114.7023	−202.1950

The BIC criteria is minimized for the two-compartment SC uptake model for both types of insulin. The value of the log-likelihood function is approximately the same for the two models but because of the more parsimonious two-compartment model, it is preferred in preference to the hexamer/dimer model.

Model Validation

The estimated insulin concentration and the insulin residuals for the two SC uptake models are shown in Figure 7.2 and Figure 7.3.

The simulated time series of the plasma insulin are shown in Figure 7.2(a) and Figure 7.3(a) for the hexamer/dimer and two-compartment SC uptake model, respectively, and are very similar to the concentration-time profiles of plasma insulin predicted by the single-compartment model.

The SC insulin calculated to reside in the SC compartments clearly shows the different PK of the two types of insulin. Since the injected insulin is assumed to be hexameric for both types of insulin in the hexamer/dimer model, the steep ascent in hexameric insulin at $t = 0$ min. is the same. Since the dimeric form of insulin is stabilized in insulin B, the equilibrium between the hexamer and dimer is shifted much more rapidly towards the dimer and thereby absorbed faster into the plasma for insulin B than A in the hexamer/dimer

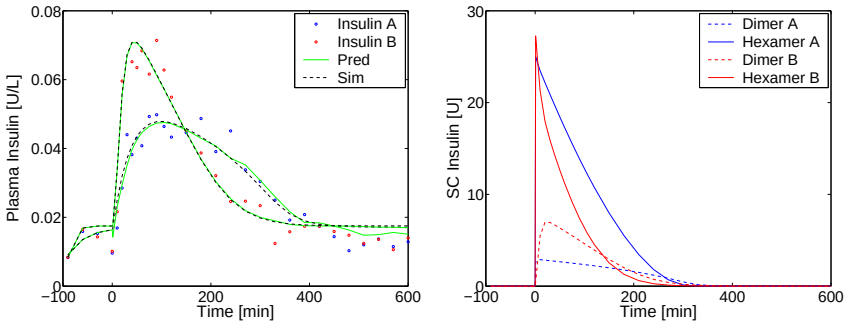

(a) Plasma Insulin

(b) SC Insulin

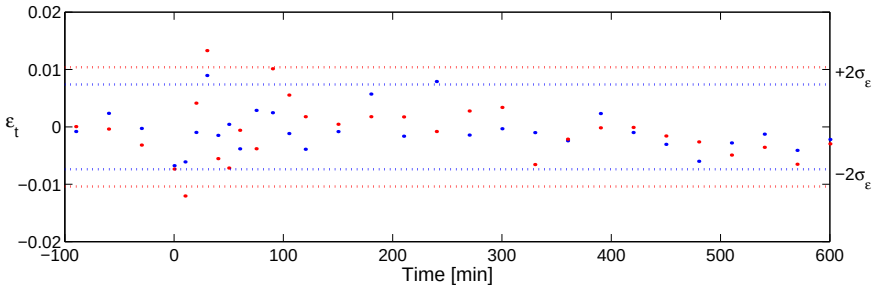

(c) Residuals

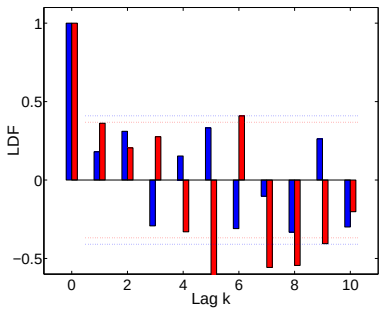

(d) LDF

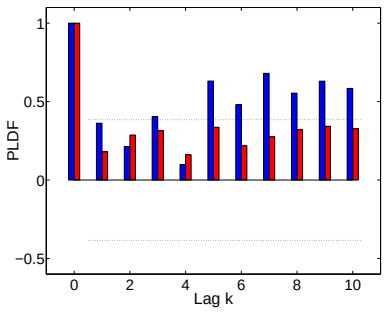

(e) PLDF

Figure 7.2: Results from hexamer/dimer SC uptake model for insulin A (Blue) and insulin B (Red).

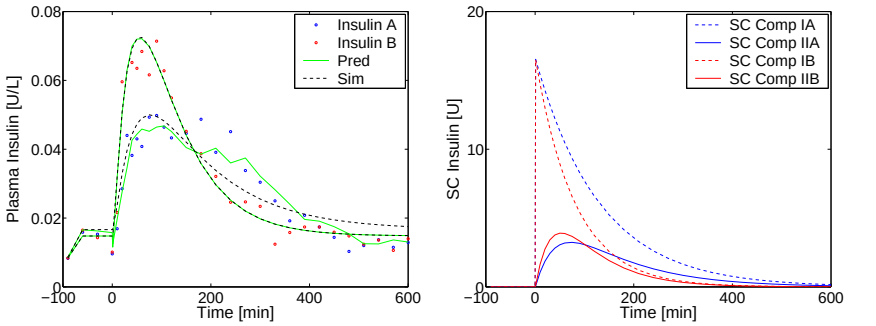

(a) Plasma Insulin

(b) SC Insulin

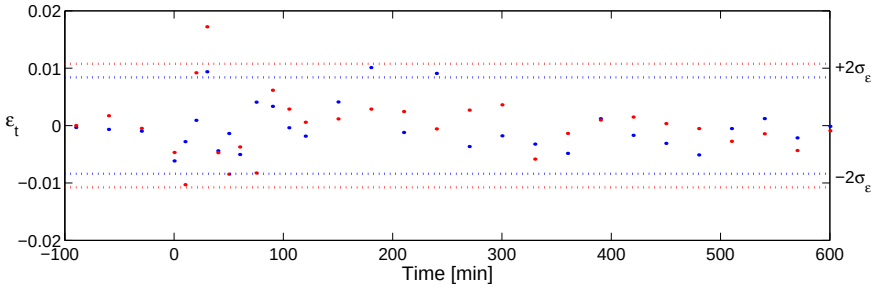

(c) Residuals

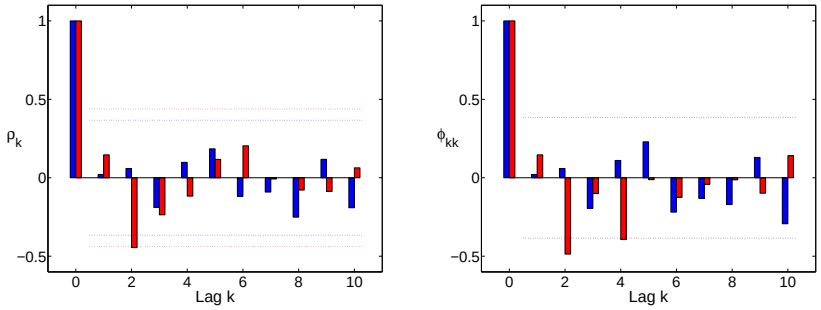

(d) ACF

(e) PACF

Figure 7.3: Results from two-compartment SC uptake model for insulin A (Blue) and insulin B (Red).

model. The same characteristics for insulin B are observed in the two-compartment model where the SC insulin is shifted faster towards SC Compartment II than that of insulin A.

By looking at the lag-dependency function (LDF) and partial lag-dependency function (PLDF), the residuals are clearly not white noise for the hexamer/dimer model while those of the two-compartment SC uptake model more or less can be considered as white noise with only lag k=2 being significant for insulin B.

7.1.3 Peripheral-Compartment Model

Finally, the single-compartment is expanded with a peripheral compartment and the elimination from the central compartment is described by Michaelis-Menten kinetics.

Grey-box Model

The NL state space model for the peripheral-compartment model with Michaelis-Menten elimination kinetics, consisting of three continuous time system equations and a discrete time observation equation, is shown below:

$$\begin{pmatrix} dI_{sc} \\ dI_c \\ dI_p \end{pmatrix} = \begin{pmatrix} -k_a I_{sc} + D \\ k_a I_{sc} - \left(\frac{V_{max} V_d}{V_d K_M + I_c} + k_{cp}\right) I_c + k_{pc} I_p + R_{in} \\ k_{cp} I_c - k_{pc} I_p \end{pmatrix} dt + \boldsymbol{\sigma}\, dw_t$$

$$C_I = \frac{I_c}{V_d} + e_k$$

where I_{sc}, I_c, and I_p are the states representing the SC, central, and peripheral compartment, respectively. The rate constants k_{cp} and k_{pc} describe the equilibrium between the central and peripheral compartment while V_{max} and K_M are the Michaelis-Menten parameters.

Parameter Estimates

The estimates of the parameters in the grey-box state space model for the peripheral-compartment model are shown in Table 7.4 along with the standard deviations and the corresponding t-score, and the probability for insignificance.

The system noise is yet again estimated to zero in the three system equations while the derived PK parameters are close to the ones found in the three previous models. The standard deviation of the initial amount of insulin in the unobservable peripheral compartment is notably large compared to the estimated value of $I_{p,0}$ for insulin B.

The apparent volume of distribution for insulin A is reduced with approximately 160 L down to 20 L compared with the single-compartment model and seems much more reasonable from a physiological point of view. The reduction in the apparent volume of distribution of insulin A might stem from the added peripheral compartment where the binding of insulin in the tissue is accounted for. The parameter V_d for insulin B is on the other hand slightly larger than the one estimated in the single-compartment model but with a very large standard deviation.

The difference in k_a for the two types of insulin is in agreement with the intended enhancement of insulin absorption for insulin B. The estimated value for k_a is approximately four times as large for insulin B than A, i.e. $k_a = 0.0023$ for insulin A and $k_a = 0.0094$ for insulin B.

The Michaelis-Menten parameter K_M for insulin A is estimated to $0.0110\,U/L$ which is equal to the insulin concentration at which the rate of elimination is half its maximal value $V_{max} = 0.0025\,U/(L \cdot min)$. The estimated Michaelis-Menten parameters for insulin B are about ten times as large as those for insulin A and with large standard deviations which suggests that the uncertainty of the estimates is quite high.

Table 7.4: Parameter estimates for the peripheral-compartment model for treatment with insulin A and B.

		Insulin A				Insulin B			
Parameter	Unit	$\hat{\theta}$	Std. dev.	t-score	p(> |t|)	$\hat{\theta}$	Std. dev.	t-score	p(> |t|)
$I_{c,0}$	[U]	0.1599	0.1307	1.2228	0.2374	0.5007	0.3676	1.3621	0.1902
$I_{p,0}$	[U]	1.9742	0.5507	3.5849	0.0024	4.1754	15.6940	0.2660	0.7933
k_a	[min^{-1}]	0.0023	0.0014	1.7001	0.1067	0.0094	0.0047	1.9977	0.0616
k_{pc}	[min^{-1}]	0.0168	0.0082	2.0552	0.0552	0.0018	0.0089	0.2077	0.8378
V_d	[L]	19.7060	13.8560	1.4221	0.1724	48.6530	29.4390	1.6527	0.1161
V_{max}	[U (L min)$^{-1}$]	0.0025	0.0008	3.1604	0.0058	0.0274	0.0222	1.2354	0.2328
K_M	[U/L]	0.0110	0.0105	1.0474	0.3089	0.9563	0.6095	1.5690	0.1344
k_{cp}	[min^{-1}]	0.0152	0.0086	1.7711	0.0939	0.0061	0.0058	1.0575	0.3044
σ_{sc}	[-]	0.0000	0.0000	0.1315	0.8968	0.0000	0.0000	0.0039	0.9970
σ_c	[-]	0.0000	0.0000	0.0826	0.9351	0.0000	0.0000	0.0084	0.9934
σ_p	[-]	0.0000	0.0000	0.0631	0.9504	0.0000	0.0000	0.0038	0.9970
S_I^2	[-]	0.0000	0.0000	3.7824	0.0016	0.0000	0.0000	3.5003	0.0029
t_{max}	[min]	120.00				60.00			
c_{max}	[U/L]	0.05				0.07			
AUC_0^∞	[U/L min]	18.09				18.47			

Model Validation

The results and the plasma insulin residuals for the peripheral-compartment model are plotted in Figure 7.4.

The model captures the initial rise and decline at $t < 0$ for insulin A but not for insulin B. Furthermore, the simulated plasma insulin concentration of insulin B is below that of insulin A for $t \geq 500$ min. which is in agreement with the observed time series of insulin.

The estimated time series of peripheral insulin in Figure 7.4(b) shows an initial decline for both types of insulin followed by a more distinct rise for insulin B than A. The very high level of peripheral insulin for insulin B compared to that of insulin A is due to the large uncertainty of the estimated initial amount of insulin in the peripheral compartment $I_{p,0}$ for insulin B.

The residuals seem reasonable from a visual point of view and can almost be assumed to be white noise when looking at LDF and PLDF.

7.1.4 Comparison of PK Models

Each of the four PK models add different insights to the understanding of the PK of insulin A and B. Unfortunately, the available data is not informative enough to combine them all into one big model. The four proposed PK models are compared by means of the BIC to determine which one of the models should be used as the PK model in the following PK/PD models. The BIC for the four models are shown in Table 7.5.

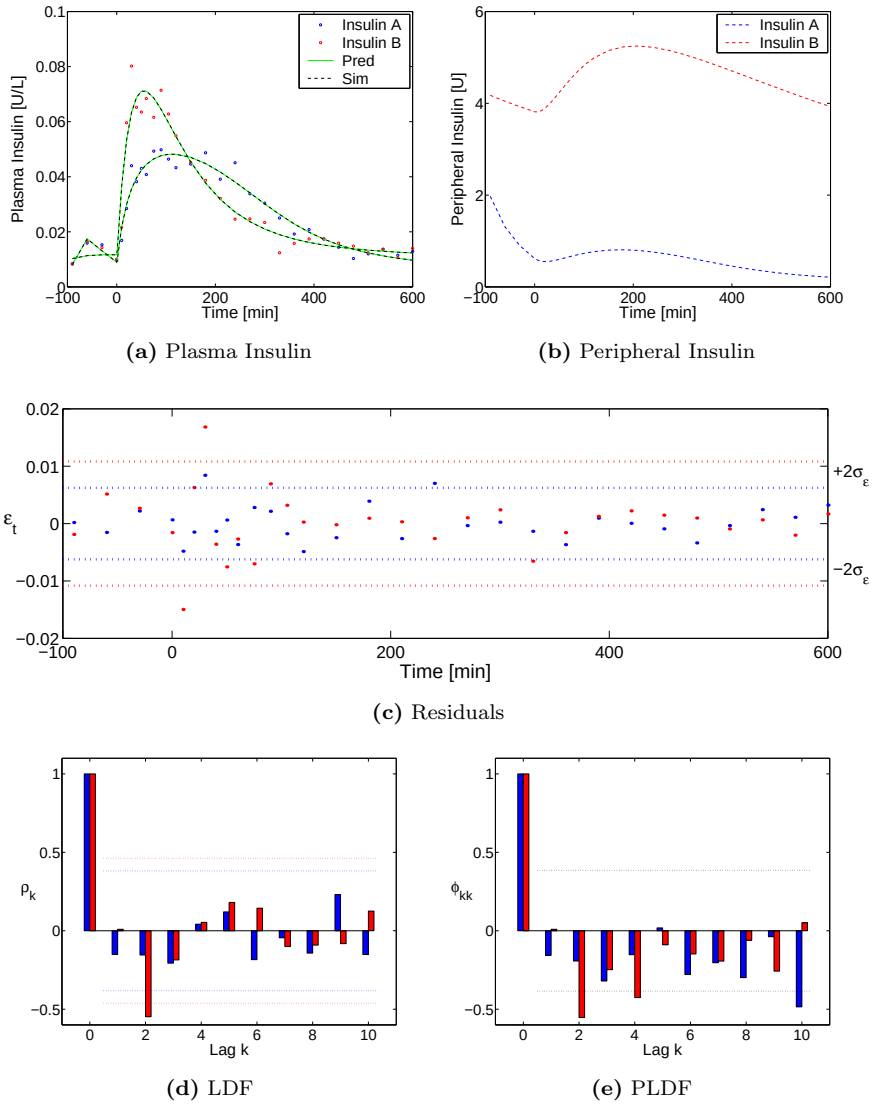

(a) Plasma Insulin **(b)** Peripheral Insulin

(c) Residuals

(d) LDF **(e)** PLDF

Figure 7.4: Insulin concentration-time profiles, residuals, LDF, and PLDF for insulin A (Blue) and insulin B (Red).

Table 7.5: Test for model structure for PK models.

Model	p	$\log L(\boldsymbol{\theta}, \mathcal{Y}_N)$	BIC
Single-Compartment			
Insulin A	7	125.1088	−226.4091
Insulin B	7	113.9663	−204.1243
Hex/Dim SC Uptake			
Insulin A	10	125.0553	−216.0986
Insulin B	10	115.1349	−196.2578
Two-Comp. SC Uptake			
Insulin A	8	122.1275	−217.0454
Insulin B	8	114.7023	−202.1950
Peripheral-Compartment			
Insulin A	12	131.0513	−221.2882
Insulin B	12	114.5537	−188.2929

The choice of model is clearly the single-compartment model using the BIC since it is minimized for both types of insulin. The value of the log-likelihood functions are close to being the same for the three models. The single-compartment is therefore preferred because of its fewer parameters.

The single-compartment representation is the simplest possible model for the PK of insulin. It is a very simplified but adequate description of the insulin in the plasma but the estimated parameters are somewhat unrealistic from a physiological point of view. However, with sampling intervals larger than 10 min., the model seems to capture the relevant characteristics of the PK of insulin considering the rather parsimonious model.

The hexamer/dimer SC uptake model stands out as the physiologically most likely description of the SC insulin absorption kinetics that enables prediction of various insulin preparations. Despite the advantages of the model, the use of three more parameters compared to the single-compartment model does not increase the value of the

log-likelihood function considerably. Furthermore, the model needs to be expanded with a monomer compartment if monomer stabilized insulin is to be investigated since the monomer has a greater affinity for binding to the tissue which will complicate the system dramatically.

The assumption in the two-compartment SC uptake model about the rate constant for the transfer from the SC compartment I to II is the same as the absorption to the central compartment cannot be validated from the experimental data. The assumption about the degradation of insulin only is present at SC compartment II and fixed at a particular value can neither be validated using the measured plasma insulin. The two-compartment SC uptake model is therefore discarded since there are too many assumptions that cannot be validated and the fit between the observed and simulated plasma insulin is not significantly better than the single-compartment model.

The peripheral-compartment model with Michaelis-Menten kinetics is a widely accepted description of drug elimination from the plasma. The peripheral-compartment model captures both the initial rise and decline of insulin A and the estimated values of the apparent volume of distribution are reasonable. Furthermore, the rate constant for absorption is four times as large for insulin B than A which is in agreement with the intended enhancement of the absorption kinetics for insulin B. The drawback of the model is the rather high uncertainty of the estimated parameters and a high degree of correlation in the correlation matrix which is why this model is not chosen for the following PK/PD models.

The PK models presented in this chapter describe the time course of plasma insulin equally well. Since the value of BIC is minimized for the single-compartment model, it is chosen to be the most suitable PK model to use in the following PK/PD models.

To be able to investigate and validate a physiological more likely model for the SC absorption, distribution, and elimination of insulin, it is necessary to obtain data from other insulin studies using several

different doses of both unlabelled and labelled insulin.

7.1.5 Parameter Estimates for All Twenty Subjects

The single-compartment model with $F = 1$ is used in the following since it is structural identifiable, the null hypothesis of the LRT was accepted and the value of the log-likelihood function was not significantly worse than the three model expansions when using the BIC. The estimated parameters in the single-compartment model with $F = 1$ for all twenty subjects are shown in Table 7.6 on the following page along with the sample mean and standard deviation for each parameter.

The value of the penalty function is insignificant compared to the value of the objective function for all the subjects which is an indication that the parameter limits in the estimation procedure are reasonable. Furthermore, the values of the normalized derivatives of the objective function $\mathcal{F}$ with respect to the particular parameters are all close to zero which suggests that the solution found is the true optimum.

The discrepancy between the estimated apparent volume of distribution V_d for the two types of insulin in the same subject and for the same type of insulin in the twenty subjects is rather large and might seem physiological unlikely at first hand. If the individual variability among the twenty subjects in the study are taken into account, the difference between V_d for the twenty subjects seems more reasonable. The correlation between the estimated apparent volume of distribution V_d and three anthropometric measurements (height, body weight (BW), and body mass index (BMI) in Table A.1) are estimated to see if these measurements can account for the physiological variability of V_d among the twenty subjects. The correlation matrix is shown in Table 7.7.

Table 7.6: Single-compartment model PK parameter estimates for subject 1-20.

	Insulin A							Insulin B						
Subject	$I_{c,0}$ [U/L]	k_a [min^{-1}]	k_e [min^{-1}]	V_d [L]	σ_{SC}	σ_c	S^2 $\cdot 10^4$	$I_{c,0}$ [U/L]	k_a [min^{-1}]	k_e [min^{-1}]	V_d [L]	σ_{SC}	σ_c	S^2 $\cdot 10^4$
1	0.6477	0.0054	0.0201	52.4262	0.0	0.0000	0.5	0.3524	0.0075	0.0422	22.0159	0.0000	0.0000	0.4
2	0.4332	0.0031	0.0161	52.8284	0.0	0.0453	0.0	0.3687	0.0054	0.0234	50.0070	0.0000	0.0560	0.0
3	2.4154	0.0108	0.0078	177.5967	0.0	0.0000	0.1	0.3676	0.0073	0.0394	34.0248	0.0000	0.0000	0.3
4	4.0766	0.0101	0.0054	241.9810	0.0	0.0000	0.2	0.6079	0.0087	0.0210	58.9601	0.0000	0.0000	0.2
5	3.8966	0.0130	0.0055	282.2412	0.0	0.0000	0.1	0.2947	0.0091	0.0623	24.5001	0.0000	0.0000	0.3
6	0.9362	0.0064	0.0186	93.6259	0.0	0.0000	0.1	1.4805	0.0228	0.0141	128.7584	0.0568	0.0000	0.2
7	1.9710	0.0074	0.0075	170.8192	0.0	0.0000	0.1	0.5969	0.0113	0.0308	44.9651	0.0788	0.0000	0.3
8	2.0685	0.0082	0.0079	158.3835	0.0	0.0000	0.3	0.8852	0.0138	0.0138	100.9721	0.0000	0.0000	0.4
9	2.0706	0.0102	0.0076	151.6026	0.0	0.0000	0.2	1.0664	0.0086	0.0246	48.5374	0.0000	0.0000	0.5
10	1.9052	0.0101	0.0094	145.5388	0.0	0.0000	0.2	0.6878	0.0177	0.0178	76.3576	0.0000	0.0000	0.4
11	0.8375	0.0072	0.0253	45.8148	0.0	0.0000	0.2	0.1825	0.0103	0.0421	31.6677	0.0000	0.0000	0.5
12	1.5746	0.0097	0.0086	152.2096	0.0	0.0000	0.1	0.4417	0.0100	0.0284	53.6280	0.0000	0.0000	0.1
13	5.9034	0.0062	0.0048	247.4544	0.0	0.0000	0.2	0.8733	0.0062	0.0233	64.0119	0.0000	0.0000	0.3
14	0.6818	0.0058	0.0120	104.1347	0.0	0.0732	0.0	0.0	0.0166	0.0170	83.0035	0.0000	0.0000	0.4
15	1.8281	0.0126	0.0106	111.2920	0.0	0.0000	0.3	0.7347	0.0161	0.0164	84.1414	0.0229	0.0000	0.2
16	0.7016	0.0085	0.0224	52.0394	0.0	0.0000	0.3	0.5213	0.0234	0.0234	65.8626	0.0377	0.0163	0.4
17	2.0184	0.0093	0.0082	145.4131	0.0	0.0000	0.1	0.5009	0.0136	0.0228	54.5802	0.0000	0.0000	0.4
18	1.5337	0.0118	0.0093	143.1262	0.0	0.0000	0.1	0.7365	0.0212	0.0200	70.6127	0.0000	0.0000	0.2
19	1.1603	0.0054	0.0112	120.8677	0.0	0.0884	0.0	1.4036	0.0114	0.0119	109.3328	0.0000	0.0000	0.3
20	0.7821	0.0082	0.0080	128.3665	0.0	0.0000	0.6	0.4103	0.0092	0.0310	32.8359	0.0000	0.0000	0.3
$\bar{\theta}$	1.8721	0.0085	0.0113	138.8881	0.0	0.0103	0.2	0.6256	0.0125	0.0263	61.9388	0.0098	0.0036	0.3
$\bar{s}$	1.3730	0.0026	0.0059	65.6336	0.0	0.0262	0.2	0.3769	0.0055	0.0123	28.7954	0.0223	0.0129	0.1

Table 7.7: Correlation matrix for the estimated $V_{d,A}$ and $V_{d,B}$ for treatment with insulin A and B, respectively, and three anthropometric measurements.

	$V_{d,A}$	$V_{d,B}$	Height	BW	BMI
$V_{d,A}$	1				
$V_{d,B}$	−0.1244	1			
Height	0.1021	0.3937	1		
BW	0.5781	0.3968	0.7248	1	
BMI	0.7524	0.1497	−0.0152	0.6751	1

From the correlation matrix, it is seen that there is a strong positive correlation between the estimated volume $V_{d,A}$ for insulin A and BMI while the correlation is not that apparent for $V_{d,B}$. In [41], values ranging from a few mL to 100 L are cited for the apparent volume of distribution in different models. The observed correlation between BMI and V_d along with the values cited in the literature seem to indicate that the estimated volumes for the twenty subjects for treatment with insulin A and B are reasonable.

Statistical Analysis

The rate constants k_a and k_e for all twenty subjects for treatment with insulin A are tested if they could come from the same distribution with the mean vector of k_a and k_e for treatment with insulin B. The same test is performed for treatment with insulin B. This is done by Hotelling's T^2 test where the test scores for the two tests are:

$$\begin{aligned} F_A &= 44.69 \\ F_B &= 131.39 \end{aligned}$$

with treatment of insulin A and B, respectively.

The test scores are clearly significant on a 95 % confidence level since $F(2, 20-2)_{0.95} = 3.55$. The estimated rate constants k_a and k_e for all twenty subjects for treatment with insulin A/B can therefore not be assumed to come from the same distribution with the mean vector of the same two parameters for treatment with insulin B/A, respectively. Therefore, insulin A and B have significantly different absorption and elimination kinetics from a statistical point of view.

7.2 PK/PD Models

Next, the results for the two PK/PD models in Section 6.2 are presented. The main difference between the two models is that the time delay between the plasma insulin concentration and response in the effect-compartment model is assumed to be related to a distributional delay while the indirect response model assumes that the delay is related to an indirect response mechanism. The two models are compared at the end of the section and the best model is used for parameter estimation for all twenty subjects in the study.

7.2.1 Effect-Compartment Model

The PK and PD parameters in the effect-compartment model are estimated simultaneously in this section. In previous studies, the PK parameters are estimated while the PD parameters are fixed at values found from *in vitro* studies. It is therefore interesting to see whether the simultaneous estimation of PK and PD parameters are different from the ones estimated separately.

Grey-box Model

The LTI state space model for the effect-compartment model, consisting of three continuous time system equations and two discrete

time observation equations, is shown below:

$$\begin{aligned}
\begin{bmatrix} dI_{sc} \\ dI_c \\ dC_e \end{bmatrix} &= \left(\begin{bmatrix} -k_a & 0 & 0 \\ k_a & -k_e & 0 \\ 0 & K_{e0}/V_d & -K_{e0} \end{bmatrix} \begin{bmatrix} I_{sc} \\ I_c \\ C_e \end{bmatrix} + \begin{bmatrix} 1 & 0 \\ 0 & 1 \\ 0 & 0 \end{bmatrix} \begin{bmatrix} D \\ R_{in} \end{bmatrix} \right) dt + \boldsymbol{\sigma}\, dw_t \\
C_I &= \frac{I_c}{V_d} + e_{1,k} \\
GIR &= \frac{E_{max}}{EC_{50}^{\gamma} + C_e^{\gamma}} \cdot C_e^{\gamma} + e_{2,k}
\end{aligned}$$

where K_{e0} is the equilibrium constant for the passive diffusion between the central and effect compartment while the PD parameters in the model are E_{max}, EC_{50}, and γ.

The PK/PD parameters in the effect-compartment model are estimated using only the observations at time instants where both insulin and GIR are observed (see Appendix A.5 which includes the input and output files from CTSM). The parameters are first estimated for insulin B. Next, the estimated value of E_{max} for insulin B is used as a fixed variable and the rest of the parameters are estimated for insulin A. This procedure is necessary for the estimation to converge for insulin A. Since the effect of the injected insulin does not come close to the maximum effect E_{max} in this study, it is reasonable to assume that E_{max} is the same for insulin A and B for the same subject.

Parameter Estimates

The parameter estimates ($\hat{\theta}$) for the effect-compartment model for treatment with insulin A and B are shown in Table 7.8 along with their standard deviation (Std. dev.).

The estimated PK parameters are similar to the ones discussed in Section 7.1.1 where the results from the single-compartment PK model are mentioned and will therefore not be discussed any further in this section.

Table 7.8: PK/PD model parameter estimates for the effect-compartment model for treatment with insulin A and B.

		Insulin A		Insulin B	
Parameter	Unit	$\hat{\theta}$	Std. dev.	$\hat{\theta}$	Std. dev.
$I_{c,0}$	[nmol]	15.8860	5.1881	2.6384	1.2955
$C_{e,0}$	[nM]	0.0735	0.0235	0.1078	0.0318
k_a	[min^{-1}]	0.0108	0.0038	0.0073	0.0007
k_e	[min^{-1}]	0.0078	0.0025	0.0391	0.0067
K_{e0}	[min^{-1}]	0.0183	0.0028	0.0261	0.0044
V_d	[L]	177.4400	55.8310	34.3590	6.3678
σ_{sc}	[-]	0.0000	0.0000	0.0000	0.0307
σ_c	[-]	0.0000	0.0025	0.0000	0.0015
σ_e	[-]	0.0000	0.0002	0.0000	0.0000
E_{max}	[mmol/min]	9.2		9.1570	2.3370
EC_{50}	[nM]	0.3097	0.0162	0.2684	0.0773
γ	[-]	1.7554	0.1784	2.0325	0.4334
S_I^2	[-]	0.0006	0.0001	0.0013	0.0004
S_{GIR}^2	[-]	0.0017	0.0004	0.0038	0.0009
t_{max}	[min]	107.00		53.00	
C_{max}	[pM]	328.29		465.84	
AUC_0^∞	[μM min]	0.1207		0.1223	
TR_{max}	[min]	171.00		101.00	
R_{max}	[mmol/min]	4.43		6.31	
GIR_0^∞	[mol]	1.66		1.82	

The physical meaning of the PD parameters E_{max} and EC_{50} are the maximum GIR concentration and the insulin concentration producing 50 % of the maximum GIR, respectively. The estimated value of $E_{max} = 9.157$ for treatment with insulin B is used as a fixed variable in the estimation with insulin A which is why no standard deviation is available for that parameter. The estimated value of E_{max} is much higher than the value of the derived parameter $R_{max} = 6.3$ (maximum GIR) which indicates that the maximal effect is not reached. In [59, 60], the parameters in a similar effect-compartment model

are estimated using the computer program *ADAPT II* [16] using algebraic PK equations while the PD parameters E_{max}, EC_{50} and γ are fixed at 5.56 mmol/min, 0.44 nM, and 2.00, respectively. The proposed values are suggestions from unpublished work by the authors of [59]. The estimated values of the PD parameters from the treatment with insulin A are close to those cited in [59].

It is very interesting to see that the parameter γ is estimated close to 2 for both types of insulin. The theoretical meaning of the parameter γ in the sigmoidal E_{max} model is that γ insulin molecules and one receptor elicit the effect (see Section 3.2.1). The estimated value of 2 is therefore also in agreement with the illustration of the insulin receptor in Figure 2.5 where two insulin molecules interact with the insulin receptor resulting in an increase in the activity of the glucose transporters. Normally, the value of $\gamma = 2$ is estimated in a static environment using *in vitro* cells exposed to insulin [54]. The estimation of the parameter γ in the grey-box effect-compartment model is therefore very reasonable.

Since the PK and PD parameters all are estimated simultaneously, the correlation between the PK and PD parameters can be assessed. The sample correlation matrix for insulin B is shown in Table 7.9.

The PK and PD parameters in Table 7.9 do not seem to be very correlated. The correlation between the PD parameters are quite high, especially between E_{max} and EC_{50} where the correlation coefficient is estimated to 0.9853. The correlation between all three parameters for the system noise (σ_{sc}, σ_c, and σ_e) is estimated to 1.0 which also is observed in the previously described PK models.

Model Validation

The validation of the effect-compartment model is carried out using all the available data with missing observations entered into the validation data files when the insulin concentration is not available. Thereby, all 690 measurements of GIR are used along with the 30

Table 7.9: Sample correlation matrix for insulin B.

	$I_{c,0}$	$C_{e,0}$	k_a	k_e	K_{e0}	V_d	σ_{sc}	σ_c	σ_e	E_{max}	EC_{50}	γ	S_I^2	S_{GIR}^2
$I_{c,0}$	1													
$C_{e,0}$	−0.1578	1												
k_a	0.3538	−0.2777	1											
k_e	−0.4430	0.1856	−0.7273	1										
K_{e0}	0.0527	−0.0681	−0.0811	−0.3472	1									
V_d	0.4518	−0.2309	0.8106	−0.9798	0.2733	1								
σ_{sc}	−0.0328	0.0406	−0.0274	0.0787	−0.0826	−0.0797	1							
σ_c	−0.0328	0.0405	−0.0274	0.0787	−0.0826	−0.0797	1.0000	1						
σ_e	−0.0328	0.0406	−0.0274	0.0787	−0.0826	−0.0797	1.0000	1.0000	1					
E_{max}	−0.1588	−0.1623	−0.1544	0.1821	0.0790	−0.1814	−0.0393	−0.0393	−0.0393	1				
EC_{50}	−0.1634	−0.1300	−0.1877	0.1768	0.1446	−0.1972	−0.0407	−0.0407	−0.0407	0.9853	1			
γ	0.0744	0.3361	−0.1092	0.0614	−0.2132	−0.0794	0.0735	0.0735	0.0735	−0.8828	−0.8783	1		
S_I^2	−0.0339	0.0271	−0.1037	0.1855	−0.1298	−0.1887	0.0845	0.0845	0.0845	0.0178	0.0217	0.0379	1	
S_{GIR}^2	−0.1066	0.0562	−0.0452	0.0581	−0.0615	−0.0645	0.0316	0.0316	0.0316	−0.0078	−0.0104	0.0192	−0.0606	1

observations of the plasma insulin concentration. The results from the effect-compartment model are plotted along with the observed plasma insulin concentration and GIR for treatment with insulin A in Figure 7.5 and for treatment with insulin B in Figure 7.6. Only the pure simulation of the estimated models are shown since the system noise is estimated to zero.

The effect compartment concentration is slightly shifted towards the right compared with the observed plasma insulin concentration (see Figure 7.5(a) and Figure 7.6(a)). The reason is that the insulin residing in the central compartment is not at steady-state resulting in the hysteresis loop shown in Figure 6.5 while the effect compartment concentration is assumed to be at steady-state and thereby shifted to the right compared to the insulin in the central compartment. Furthermore, the volume of the effect compartment must be much smaller than V_d if the assumption about a negligible amount is transferred from the central compartment to the effect compartment is valid since the concentration in the two compartments is almost the same.

The simulated GIR follows the observed GIR very well. The oscillations in GIR are not captured by the estimated model since only 30 observations are used in the estimation and because it is a nurse who is regulating the GIR by observing the BG. From Figure 7.5 and Figure 7.6, the time delay between time to maximum insulin concentration (C_{max}) and maximum effect (R_{max}) is clearly seen while the peak on the effect concentration curve seem to be aligned with that of GIR.

The phase-plot of the observed GIR vs. the predicted concentration at the effect site C_e in Figure 7.5(c) and Figure 7.6(c) follows the estimated sigmoidal-shaped curve very nicely for both types of insulin. The phase-plots clearly show that the observed GIR for treatment with insulin B is distributed along most of the sigmoidal curve while that of insulin A only is in the linear area between 20 % and 80 % effect. This explains why it is not possible to estimate a reasonable value of the parameter E_{max} for insulin A.

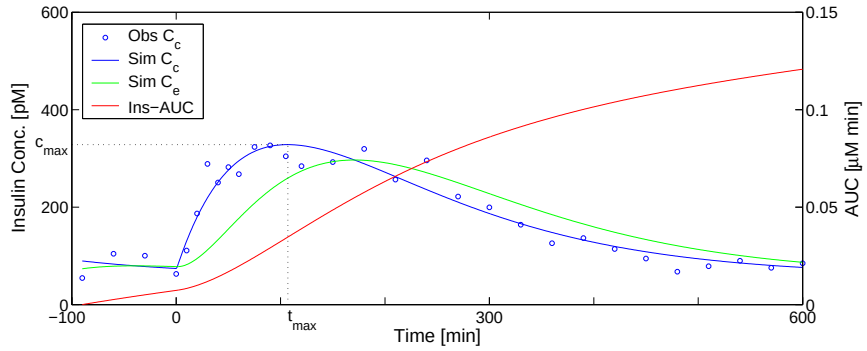

(a) Concentration-time profiles

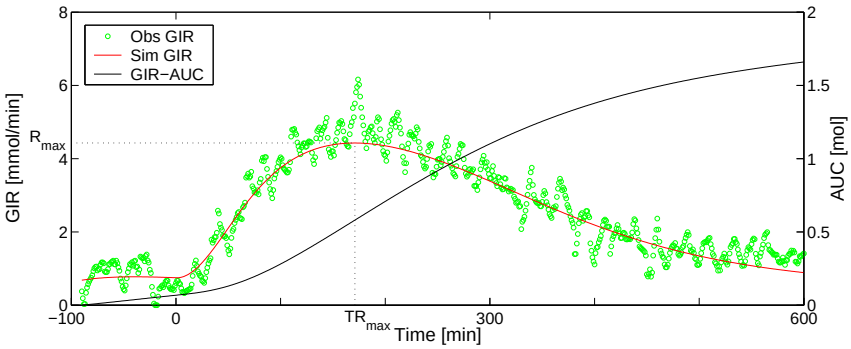

(b) GIR

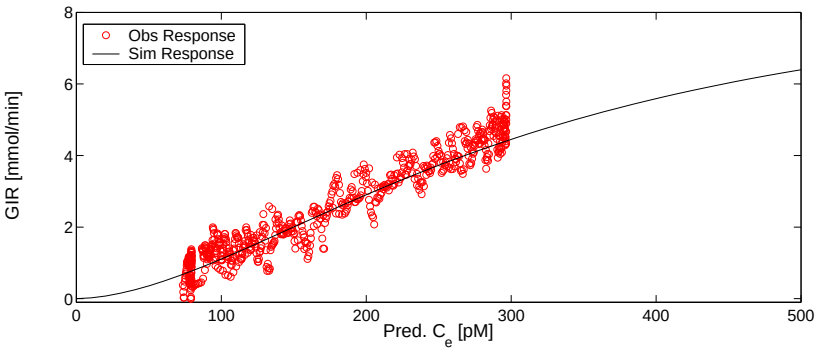

(c) Phase-plot

Figure 7.5: Plot of results from effect-compartment model for insulin A.

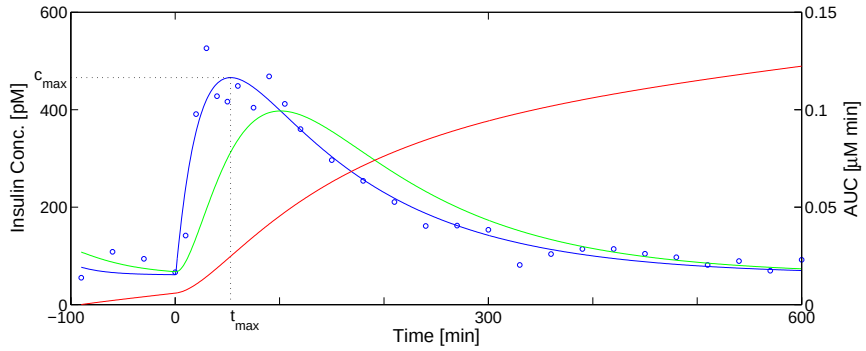

(a) Concentration-time profiles

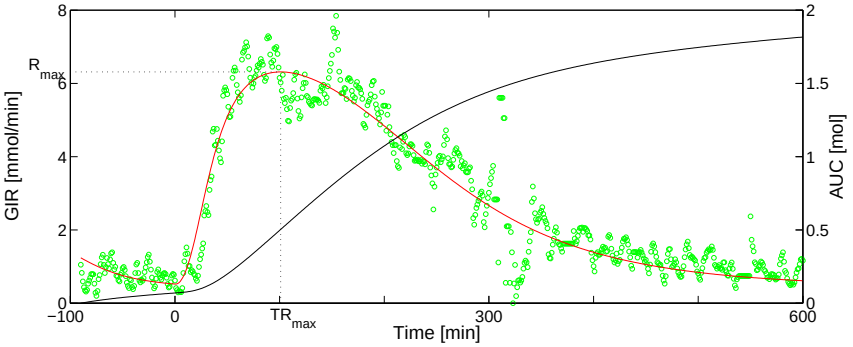

(b) GIR

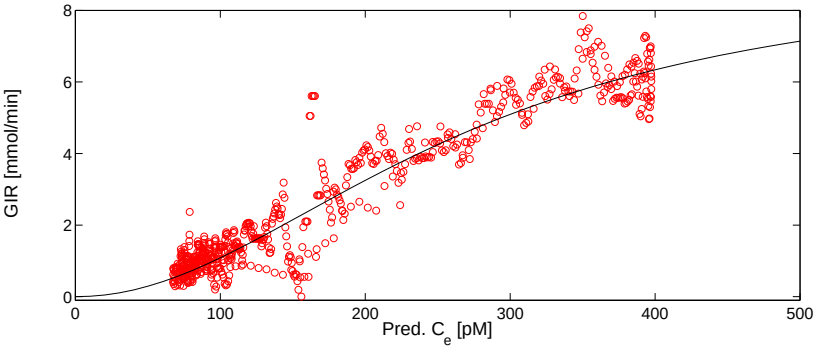

(c) Phase-plot

Figure 7.6: Plot of results from effect-compartment model for insulin B.

The plasma insulin residuals for insulin A and B are the exact same as the ones shown in Figure 7.1(b) on page 85 for the single-compartment PK model and therefore not shown here.

The GIR residuals for treatment with insulin A and B are shown in Figure 7.7 along with LDF and PLDF.

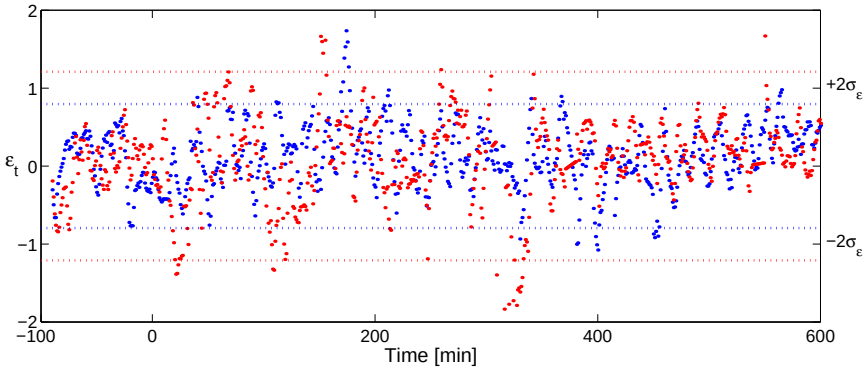

(a) GIR residuals

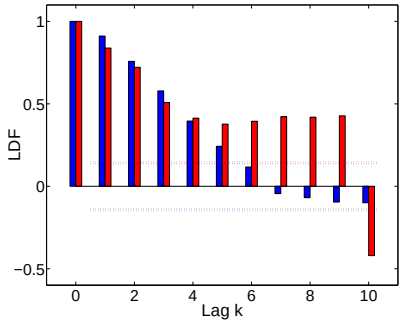

(b) LDF

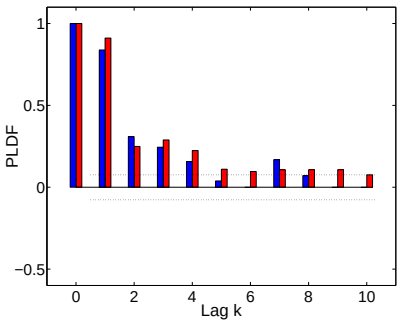

(c) PLDF

Figure 7.7: Residual analysis of GIR for treatment with insulin A (Blue) and insulin B (Red).

The residuals in Figure 7.7(a) are clearly not white noise but considering that it is a nurse who regulates the GIR by observing the BG,

one would not expect the residuals to be white noise. In the light of that, the estimated sigmoidal E_{max} model seem to capture the PD of the insulin/glucose system very well.

7.2.2 Indirect Response Model

The last model in this chapter is the indirect response model where the delay between plasma insulin and the effect on the BG concentration is assumed to be related to an indirect response mechanism. It has not previously been used in clamp studies because of the nature of the study where glucose is infused to keep a clamped glucose level. It is therefore doubtful whether the GIR can be used as an input variable.

Grey-box Model

The NL state space model for the indirect response model, consisting of three continuous time system equations and two discrete time observation equations, is shown below:

$$\begin{aligned}
\begin{pmatrix} dI_{sc} \\ dI_c \\ dG \end{pmatrix} &= \begin{pmatrix} -k_a I_{sc} + D \\ k_a I_{sc} + R_{in} - k_e I_c \\ GIR - k_{out}\Big(1 + \frac{S_{max} \cdot \left(\frac{I_c}{V_d}\right)^{\gamma}}{SC_{50}^{\gamma} + \left(\frac{I_c}{V_d}\right)^{\gamma}}\Big) G \end{pmatrix} dt + \boldsymbol{\sigma}\, dw_t \\
C_I &= \frac{I_c}{V_d} + e_{k,1} \\
BG &= \frac{G}{V_G} + e_{k,2}
\end{aligned}$$

where D, R_{in}, and GIR are input variables while G is the state variable for the amount of glucose in the blood. The parameter k_{out} is the first-order rate constant for elimination of G while SC_{50} is the insulin concentration producing 50% of the maximum stimulating effect S_{max}. The volume of the glucose compartment is fixed at $V_G = 10\ L$ to prevent the estimation of yet another volume.

Parameter Estimates

The parameter estimates ($\hat{\theta}$) for the indirect response model for treatment with insulin A and B are shown in Table 7.10 along with the standard deviation (Std. dev.).

The sigmoidicity parameter γ is estimated with quite a large standard deviation to 4.77 and 14.67 for treatment with insulin A and B, respectively. These values do not agree with the estimated value of γ found in the effect-compartment model or the fact that two insulin molecules are needed to activate the insulin receptor. Furthermore, the value of $\gamma = 14.67$ is very close to the maximal value of 15 specified in CTSM.

The insulin needed to produce 50 % of the maximal stimulating effect S_{max} is about 1/3 of the similar parameter EC_{50} from the effect-compartment model. This can be explained by the BG is also eliminated without the stimulation effect of insulin described by the first-order rate constant k_{out}.

Model Validation

The results from the indirect response model are plotted along with the observed plasma insulin and BG concentration for treatment with insulin A and B in Figure 7.8.

It is clearly seen in Figure 7.8(a) that the estimated model captures the PK of insulin as well as the effect-compartment model which is expected since the same PK model is used. The simulated time course of BG oscillates around the observed BG, which probably is due to the oscillating nature of the input variable GIR or disturbances and unmodelled dynamics.

The 1-step prediction of BG seem to capture the time course of BG and is further investigated by plotting the BG residuals for treatment with insulin A and B in Figure 7.9 along with LDF and PLDF.

Table 7.10: PK/PD Model parameter estimates for the indirect response model for treatment with insulin A and B.

		Insulin A				Insulin B			
Parameter	Unit	$\hat{\theta}$	Std. dev.	t-score	p(> |t|)	$\hat{\theta}$	Std. dev.	t-score	p(> |t|)
$I_{c,0}$	[nmol]	13.1390	5.5371	2.3729	0.0219	2.5861	1.1678	2.2145	0.0318
BG_0	[mM]	5.4173	0.5669	9.5559	0.0000	4.8240	0.6147	7.8473	0.0000
k_a	[min^{-1}]	0.0098	0.0039	2.5141	0.0155	0.0073	0.0007	10.6275	0.0000
k_e	[min^{-1}]	0.0082	0.0031	2.6373	0.0114	0.0370	0.0064	5.7441	0.0000
k_{out}	[min^{-1}]	0.0183	0.0104	1.7618	0.0847	0.0237	0.0041	5.8260	0.0000
S_{max}	[-]	3.2002	2.5775	1.2416	0.2206	3.3596	0.8007	4.1961	0.0001
SC_{50}	[nM]	0.1408	0.0218	6.4450	0.0000	0.1395	0.0125	11.1272	0.0000
γ	[-]	4.7723	2.9789	1.6020	0.1159	14.6690	3.3050	4.4385	0.0001
V_d	[L]	165.4500	62.7890	2.6350	0.0114	36.1830	6.8426	5.2879	0.0000
σ_{sc}	[-]	0.0000	0.0000	0.0355	0.9718	0.0000	0.0007	0.0000	1.0000
σ_c	[-]	0.0000	0.0000	0.0110	0.9912	0.0000	0.0003	0.0000	1.0000
σ_G	[-]	0.3439	0.0477	7.2146	0.0000	0.4010	0.0552	7.2591	0.0000
S_I^2	[-]	0.0006	0.0002	3.4446	0.0012	0.0011	0.0003	3.6094	0.0008
S_{BG}^2	[-]	0.0000	0.0000	0.0134	0.9894	0.0000	0.0000	0.0000	1.0000
t_{max}	[min]	110.00				55.00			
C_{max}	[pM]	327.00				459.90			
AUC_0^∞	[nM min]	121.20				122.50			

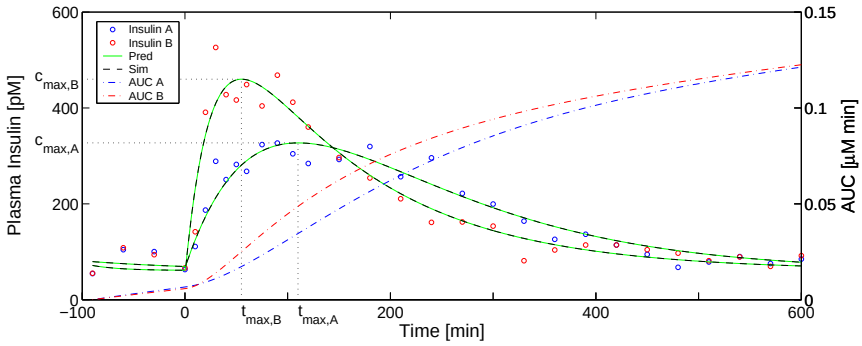

(a) Insulin

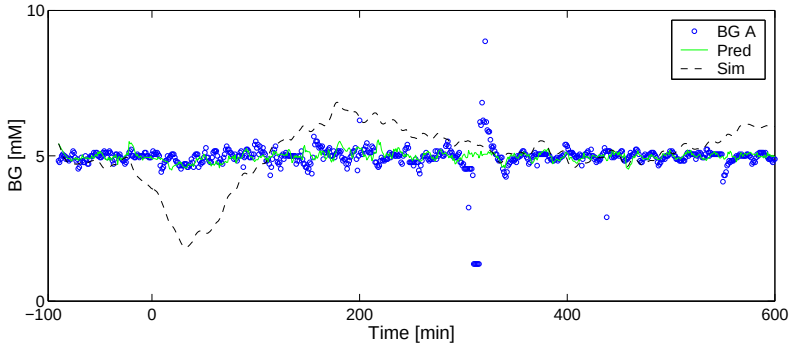

(b) BG A

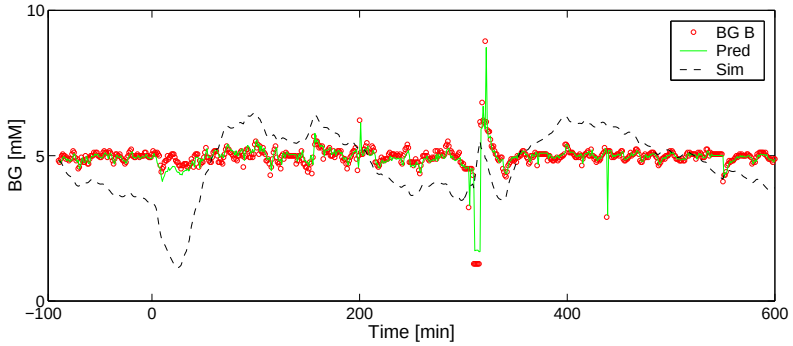

(c) BG B

Figure 7.8: Plot of results from indirect response model for insulin A (Blue) and insulin B (Red).

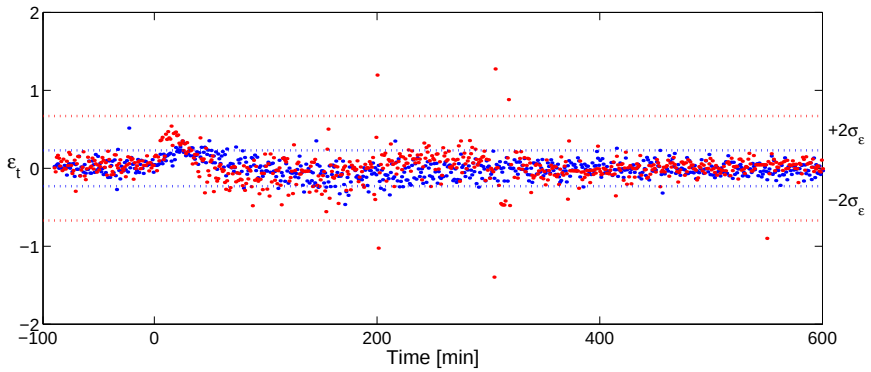

(a) BG residuals

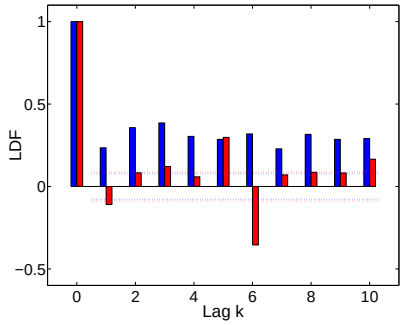

(b) LDF

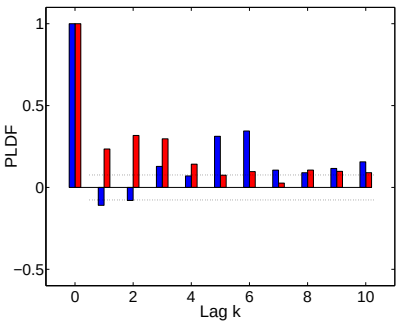

(c) PLDF

Figure 7.9: Residual analysis of BG for treatment with insulin A (Blue) and insulin B (Red).

The residual plot shows that the *BG* residuals almost are within the approximative 95 % confidence interval of $\pm 2\sigma_\varepsilon$. The same is not true when looking at LDF and PLDF, where almost all the lags from 1 to 10 are significant for treatment with insulin A and B.

7.2.3 Comparison of PK/PD Models

The two PK/PD models presented in the previous sections for the insulin/glucose system are compared using the BIC in Table 7.11.

Table 7.11: Test for model structure for PK/PD models.

Model	p	$\log L(\boldsymbol{\theta}, \mathcal{Y}_N)$	BIC
Effect-Compartment			
Insulin A	14	123.9301	−156.3465
Insulin B	14	100.0970	−108.6802
Indirect Response			
Insulin A	14	97.2005	−102.8873
Insulin B	14	115.1349	−72.7181

Since both of the models have 14 parameters and are estimated using the same number of observations, the value of the likelihood function can be used as well as the BIC which shows that the effect-compartment model is chosen as the best model.

From physiology studies, it is known that the delay between plasma insulin concentration and observed response is due to an indirect response mechanism downstream from the insulin receptor. The indirect response model is therefore the physiological most likely representation of the insulin/glucose system but in this study where the glucose level is clamped and glucose is infused, the effect-compartment model is superior to the indirect response model when comparing the two models with the BIC.

The effect-compartment model is therefore chosen as the best representation of the insulin/glucose system and is used in the following parameter estimation for the twenty subjects in the study.

7.2.4 Parameter Estimates for All Twenty Subjects

The parameter estimates obtained for each subject with the effect-compartment model along with the sample mean and standard deviation for each parameter are reported in Table 7.12 for insulin A while the estimates for insulin B are shown in Table 7.13.

The maximal value of the parameter E_{max} is specified in CTSM as 15.0 mmol/min while the maximal value of EC_{50} is set to 1.0 nM to make the estimation converge. E_{max} is close to the maximal value of 15 mmol/min for half of the subjects for insulin A and 7 out of 20 for insulin B. The range of the estimated parameter EC_{50} is from 0.1 nM to the maximal allowable value of 1.0 nM. The estimates of E_{max} and EC_{50} for subject 2, 9, and 15 for insulin A and subjects 8, 11, and 20 for insulin B are therefore doubtful since they are close to the limits specified in CTSM. The value of the penalty function is on the other hand not significant compared to the likelihood-function, which is why the estimates of those subjects are not taken out.

The sample mean of γ is close to 2 but with quite a large standard deviation due to the variation of γ among subjects. Especially the value of $\gamma = 4.16$ for subject 7 seem unreasonable since it means that four insulin molecules would need to interact to facilitate the transport of glucose into the cell.

Table 7.12: Effect-compartment model PK/PD parameter estimates for insulin A for subject 1-20.

Subject	$I_{c,0}$ [nmol]	$C_{e,0}$ [nM]	k_a [min^{-1}]	k_e [min^{-1}]	K_{e0} [min^{-1}]	V_d [L]	σ_{SC}	σ_c	σ_e	E_{max} [mmol/min]	EC_{50} [nM]	γ	S_I^2	S_{GIR}^2
1	1.8486	0.0766	0.0040	0.0348	0.0290	28.5000	0.0000	0.3160	0.0000	14.7	0.6919	1.4439	0.0012	0.0007
2	2.0417	0.0561	0.0026	0.0210	0.0185	38.2960	0.0000	0.2406	0.0035	14.6	0.9967	1.2508	0.0000	0.0013
3	15.8860	0.0735	0.0108	0.0078	0.0183	177.4400	0.0000	0.0000	0.0000	9.2	0.3097	1.7554	0.0006	0.0017
4	19.8740	0.0333	0.0076	0.0072	0.0423	178.8500	0.0000	0.0000	0.0000	14.7	0.5122	1.4669	0.0008	0.0038
5	19.8080	0.0338	0.0093	0.0073	0.0375	211.9700	0.0000	0.0000	0.0000	7.6	0.1567	2.5414	0.0006	0.0055
6	9.0295	0.1321	0.0075	0.0153	0.0270	115.9800	0.0000	0.0001	0.0000	5.9	0.1487	2.8308	0.0006	0.0044
7	14.3020	0.1624	0.0071	0.0075	0.0171	169.3300	0.0000	0.2555	0.0051	7.6	0.2216	4.1641	0.0002	0.0003
8	14.2920	0.0877	0.0082	0.0079	0.0134	158.9100	0.0000	0.0000	0.0000	14.6	0.4281	1.9988	0.0011	0.0028
9	14.6670	0.0592	0.0107	0.0073	0.0192	159.1000	0.0000	0.0000	0.0000	14.8	0.9926	1.2204	0.0008	0.0007
10	14.6530	0.0417	0.0102	0.0092	0.0199	150.0600	0.0000	0.0000	0.0000	7.3	0.1785	1.7053	0.0010	0.0052
11	6.0196	0.1127	0.0073	0.0247	0.1054	47.1040	0.0000	0.0000	0.0000	14.8	0.7656	1.2713	0.0008	0.0018
12	11.0360	0.0977	0.0099	0.0085	0.0581	154.8800	0.0000	0.0000	0.0000	4.5	0.1859	1.9208	0.0003	0.0026
13	39.7700	0.0000	0.0062	0.0047	0.0239	249.2500	0.0000	0.0000	0.0000	10.6	0.3419	2.2668	0.0009	0.0040
14	15.1410	0.1000	0.0089	0.0082	0.0175	159.6300	0.0000	0.0000	0.0000	6.1	0.1290	3.0893	0.0007	0.0043
15	15.1560	0.0909	0.0134	0.0098	0.0466	121.9100	0.0000	0.0000	0.0000	14.9	0.9963	1.0894	0.0014	0.0033
16	11.6200	0.0000	0.0225	0.0085	0.0162	139.2200	0.0000	0.0000	0.0000	14.7	0.5636	1.1512	0.0011	0.0036
17	14.3530	0.0299	0.0093	0.0082	0.0221	146.9700	0.0000	0.0000	0.0029	4.6	0.1602	2.1777	0.0006	0.0052
18	10.1200	0.1036	0.0115	0.0096	0.0166	139.5100	0.0000	0.0000	0.0000	5.3	0.1387	2.2422	0.0006	0.0017
19	7.2835	0.0505	0.0052	0.0115	0.0184	115.9400	0.0000	0.5669	0.0000	4.6	0.1333	2.5341	0.0000	0.0016
20	6.7928	0.0240	0.0080	0.0080	0.0394	128.7900	0.0000	0.0000	0.0000	14.9	0.7152	1.4597	0.0028	0.0014
$\bar{\theta}$	13.1847	0.0683	0.0090	0.0114	0.0303	139.5820	0.0000	0.0690	0.0006	10.3	0.4383	1.9790	0.0008	0.0028
$\bar{s}$	8.0525	0.0432	0.0041	0.0074	0.0215	53.9870	0.0000	0.1538	0.0014	4.4	0.3181	0.7807	0.0006	0.0016

Table 7.13: Effect-compartment model PK/PD parameter estimates for insulin B for subject 1-20.

Subject	$I_{c,0}$ [nmol]	$C_{e,0}$ [nM]	k_a [min^{-1}]	k_e [min^{-1}]	K_{e0} [min^{-1}]	V_d [L]	σ_{SC}	σ_c	σ_e	E_{max} [mmol/min]	EC_{50} [nM]	γ	S_I^2	S_{GIR}^2
1	2.3732	0.0000	0.0077	0.0400	0.0298	23.3550	0.2309	0.0000	0.0000	14.732	0.8319	1.3906	0.0015	0.0053
2	2.4043	0.0923	0.0053	0.0257	0.0216	44.9680	0.0000	0.3242	0.0000	14.639	0.5555	1.6562	0.0003	0.0057
3	2.6384	0.1078	0.0073	0.0391	0.0261	34.3590	0.0000	0.0000	0.0000	9.157	0.2684	2.0325	0.0013	0.0038
4	3.6934	0.0985	0.0088	0.0203	0.0371	60.9220	0.0000	0.1577	0.0000	14.699	0.5561	1.4046	0.0007	0.0033
5	1.7460	0.0000	0.0088	0.0638	0.0234	23.6150	0.0000	0.0000	0.0000	7.616	0.1796	2.0499	0.0013	0.0020
6	7.2193	0.0000	0.0192	0.0169	0.0277	107.5100	0.5357	0.0000	0.0000	5.869	0.1616	3.7393	0.0008	0.0034
7	9.9450	0.0568	0.0236	0.0145	0.0175	97.9920	0.5323	0.0000	0.0000	7.635	0.2327	2.0357	0.0011	0.0021
8	4.6586	0.0754	0.0138	0.0137	0.0119	100.8100	0.0000	0.0000	0.0000	14.619	0.9702	1.1012	0.0016	0.0026
9	5.5890	0.1797	0.0081	0.0269	0.0104	43.7950	0.0000	0.0000	0.0000	14.791	0.6766	1.6488	0.0019	0.0030
10	4.1391	0.0000	0.0186	0.0172	0.0351	77.7820	0.0000	0.3837	0.0000	7.270	0.2841	1.4871	0.0013	0.0010
11	0.9602	0.0669	0.0106	0.0392	0.0220	34.2550	0.0000	0.0000	0.0000	14.779	0.9710	1.0697	0.0020	0.0014
12	2.1344	0.0000	0.0095	0.0302	0.0216	49.8650	0.0000	0.0682	0.0000	4.517	0.1439	2.0940	0.0005	0.0017
13	9.5792	0.0365	0.0072	0.0185	0.0377	82.8650	0.0000	0.0000	0.0000	10.592	0.3122	1.2465	0.0014	0.0037
14	0.7372	0.0994	0.0170	0.0162	0.0212	86.3490	0.0000	0.0000	0.0000	6.138	0.1605	1.8661	0.0017	0.0020
15	5.1628	0.0000	0.0172	0.0150	0.0172	91.3350	0.0000	0.2198	0.0138	4.862	0.5168	1.8851	0.0008	0.0000
16	3.0949	0.1209	0.0236	0.0230	0.0078	66.7750	0.0000	0.3023	0.0101	4.655	0.3832	1.9165	0.0016	0.0000
17	6.2303	0.0437	0.0220	0.0141	0.0231	88.8310	0.0000	0.0000	0.0000	4.640	0.1456	1.8235	0.0015	0.0028
18	4.0973	0.0000	0.0209	0.0205	0.0150	68.8760	0.0000	0.0000	0.0000	5.328	0.1422	1.1603	0.0010	0.0040
19	7.8904	0.0445	0.0114	0.0120	0.0122	108.4700	0.0000	0.0000	0.0000	4.604	0.1329	2.3581	0.0011	0.0044
20	2.8247	0.0929	0.0094	0.0297	0.0166	34.3360	0.0000	0.0000	0.0031	14.860	0.9088	1.3007	0.0012	0.0011
$\bar{\theta}$	4.3559	0.0558	0.0135	0.0248	0.0217	66.3533	0.0649	0.0728	0.0013	10.300	0.4267	1.7633	0.0012	0.0027
$\bar{s}$	2.6807	0.0522	0.0061	0.0128	0.0086	28.6696	0.1685	0.1289	0.0037	4.363	0.3008	0.5974	0.0005	0.0016

Chapter 8

Glucose Tolerance Models

The development of type II diabetes is preceded and predicted by defects in both the insulin-dependent and insulin-independent glucose uptake. The defects are detectable when the patients are normoglycaemic and in most cases more than a decade before diagnosis of the disease. On that background, glucose tolerance tests are performed on patients to derive metabolic indices of the insulin-dependent and insulin-independent glucose uptake which can be used to determine whether or not the patient is likely to develop diabetes.

A brief definition of insulin resistance is given in the following section followed by a description of the models considered for the glucose tolerance tests.

8.1 Insulin Resistance

Insulin resistance (the opposite of insulin sensitivity) is defined as an impaired biological response to insulin [5]. When the insulin receptor sensitivity is decreased, glucose is not transported into the cell, which consequently causes an excess of glucose to build up in the blood.

Several procedures, such as the euglycaemic clamp and glucose tolerance tests, have been developed in an attempt to find ways of measuring insulin resistance and determining whether a patient has normal glucose tolerance (NGT), impaired glucose tolerance (IGT) or is type II diabetic. Among those, the three most widely used techniques are described in the following.

Euglycaemic Clamp: The total amount of infused glucose can be used as an index of insulin action on glucose metabolism since an insulin resistant patient would require much less glucose to maintain the clamped plasma glucose level than a normal patient. The more glucose infused, the greater the sensitivity to insulin of the patient. The advantage of this test is that the effect of insulin can be assessed in absence of the insulin/glucose feedback system since the pancreatic secretion of insulin has been suppressed. The limitations of this technique are however that several doses of insulin are needed to estimate the full spectrum of insulin resistance. The complexity and expenses associated with that are many, which is why the use of the clamp technique is limited to research laboratories only [5].

IV Glucose Tolerance Test: A more practical method to measure insulin resistance is by using an intravenous glucose tolerance test (IVGTT). The measure of insulin resistance is highly correlated with the results obtained with the clamp technique for non-diabetic but not for diabetic patients. The flaws of this method is that the peripheral and hepatic glucose metabolism are not separated. The focus is primarily on glucose ignoring all other insulin-sensitive issues. The advantage of IVGTT is that the results obtained from the IVGTT are generally better at predicting type II diabetes than that of the clamp technique. It provides information on both the insulin action and secretion. The IVGTT is relative simple compared to the clamp technique but is still too complex and costly to be used for clinical evaluation of insulin resistance.

Oral Glucose Tolerance Test: The oral glucose tolerance test (OGTT) is less invasive than the IVGTT since the glucose dose is given orally. The OGTT and IVGTT are otherwise the same. The advantage of OGTT over IVGTT is that it can be used in various clinical settings because it is more practical and less costly than the IVGTT. The modelling of the OGTT is more difficult than IVGTT since the glucose is no longer IV administered but absorbed from the gut.

8.2 IVGTT Models

In the following, the minimal model (MM) initially proposed by Dr. Richard N. Bergman *et al.* [7] in 1979 is presented. The model was introduced for the interpretation of the glucose and plasma insulin concentrations following an IVGTT.

The MM is different from the clamp models since there is no suppression of insulin secretion in the IVGTT. Therefore, the insulin/glucose feedback mechanisms has to be included in the MM.

The glucose kinetics in the MM have recently been reassessed by Ni *et al.* [38] where it is concluded that it is too simple. Several model expansions have been cited in the literature to try and come up with better models. Those expansions include two instead of one compartment for glucose [10, 11] and a circulatory model for glucose kinetics [34]. The reason why these models have not been included in this thesis, is because a labelled IVGTT is needed to estimate the model parameters.

The MM consists of two parts which will be explained in the following sections. The first MM is for the glucose kinetics while the second part is for the insulin kinetics. Metabolic indices can be derived from each of the two models to assess the insulin sensitivity and the beta-cell function.

8.2.1 Minimal Model of Glucose Kinetics

The MM of glucose kinetics consists of a compartment for glucose along with two compartments for plasma and remote insulin. The controlling action of insulin on hepatic glucose production and utilization of glucose in the peripheral tissue is modelled using the insulin in the remote compartment. The cold[1] MM of glucose kinetics during an IVGTT is illustrated in Figure 8.1.

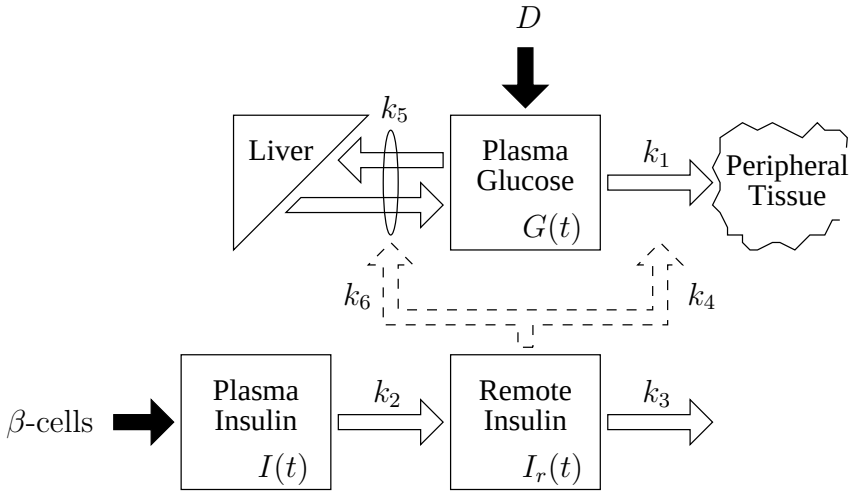

Figure 8.1: Minimal model of glucose kinetics. $G(t)$ is plasma glucose, $I(t)$ is plasma insulin, and $I_r(t)$ is remote insulin. The inputs to the system are D (IV infused glucose dose) along with the secreted insulin from the beta-cells shown as solid black arrows. The parameters k_i are rate constants characterizing material fluxes (solid white arrows) and control action (dashed arrows).

The rate constants k_1 and k_5 represent the effect of glucose to accelerate its utilization by the peripheral tissues and the liver, respectively,

[1] Cold, meaning that the insulin is not labelled, opposed to the hot model where the injected glucose is radioactive or a stable isotope acting as a tracer.

independent of insulin levels. k_2 describes the efficiency with which plasma insulin fills the remote compartment. k_3 is a measure of the rate of disappearance of the insulin effect while k_4 and k_6 correspond to the effect of remote insulin in enhancing glucose disappearance [4].

Model Equations

The rate of change of glucose G is the difference between the net hepatic glucose balance B and the disappearance of glucose into the peripheral tissue U_p. The equations for B and U_p are introduced in the following and later combined in a differential equation for the rate of change of glucose.

The equation for the hepatic glucose can be written as [7]:

$$B = B_0 - \big(k_5 + k_6 I_r\big)G \tag{8.1}$$

where B_0 is the extrapolated hepatic glucose production at zero glucose concentration, I_r is the insulin in the remote compartment, and G is the plasma glucose. Depending whether the liver is producing or consuming glucose, B can assume both positive and negative values.

The expression for the glucose utilization U_p into the peripheral tissue where the remote insulin I_r is assumed to increase the mobility of the glucose across the cell membrane is shown below [7]:

$$U_p = \big(k_1 + k_4 I_r\big)G \tag{8.2}$$

where k_1 and k_4 are the rate constants for insulin-independent and insulin-dependent glucose uptake, respectively.

The equation for the rate of change of plasma glucose is obtained by combining equation (8.1) and (8.2) (see Appendix B.2) and shown in equation (8.3) along with the equation for the rate of change of

remote insulin:

$$\begin{aligned}\frac{dG}{dt} &= -\Big[\big(k_1+k_5\big)+\big(k_4+k_6\big)I_r\Big]G \\ &\qquad + \big(k_1+k_5\big)C_{G_b}V + D\cdot\delta(t) \qquad (8.3a)\\ \frac{dI_r}{dt} &= k_2\big(C_I - C_{I_b}\big) - k_3 I_r \qquad (8.3b)\end{aligned}$$

where C_{G_b} and C_{I_b} are the basal plasma glucose and insulin concentrations, respectively, typically measured 180 minutes after the glucose bolus injection.

To obtain a model which is uniquely identifiable from glucose and insulin measurements, equation (8.3) is reparameterized as in the MM, i.e. [7, 53]:

$$\begin{aligned}p_1 &= k_1 + k_5\\ p_2 &= k_3\\ p_3 &= k_2\big(k_4+k_6\big)\\ X &= (k_4+k_6)I_r\end{aligned}$$

where X is the insulin action proportional to the insulin in the remote compartment I_r. The parameter p_1 is the insulin-independent rate constant of glucose uptake, also referred to as glucose effectiveness while p_3 describes the insulin-dependent increase in tissue glucose uptake ability pr. unit of insulin concentration above baseline insulin. The parameter p_2 corresponds to the spontaneous decrease of tissue glucose uptake ability [20].

The MM of glucose kinetics thereby consists of two differential equations describing the glucose plasma concentration and insulin action as shown below with the new parameters mentioned above:

$$\begin{aligned}\frac{dG}{dt} &= -\big(p_1+X\big)G + p_1 C_{G_b}V + D\cdot\delta(t) \qquad (8.4a)\\ \frac{dX}{dt} &= p_3\big(C_I - C_{I_b}\big) - p_2 X \qquad (8.4b)\end{aligned}$$

where $G(0) = G_0$ and $X(0) = 0$.

The glucose is utilized at a constant rate p_1 and by the feedback effect of the insulin action X represented by $-X \cdot G$. An additional amount of plasma insulin will cause an increase in X and thereby cause the rate of glucose utilization to be lowered.

8.2.2 Minimal Model of Insulin Kinetics

The second part of the MM is for insulin kinetics as illustrated in Figure 8.2 [8].

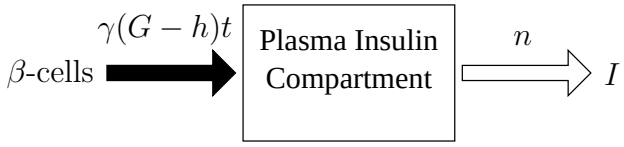

Figure 8.2: Minimal model of insulin kinetics.

The secreted insulin from the beta-cells enters the plasma insulin compartment at a rate proportional by γ to the degree by which the glucose exceeds a threshold level h and to the time from the glucose injection. The insulin is cleared from the plasma compartment at a rate proportional to the amount of insulin in the plasma compartment.

The minimal model of insulin kinetics is described by the following equation:

$$\frac{dI}{dt} = \gamma \left[G - h\right]^{+} t - nI \tag{8.5}$$

where γ is the proportionality factor between the glucose concentration and the rate of change in plasma insulin, h is the threshold level while n is the first-order rate constant for insulin disappearance and t is the time elapsed from the glucose stimulus. The '+' in (8.5) symbolizes that it is only the positive part of $[G - h]$ which is used.

The estimation of parameters in the two minimal models of glucose and insulin kinetics has to be conducted in two steps using the measured insulin and glucose concentrations as known forcing functions in (8.4) and (8.5), respectively. It has been shown in [20] that coupling of the two parts of the MM will not admit an equilibrium and the concentration in the remote insulin compartment will increase without any bounds.

8.2.3 Metabolic Indices

The sensitivity index S_I, representing the insulin-dependent glucose elimination, is derived from the MM of glucose kinetics along with a measure for the insulin-independent glucose elimination called glucose effectiveness index S_G.

With the notation used in (8.3), the insulin sensitivity index and glucose effectiveness translates into:

$$S_I = \frac{k_2\big(k_4 + k_6\big)}{k_3} = \frac{p_3}{p_2} \tag{8.6a}$$

$$S_G = k_1 + k_5 = p_1 \tag{8.6b}$$

The two metabolic indices which can be obtained from the MM of insulin kinetics are the first- and second-phase pancreatic responsitivity indices (ϕ_1 and ϕ_2).

The first- and second-phase pancreatic responsivity index can be calculated from the minimal model for insulin kinetics as [8]:

$$\phi_1 = \frac{I_0}{n \cdot \Delta G} \tag{8.7a}$$

$$\phi_2 = \gamma \cdot 10^4 \tag{8.7b}$$

where I_0 is the early peak in insulin plasma concentration while $\Delta G = G_0 - G_b$ is the maximum change in the glucose concentration due to the glucose injection.

The first-phase pancreatic responsivity index ϕ_1 is a measure of the size of the first peak of plasma insulin due to the bolus of glucose. The second-phase pancreatic responsivity index ϕ_2 represents the sensitivity of the rate of rise of the second-phase to glucose. This peak is enhanced by injecting tolbutamide at $t = 20$ min. in the present IVGTT (see Figure 5.3).

As a measure of the beta-cell function, the acute insulin response (AIR) can be calculated as the area under the insulin curve from $t = 0$ to 8 min. The value of AIR_{0-8} is often used in combination with the insulin sensitivity index S_I to distinguish between NGT and IGT subjects.

8.3 OGTT Models

The OGTT is not modelled using differential equations since the glucose is not injected IV but given orally. The glucose is therefore absorbed from the gut which makes the modelling a bit more complicated. Instead, regression models are commonly used for deriving insulin sensitivity and pancreatic beta-cell function indices from the OGTT. The purposes of these models are to estimate indices which are correlated with the indices from the MM during an IVGTT using as few measurements from the OGTT as possible.

Four commonly used insulin sensitivity indices and two indices for the pancreatic beta-cell function derived from the OGTT are briefly described in the following sections.

8.3.1 Insulin Sensitivity

During the oral glucose load, the suppression of hepatic glucose production is not very complete. The insulin sensitivity index therefore reflects both suppression of hepatic glucose production as well as glucose disposal by all tissues in the body. The more resistant the

liver and peripheral tissues are, the greater the rise will be in mean plasma glucose concentrations during the OGTT. The following regression models try to model these dependencies using insulin and glucose measurements entered in the formulas as mM and pM (unless otherwise is stated) along with simple demographic parameters.

The insulin sensitivity index calculated using the homeostasis model assessment (HOMA) is the simplest of the four models. It only requires fasting glucose and insulin samples and is calculated as [2, 22, 35]:

$$\text{HOMA} = \frac{\text{ins0}'}{22.5 \exp(-\log \text{glu0}')} \tag{8.8}$$

where ins0′ and glu0′ are the plasma insulin and glucose concentrations at $t = 0$ min, respectively.

In the Cederholm index, the prediction of the insulin sensitivity is based on four samples of insulin and glucose (t=0, 30, 60, 120 min.) along with measurements of the bodyweight BW [2, 22].

$$\text{Cederholm} = \frac{75 + (\text{glu0}' - \text{glu120}') \cdot 1.15 \cdot 180 \cdot 0.19 \cdot \text{BW}}{120 \cdot \log(\text{mean ins}) \cdot \text{mean glu}} \tag{8.9}$$

where the mean values of the insulin and glucose concentration are calculated using the four samples of insulin and glucose, respectively.

The Stumvoll index for insulin sensitivity is calculated using a simple demographic parameter (BMI) along with only two measurements from the OGTT [50].

$$\text{Stumvoll} = 18.8 - 0.271 \cdot \text{BMI} - 0.0052 \cdot \text{ins120}' - 0.27 \cdot \text{glu90}' \tag{8.10}$$

Finally, the Matsuda index uses the mean of seven insulin and glucose measurements (t=-30, -15, 0, 30, 60, 90, 120 min.) along with the samples of fasting insulin and glucose [36]. The insulin sensitivity index is calculated as a constant divided by the square root of the product of fasting and mean values of insulin and glucose, i.e.:

$$\text{Matsuda} = \frac{10,000}{\sqrt{(\text{glu0}' \cdot \text{ins0}')(\text{mean glu} \cdot \text{mean ins})}} \tag{8.11}$$

where the plasma insulin and glucose are entered in the formula as mg/dL and mU/L.

8.3.2 Pancreatic Beta-Cell Function

The following two indices of the pancreatic beta-cell function are to be compared with the acute insulin response (AIR_{0-8}) from the IVGTT.

The HOMA index for the pancreatic beta-cell function is calculated using only the fasting glucose and insulin measurements, i.e.:

$$\text{HOMA} = \frac{20 \cdot \text{ins}0'}{\text{glu}0' - 3.5} \tag{8.12}$$

while the Stumvoll index for the pancreatic beta-cell function is calculated using the following formula:

$$\text{Stumvoll} = 1283 + 1.829 \cdot \text{ins}30' - 138.7 \cdot \text{glu}30' + 3.772 \cdot \text{ins}0' \tag{8.13}$$

Chapter 9

Results from Glucose Tolerance Models

The results from the glucose tolerance models are presented in this chapter. First, the grey-box estimates of the parameters in the MM of glucose kinetics for the IVGTT are presented and validated. Next, the derived metabolic indices are tested if they can be used in a discriminant analysis to distinguish between NGT and IGT subjects and compared with estimates from previous studies. Finally, the indices from the IVGTT are compared with those from the OGTT to examine the correlation between them.

9.1 IVGTT Models

Since the IVGTT is modified with tolbutamide injected after 20 min., the measured insulin data cannot be used for estimation of the parameters in the differential equation (8.5) for the MM of insulin kinetics. The measured insulin is therefore only used as a forcing function in the MM of glucose kinetics, i.e. equation (8.4). Consequently,

the estimation of the first- and second-phase pancreatic responsivity indices is not possible using the present IVGTT.

9.1.1 Grey-box Model

The NL state space model for the MM of glucose kinetics, consisting of two continuous time system equations and one discrete time observation equation, is shown below:

$$\begin{aligned} \begin{pmatrix} dG \\ dX \end{pmatrix} &= \begin{pmatrix} -\big(p_1 + X\big)G + p_1 C_{G_b} V + D \\ p_3\big(C_I - C_{I_b}\big) - p_2 X \end{pmatrix} dt + \boldsymbol{\sigma}\, dw_t \\ C_G &= \frac{G}{V} + e_k \end{aligned}$$

where D is the bolus dose of glucose given at $t = 0$ min. and the insulin concentration C_I is a known forcing function. The basal glucose and insulin concentrations, i.e. C_{G_b} and C_{I_b}, are found as the average of the measurements at t=140, 160, and 180 min. of the glucose and insulin concentrations, respectively. w_t is a standard Wiener process with covariance matrix $\boldsymbol{\sigma}$ with σ_G and σ_X in the diagonal, and $e_k \in N(0, S^2)$ is a white noise process mutually independent of w_t.

9.1.2 Parameter Estimates

The grey-box parameter estimates for the MM of glucose kinetics are shown in Table 9.1 for a representative NGT and IGT subject along with the standard deviations.

The apparent volume of distribution of the glucose is estimated close to 12.6 L and 13.7 L for the NGT and IGT subject, respectively. Unlike the clamp models, the estimation of the volume V does not seem to be a problem in the MM. The values of V for the NGT and IGT subject both seem physiological reasonable.

Table 9.1: MM parameter estimates for a representative NGT and IGT subject.

		NGT		IGT	
Parameter	Unit	$\hat{\theta}$	Std. dev.	$\hat{\theta}$	Std. dev.
G_0	[mmol]	$6.5504E{+}01$	$3.5506E{+}00$	$8.6505E{+}01$	$2.9457E{+}00$
p_1	[min^{-1}]	$2.0097E{-}02$	$4.8879E{-}03$	$1.4629E{-}02$	$7.2208E{-}03$
p_2	[min^{-1}]	$5.7490E{-}02$	$1.7436E{-}02$	$2.5365E{-}01$	$2.7911E{-}01$
p_3	[$\text{min}^{-2}\text{pM}^{-1}$]	$6.9959E{-}06$	$1.7469E{-}06$	$8.3331E{-}06$	$1.4697E{-}05$
V	[L]	$1.2610E{+}01$	$3.9444E{-}01$	$1.3742E{+}01$	$4.1699E{-}01$
σ_G	[-]	$9.8176E{-}01$	$3.4316E{-}01$	$5.8172E{-}07$	$2.3523E{-}02$
σ_X	[-]	$7.9394E{-}09$	$5.3310E{-}06$	$4.5122E{-}03$	$3.6639E{-}03$
S^2	[-]	$7.3042E{-}02$	$2.5261E{-}02$	$3.3406E{-}02$	$1.1552E{-}02$
AIR_{0-8}	[pM min]	$2.3265E{+}03$		$1.0320E{+}03$	

The system noise is not estimated to zero, which was the case for most of the clamp models, since the glucose and insulin measurements from the IVGTT are much more excited than those from the clamp study. The rather large value of σ_G for the NGT subject indicates that the dynamics of the glucose is not modelled completely with the MM. The MM has not been expanded with more compartments since it would require the injected glucose to be labelled to be able to estimate yet another unobservable state as mentioned in Section 8.2.

The glucose effectiveness index can be calculated from the parameter estimate of p_1 from the MM. The estimated values of the glucose effectiveness index for the NGT and IGT subject are 0.020 and 0.015 min^{-1}, respectively. The glucose effectiveness is a measure of the insulin-independent ability to dispose glucose. S_G does not seem to be significantly different for NGT and IGT subjects when comparing the estimates of the two representative subjects.

The insulin sensitivity index is equal to the ratio between the estimated parameters p_3 and p_2 from the MM, i.e. $S_I = p_3/p_2$. It is a measure of the insulin-dependent ability to dispose glucose. Unlike the glucose effectiveness, the values of S_I are quite different for the two glucose tolerance groups. The estimated values are $S_I = 1.217$ and $S_I = 0.329$ for the NGT and IGT subject, respectively[1].

The parameter AIR_{0-8} is the acute insulin response which is used as a measure of the beta-cell function, i.e. the ability of the beta-cells to produce insulin when exposed to a bolus of glucose. It is calculated as the area under the insulin curve from 0 to 8 min. using the Trapezoidal-method. The value of AIR_{0-8} is about twice as large for the NGT subject compared with the IGT subject, which indicates that the response to the glucose bolus of the NGT subject is much larger than that of the IGT subject.

The sample mean and standard deviation of the MM parameter estimates can be found in Appendix B.3 for the 108 NGT and 17 IGT subjects in the IVGTT. The sample mean of the system noise parameters σ_G and σ_X indicates that the MM of glucose kinetics is too simple.

9.1.3 Model Validation

Next, the ability of the MM model to predict and simulate the observed dynamics of the insulin/glucose system is tested. The 1-step prediction and pure simulation of the glucose concentration C_G and the insulin action X are plotted in Figure 9.1 and Figure 9.2 for a representative NGT and IGT subject, respectively. The glucose residuals are also plotted and tested whether they can be considered to be white noise using the lag-dependency function (LDF) and partial lag-dependency function (PLDF).

When comparing the time course of the measured glucose in Figure 9.1(a) and Figure 9.2(a), it is seen that the disposal of glucose

[1]The unit of S_I is $10^{-4} \cdot \mathrm{min}^{-1}\mathrm{pM}^{-1}$.

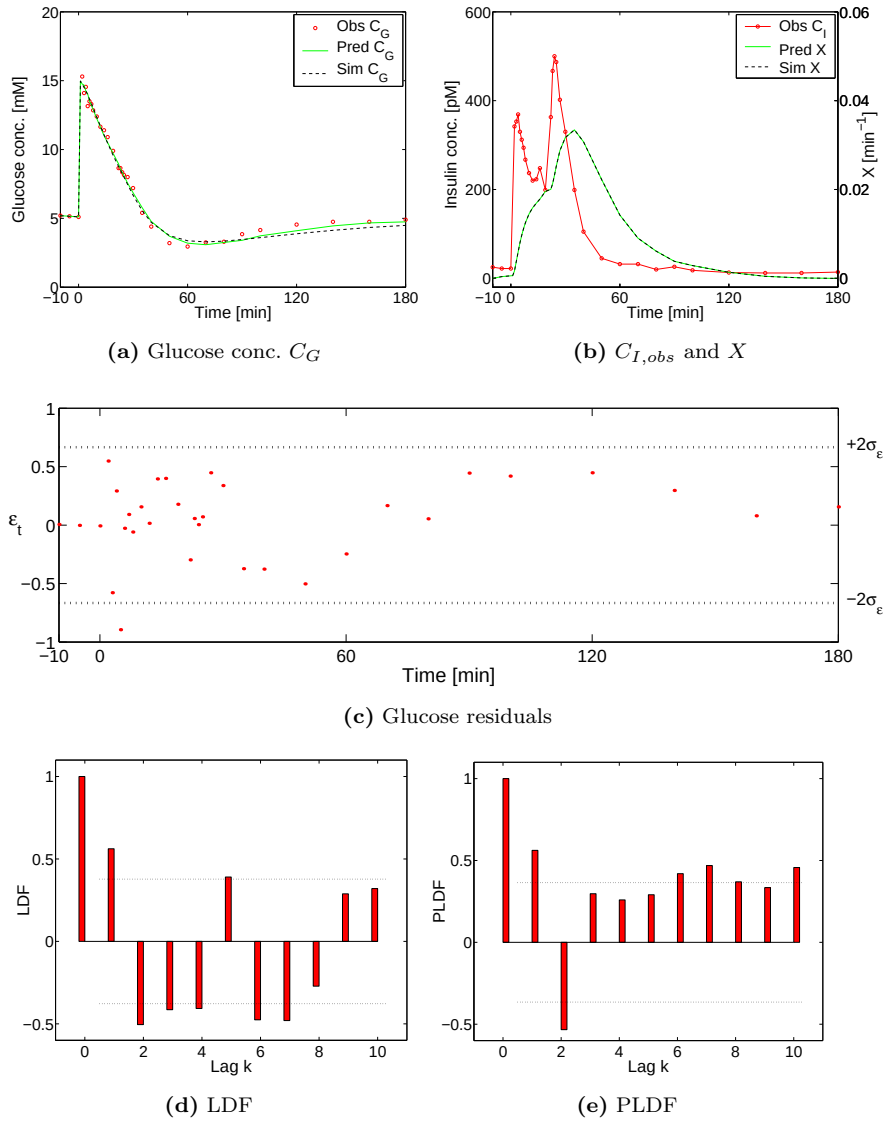

(a) Glucose conc. C_G

(b) $C_{I,obs}$ and X

(c) Glucose residuals

(d) LDF

(e) PLDF

Figure 9.1: Measured, predicted, and simulated glucose and insulin concentrations along with a residual analysis of glucose for a representative NGT subject.

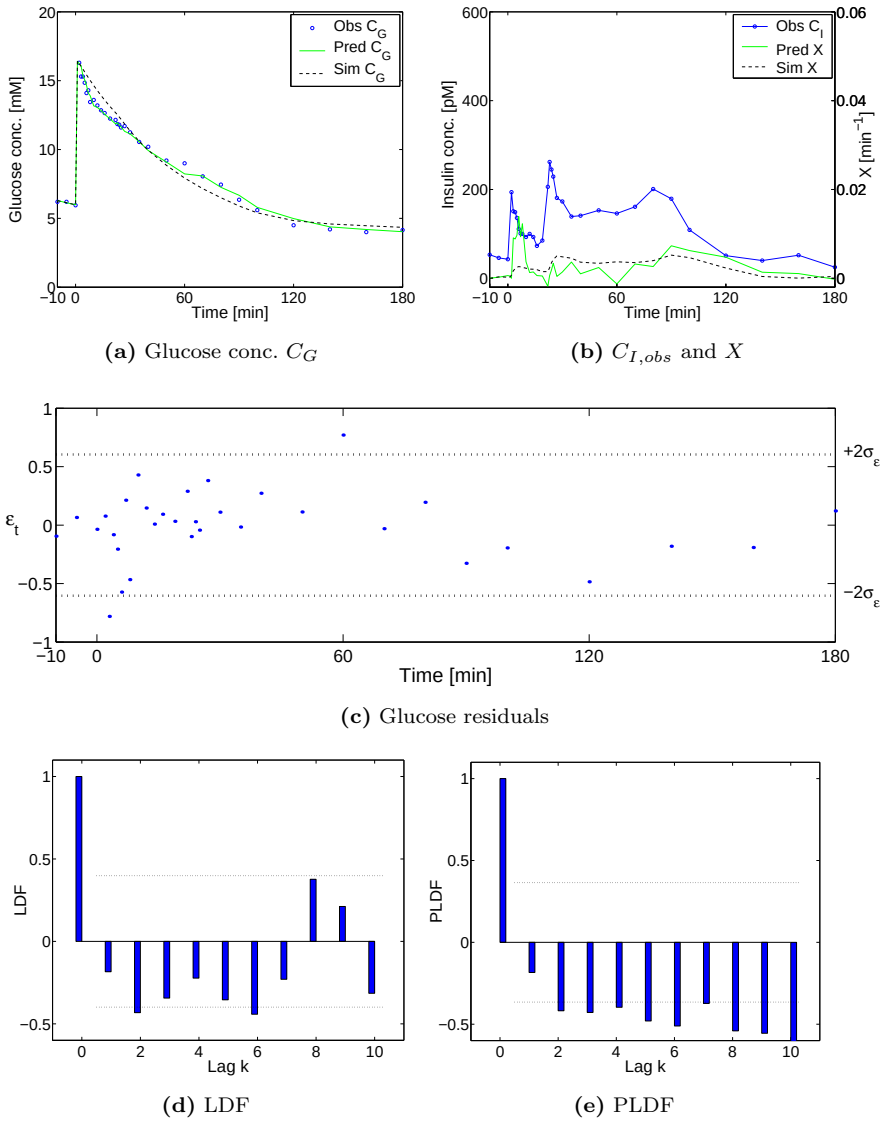

(a) Glucose conc. C_G

(b) $C_{I,obs}$ and X

(c) Glucose residuals

(d) LDF

(e) PLDF

Figure 9.2: Measured, predicted, and simulated glucose and insulin concentrations along with a residual analysis of glucose for a representative IGT subject.

for the IGT subject is not as fast as for the NGT subject. One hour after the glucose bolus, the glucose level of the NGT subject drops to a minimum which is below the basal glucose level, and then gradually returns to the level before the injection of glucose while the basal glucose level barely is reached for the IGT subject during the 180 min. of the IVGTT.

The 1-step prediction and pure simulation of the glucose concentration for both the NGT and IGT subject seem to fit the measured glucose concentration nicely. Almost all of the glucose residuals plotted in Figure 9.1(c) and Figure 9.2(c) are within $\pm 2\sigma_\varepsilon$. The plots of LDF and PLDF for the NGT and IGT subjects show that the residuals are not far from being white.

The measured insulin concentration is used as an input to the model which is why it has not been predicted or simulated. The measured insulin concentration is though plotted in Figure 9.1(b) and Figure 9.2(b) along with the 1-step prediction and simulation of the insulin action X to compare the time course of the two. For the NGT subject, the measured insulin concentration rises rapidly to a peak immediately after the glucose injection and drops shortly thereafter to a lower level still above the basal insulin concentration. At $t = 20$ min., the second-phase insulin response is boosted by the tolbutamide injection to an insulin peak higher than the first-phase response which gradually drops to the basal level. The insulin peaks for the IGT subject are not as distinct as for the NGT subject and the insulin concentration does not return to the basal level before 2 hours after the glucose bolus.

The insulin action is quite different for the NGT and IGT subject. There is an apparent delay between the measured plasma insulin and the insulin action for the NGT subject while the predicted and simulated insulin action for the IGT subject are close to zero during the whole IVGTT. This observation indicates that it is the insulin-dependent and not the insulin-independent glucose uptake which is impaired for the IGT subject.

9.1.4 Outliers and Corrupted Data

The IVGTT is performed on 261 NGT and 27 IGT subjects. Unfortunately, not all of the subjects could be used in the estimation of MM parameters because of various reasons. To ensure precise estimates of the metabolic indices which can be used to distinguish between NGT and IGT subjects in the IVGTT, it is therefore necessary to remove outliers and subjects with missing or corrupted data.

Out of the 288 subjects, only 108 NGT and 17 IGT subjects remains after the removal procedure which is summarized in Table 9.2.

Table 9.2: Removal of subjects in the IVGTT.

Subject	NGT	IGT	Total
Number of subjects	261	27	288
Missing data	37	3	40
No convergence	88	6	94
Possible misclassification	28	1	29
Remaining	108	17	125

All the glucose and insulin measurements for 40 of the subjects in the study are missing and the subjects are removed on that account. The parameter estimation of the MM is extremely dependent on the initial guesses. To reduce the time of estimating the parameters for the remaining 248 subjects, a reasonable set of initial values are specified in CTSM for the estimation of NGT subjects and another for IGT subjects. The estimation does not converge for 88 NGT and 6 IGT subjects when using those initial values and are therefore removed. Finally, 29 subjects are removed because the estimated parameters indicate a possible misclassification. Those subjects should preferably be tested further by a physician to determine whether the

preclassification is valid or not so that they can be included in the study once again. The remaining numbers of NGT and IGT subjects in the IVGTT after the removal procedure are therefore 108 and 17, respectively.

9.1.5 Statistical Analysis

The following statistical analysis of the results from the IVGTT are performed to investigate the differences between NGT and IGT subjects.

First, the sample mean and standard deviation of S_G, S_I, and AIR_{0-8} are shown in Table 9.3 for the 108 and 17 successful estimations of MM parameters for NGT and IGT subjects, respectively.

Table 9.3: Sample mean and standard deviation of S_G, S_I, and AIR_{0-8}.

		NGT		IGT	
Parameter	Unit	$\bar{\theta}$	$\bar{s}$	$\bar{\theta}$	$\bar{s}$
S_G	$[\text{min}^{-1}]$	0.0206	0.0095	0.0211	0.0102
S_I	$[10^{-4} \cdot \text{min}^{-1}\text{pM}^{-1}]$	1.0074	0.3988	0.2488	0.2068
AIR_{0-8}	[nM min]	2.2397	1.3656	2.4744	1.8780

The sample means of S_I for NGT and IGT subjects are clearly different while the sample means of the two other indices are almost identical for NGT and IGT subjects. This observation seems to indicate that it is only the insulin-dependent glucose uptake which is affected in IGT subjects.

To determine which of the three indices are best at separating the NGT and IGT subjects, a matrix of scatter plots of S_I, S_G, and AIR_{0-8} is shown in Figure 9.3. The histograms in the diagonal are divided into ten equally spaced bins on the x-axis and the frequency is shown on the y-axis to illustrate the distribution of each parameter for NGT and IGT subjects.

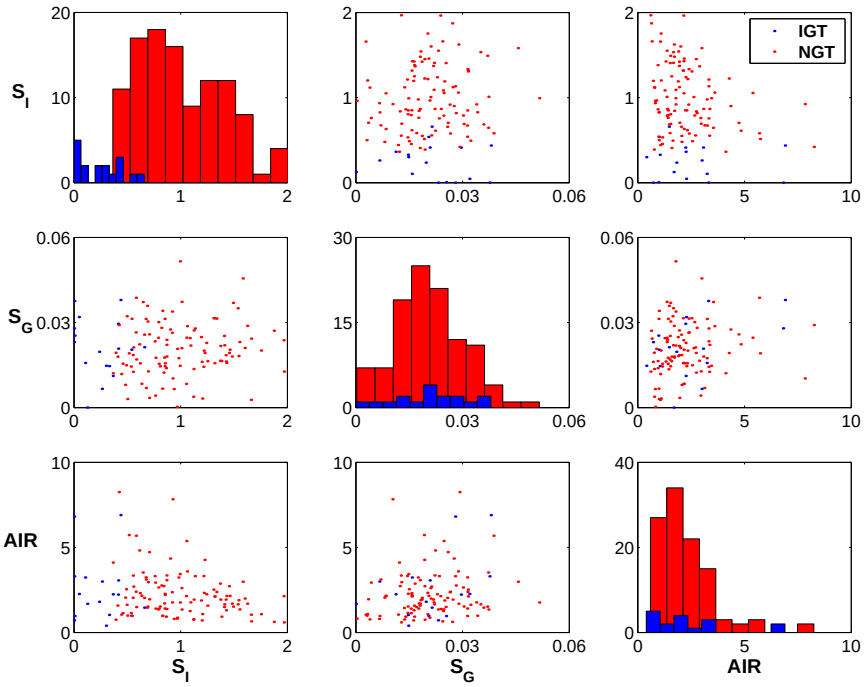

Figure 9.3: Matrix of scatter plots of S_I, S_G, and AIR_{0-8} with histograms in the diagonal for NGT (red) and IGT (blue) subjects.

The S_I values are clearly separated for NGT and IGT subjects while the S_G and AIR_{0-8} do not seem to be all that different for the two populations. The presence of S_I values indistinguishable from zero for four of the IGT subjects is a known and unexplained physiological phenomenon in the MM which suggests that it is too simple a model for the insulin/glucose system [38].

Since the disposition index, defined as the product of S_I and AIR_{0-8}, often is used to determine whether a particular NGT subject is likely to become IGT or diabetic, the scatter plot of AIR_{0-8} vs. S_I is shown in Figure 9.4 and further investigated in the following section.

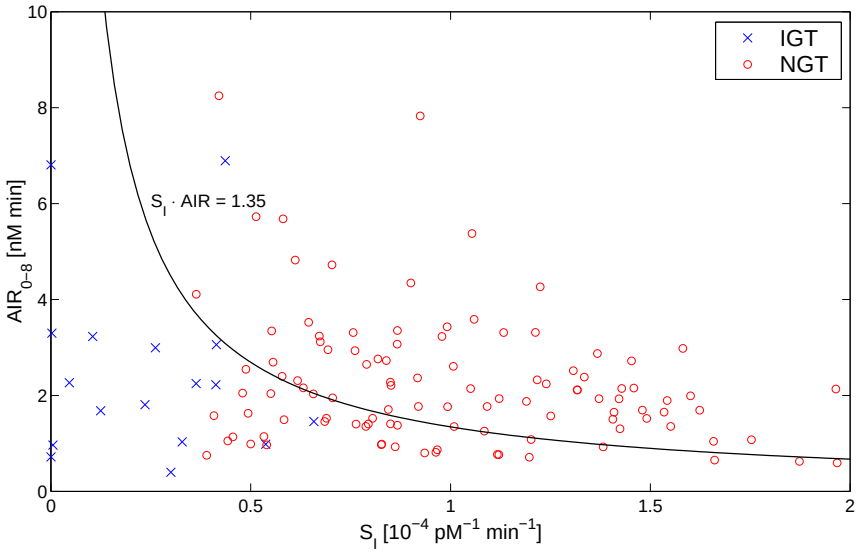

Figure 9.4: Scatter plot of AIR_{0-8} and S_I.

In the prediabetic phase, before developing IGT, the value of AIR_{0-8} tends to increase (rather than decrease) while the value of S_I decreases [54]. The value of AIR_{0-8} drops when going from NGT to IGT, causing the placement in a scatter plot of AIR_{0-8} vs. S_I of IGT subjects to be in an area just below the hyperbola of $AIR = k/S_I$ as shown in Figure 9.4. The value of k is calculated using the following discriminant function which minimizes the probability of misclassification when using only the value of the disposition index [15, p. 313]:

$$\begin{aligned} k = S_I \cdot AIR_{0-8} &= \frac{\frac{1}{2}\hat{\mu}_N^2\hat{\sigma}^{-2} - \frac{1}{2}\hat{\mu}_I^2\hat{\sigma}^{-2} + \log c}{\hat{\sigma}^{-2} \cdot (\hat{\mu}_N - \hat{\mu}_I)} \\ &= 1.35 \end{aligned} \tag{9.1}$$

where $\hat{\mu}_N$ and $\hat{\mu}_I$ are the estimated mean vectors of $S_I \cdot AIR_{0-8}$ for NGT and IGT subjects, respectively, $\hat{\sigma}$ is the estimated standard

deviation of $S_I \cdot AIR_{0-8}$, and $c = 1$ since no *a priori* knowledge about the expected loss is available.

1 IGT subject is misclassified as NGT while 35 NGT subjects are misclassified as IGT when using the discriminant function of $S_I \cdot AIR_{0-8} = 1.35$ which is equal to 6 % misclassification of the IGT subjects and 32 % of the NGT subjects. When using the information about the changes of the two indices S_I and AIR_{0-8} in the prediabetic stage, the NGT subjects just above the hyperbola and with large values of AIR_{0-8} are likely to become IGT. If the IVGTT had been performed on type I and II diabetic subjects, then the type II diabetics would be below the IGT subjects in the scatter plot and the type I diabetics would be below the type II diabetics.

A test is performed in the following to determine which indices contribute with additional information for separating the populations of NGT and IGT subjects in a discriminant analysis.

Mahalanobis' distance between the two populations is calculated using the full information from S_I, S_G, and AIR_{0-8} and on the basis of the reduced information using the estimated values of S_I only. The formula for Mahalanobis' distance is [15, pp. 309-329]:

$$D^2 = (\hat{\boldsymbol{\mu}}_N - \hat{\boldsymbol{\mu}}_I)^T \hat{\boldsymbol{\Sigma}}^{-1} (\hat{\boldsymbol{\mu}}_N - \hat{\boldsymbol{\mu}}_I) \tag{9.2}$$

where $\hat{\boldsymbol{\Sigma}}$ is the estimated dispersion matrix.

The two values of Mahalanobis' distance using the full and reduced information are:

$$\begin{aligned} D^2_{full} &= 4.1760 \\ D^2_{red} &= 3.9984 \end{aligned}$$

The test for the hypothesis that S_G and AIR_{0-8} do not contribute to an increase in the discrimination is:

$$Z = \frac{n_N - n_I - p - 1}{q} \cdot \frac{n_N \cdot n_I (D^2_{full} - D^2_{red})}{(n_N + n_I)(n_N + n_I - 2) + n_N \cdot n_I \cdot D^2_{red}} \tag{9.3}$$

where n_N and n_I are the number of NGT and IGT subjects, respectively, p is the total number of variables while $p - q$ is the reduced number of variables.

Z is thus a measure of the relative increase in the 'distance' between the two populations when going from $p - q$ to p variables. For the test to be accepted, it can be shown that $Z \in F(q, n_N + N_I - p - 1)$ and the hypothesis is rejected for large values of Z. The value of Z for the stated hypothesis is:

$$\begin{aligned} Z &= \frac{108 - 17 - 3 - 1}{2} \cdot \frac{108 \cdot 17(4.1760 - 3.9984)}{(108 + 17)(108 + 17 - 2) + 108 \cdot 17 \cdot 3.9984} \\ &= 0.8688 \end{aligned}$$

The hypothesis is therefore accepted since $Z < F(2, 108 + 17 - 3 - 1)_{0.95} = 3.071$. Thus, the additional information from the values of S_G and AIR_{0-8} does not contain additional information which can be used to distinguish between NGT and IGT subjects. The discriminant function which minimizes the probability of misclassification using only the values of S_I can be written as:

$$S_I \cdot \hat{\sigma}_{S_I}^{-2} \cdot (\hat{\mu}_N - \hat{\mu}_I) - \frac{1}{2}\hat{\mu}_N^2 \hat{\sigma}_{S_I}^{-2} + \frac{1}{2}\hat{\mu}_I^2 \hat{\sigma}_{S_I}^{-2} = \log c = 0 \tag{9.4}$$

By rewriting (9.4), the value of S_I which separates NGT and IGT subjects is estimated as:

$$\begin{aligned} S_I &= \frac{\frac{1}{2}(1.0074^2 - 0.2488^2)}{1.0074 - 0.2488} \\ &= 0.6281 \end{aligned} \tag{9.5}$$

Subjects with S_I values larger than 0.6281 are therefore classified as NGT while subjects with values below 0.6281 are classified as IGT. Only 1 IGT subject (6 %) is misclassified as NGT while 21 NGT subjects (19 %) are misclassified as IGT. The misclassification is thereby reduced using the discriminant function of S_I instead of the product of S_I and AIR_{0-8}.

9.1.6 Comparison with Estimates from MinMod

The estimates obtained with CTSM are compared with those from MinMod [25], a program for the estimation of parameters in the MM. The difference between MinMod and CTSM is that MinMod does not include a diffusion term in the system equations as CTSM does. The MinMod parameter estimates which are compared with the CTSM parameter estimates are taken from [23].

Scatter plots of the estimates of S_I and S_G from MinMod and CTSM are shown in Figure 9.5. Only 13 out of the 17 IGT subjects are plotted since the MinMod estimates of the remaining 4 IGT subjects are not available. The same applies for 11 of the 108 NGT subjects.

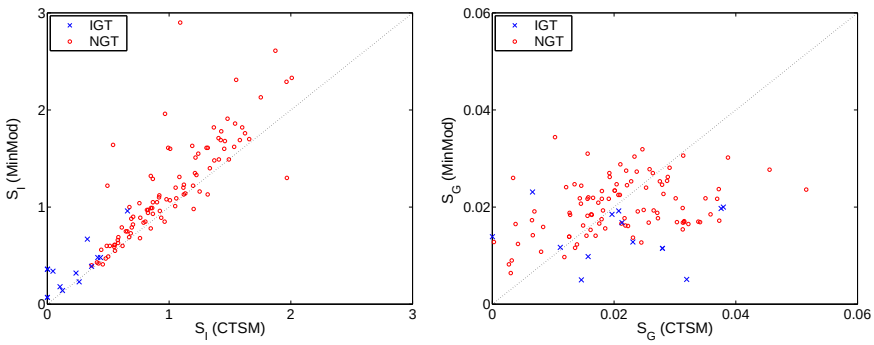

(a) S_I **(b)** S_G

Figure 9.5: Scatter plots of S_I and S_G from MinMod and CTSM.

The correlation coefficient is calculated as a measure of the strength of the association between the values of S_I estimated by MinMod and CTSM. The two estimates of S_I are reasonable correlated with a correlation coefficient of 0.8678. The scatter plot of S_I from MinMod and CTSM shows that the values are close to the dashed line dividing the scatter plot in two equal parts. The fact that most of the values are above the dashed line could be due to the noise term in the

system equations in CTSM. The estimated values of S_I from CTSM are lower than those from MinMod since the Wiener process accounts for disturbances and unmodelled dynamics of the system.

The estimates of S_G from the MM are generally less precise than those of S_I. This is partially because of the model assumption concerning the self-production of glucose which is assumed to be negligible. The correlation coefficient between the estimates of S_G using MinMod and CTSM is 0.3089 which is significantly lower than that of S_I. The big difference between the values of S_G from MinMod and CTSM shown in Figure 9.5(b) is probably due to the numerical instability of MinMod where the range of the glucose concentrations are from 0 to 10 while the range of the insulin concentrations are from 0 to 600 since the glucose is specified in mM and the insulin in pM. The accuracy of insulin is therefore much higher than that of glucose since the insulin measurements are weighted more in the calculation of the likelihood function. To avoid the numerical instability in the estimation of parameters in CTSM, the insulin concentrations are inserted in 10^{-1} μM as shown in Appendix B.4 to obtain values between 1 and 15.

9.1.7 Summary of IVGTT Results

The estimated parameters for the noise in the system equations of the MM are rather large indicating that the model is too simple and not sufficient in describing the complicated dynamical system of insulin and glucose during an IVGTT.

The sample mean of the insulin sensitivity index S_I estimated in CTSM is significantly different for NGT and IGT subjects while the values of S_G and AIR_{0-8} do not seem to be affected in the prediabetic phase. The value of S_I is therefore the only of these three measures which can be used to distinguish between NGT and IGT subjects in a statistical analysis.

The estimated values of S_I using CTSM are slightly lower than those

from the program MinMod. Since MinMod does not add noise parameters to the system equations, the values of S_I are overestimated. The correlation between the values of S_G using CTSM and MinMod is very little due to mentioned differences in the weighting of insulin and glucose measurements.

9.2 OGTT Models

The OGTT indices for the insulin sensitivity and beta-cell function presented in Section 8.3 are estimated and compared with the estimates of S_I and AIR_{0-8} from the IVGTT. The estimated indices from the OGTT are calculated for the same subjects as those from the IVGTT.

9.2.1 Insulin Sensitivity

Scatter plots of the estimates of the insulin sensitivity from four OGTT models vs. the CTSM estimates of S_I from the MM are illustrated in Figure 9.6 along with a fitted regression line and the squared multiple correlation (coefficient of determination) R^2.

The value of the R^2 statistics is generally the best indicator of the fit of a regression line and can be interpreted as the relative amount of variance of the dependent variable explained or accounted for by the explanatory variable.

The simplest of the four OGTT models is the HOMA model in the upper left hand corner of Figure 9.6. It is the only model where the regression line has a negative slope. The model with the lowest value of R^2 is the Cederholm model. The Stumvoll and Matsuda model seem to be the best OGTT models for deriving an insulin sensitivity index which is correlated with the S_I values from an IVGTT. The values of R^2 are almost the same for the two models where approximately 45 % of the variance in S_I from the MM can be explained by

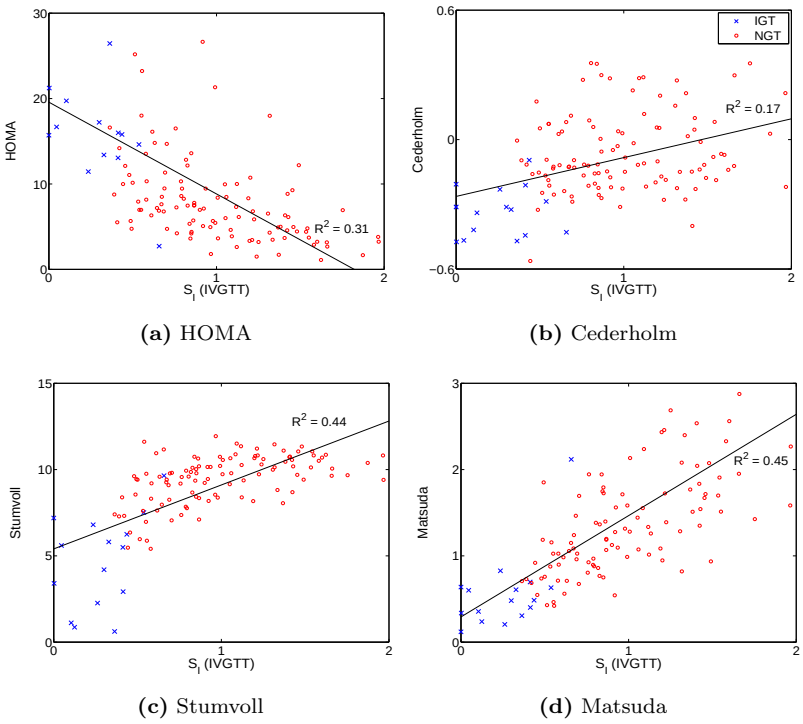

(a) HOMA **(b)** Cederholm

(c) Stumvoll **(d)** Matsuda

Figure 9.6: OGTT models for the insulin sensitivity.

the Stumvoll and Matsuda models. The values of R^2 for the regression of Stumvoll and Matsuda and the estimates of S_I from MinMod are 0.51 and 0.65, respectively [23]. The R^2 statistics are lower using the S_I estimates from CTSM than MinMod which probably is due to the OGTT models are derived using the estimates from MinMod and not CTSM.

9.2.2 Beta-cell Function

The OGTT models for the beta-cell function are compared with the values of the acute insulin response from the IVGTT. These results

are therefore not obtained using CTSM but are included for the completion of the OGTT.

The HOMA and Stumvoll index of the beta-cell function are calculated using equations (8.12) and (8.13) and compared with the estimates of AIR_{0-8} from the IVGTT in the scatter plots in Figure 9.7.

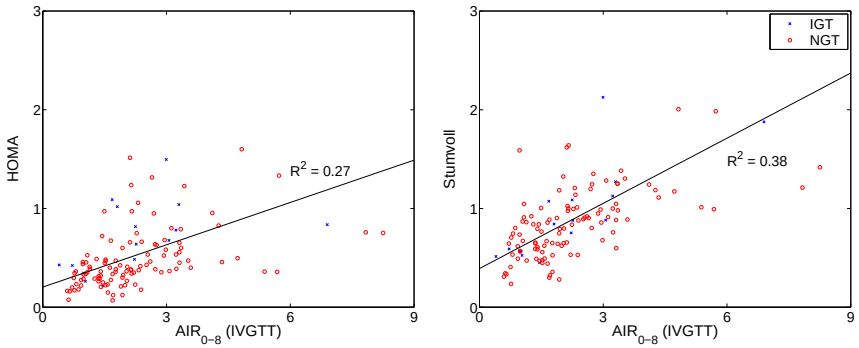

(a) HOMA **(b)** Stumvoll

Figure 9.7: OGTT models for the beta-cell function.

The OGTT models for the beta-cell function are not as accurate as the models for the insulin sensitivity. The R^2 statistics are only 0.27 and 0.38 for the HOMA and Stumvoll model, respectively. The two models therefore seem too simple at explaining the variation in AIR_{0-8} from the IVGTT.

9.2.3 Summary of OGTT Results

The results from the four OGTT models are not all equally successful in assessing the insulin sensitivity index S_I from an IVGTT estimated in CTSM. The two OGTT models which appear to be the best are the Stumvoll and Matsuda models with R^2 values of 0.44

and 0.45, respectively. These values are somewhat lower than previously published estimates using MinMod since the OGTT regression models are derived using the estimates from MinMod.

The accuracy of the two OGTT models for the beta-cell function are less than the models for the insulin sensitivity and seem to be too simple at predicting the acute insulin response from an IVGTT.

Chapter 10

Discussion

The primary focus of the discussion will be on the assumptions and results of the clamp and glucose tolerance models presented in the previous chapters along with a general discussion of the methods used for modelling the PK/PD of insulin. At the end of this chapter, the discussion is summarized as a direction for future work.

10.1 Euglycaemic Clamp Models

The euglycaemic clamp study is presented as a method of assessing the PK/PD of different types of insulin. The experiment is conducted in a way so that the secretion of insulin from the pancreas is suppressed so that it can be modelled using rather simple mathematical models.

10.1.1 PK Models and Assumptions

Since the insulin is injected both IV and SC, it is difficult to determine the PK of the absorption. Methods like the phase-plane method

[19] has been applied to the data from the clamp study but with no success since the phase-plane plots are obscured by the IV infusion of human insulin. First-order absorption of SC insulin, where the rate of absorption is dose dependent, is therefore assumed throughout this thesis while the absorption of IV insulin is assumed to follow zero-order kinetics since it is injected directly into the blood.

The bioavailability factor F is normally introduced in models with SC absorption due to degradation of insulin in the SC depot. Since the bioavailability of the SC injected insulin is not known for the two types of insulin, the value of F is fixed at 1 to ensure global identifiability of the single-compartment PK model. Compared with the estimates of the parameters in the single-compartment model where F is not fixed, the apparent volume of distribution is slightly increased when F is set equal to unity while the rate constants are not affected significantly. This assumption therefore seem quite reasonable and is not the issue of further discussion.

The obtained results with the single-compartment model are in agreement with the measured plasma insulin concentrations. The PK of insulin A and B are clearly different when considering the shape of the simulated concentration-time profiles as well as the summary measures of t_{max} and C_{max} but not the value of AUC_0^∞. Since F is eliminated from the model, k_a and k_e are the only parameters which can be used as measures of the differences between insulin A and B. The comparison indicates that it is the elimination kinetics of insulin B which are altered rather than the absorption kinetics when compared with insulin A. This observation is does not agree with the intended change in the primary structure of insulin B which should increase the absorption. This phenomena often occurs for drugs with fast elimination and is referred to as the 'flip-flop' effect. This effect is due to the fact that it is not always possible to separate what is k_a and k_e in the estimation. The 'flip-flop' effect can be circumvented by assuming that $k_a > k_e$, but since it is not possible to enter such assumptions in CTSM, the main difference between insulin A and B appears wrongly to be in the elimination kinetics.

Since the bioavailability factor cannot be used as a measure of the different availability of the two types of insulin due to identifiability issues and since the estimated parameters of the single-compartment model are physiological unlikely, the difference in SC absorption kinetics for insulin A and B are further examined by expanding the single-compartment model with compartments for the SC depot. The two different approaches considered are a model with compartments for the different association states of SC insulin and a model with a delay between the SC injection and absorption into the plasma along with degradation from the SC depot.

The hexamer/dimer SC uptake model is a modification of a similar model proposed in [55]. Five simplifying assumptions are made to make the model suitable for estimation since the original model only has been validated through simulation. The slower uptake of insulin A than B is explained by the equilibrium between hexamer and dimer is shifted faster towards that of dimer for insulin B since the dimer structure is stabilized. These different properties of insulin A and B are verified from the estimated model and the simulated plasma insulin concentrations are similar to those of the single-compartment model. The parameter estimates of the apparent volume of distribution for insulin A and B are reduced significantly to more likely values. Unfortunately, the uncertainty of the parameter estimates of the hexamer/dimer model are quite large. Especially the uncertainties of the parameters for the equilibration between hexamer and dimer, i.e. P and Q, are so high that the parameters are insignificant on a 95 % confidence level. The estimated values of the noise in the system equations of hexamer and dimer insulin also indicate that the PK of the insulin in the SC depot are not fully captured.

Since the hexamer/dimer model does not seem to be suitable for estimation even after applying some simplifying assumptions, a more empirical and parsimonious approach is attempted in the two-compartment SC uptake model. The characteristics of insulin A and B in the SC depot are the same as in the hexamer/dimer model. The estimated values of the apparent volume of distribution are almost equal

for the two types of insulin and close to the physiological plasma volume in the two-compartment model and the uncertainties of the parameters in the two-compartment model are considerably less than in the hexamer/dimer model. This model is therefore preferred compared to the hexamer/dimer model. The simplifying assumptions of the same rate constant k_a for the transfer between the two SC compartments and the absorption into the central compartment along with the fixed parameter for the SC degradation to make the model *a priori* identifiable are assumptions that cannot be validated from the measured plasma insulin concentrations. Compared with the single-compartment model, the two-compartment model adds insight to the different absorption kinetics of the two types of insulin but does not contribute with a better description of the plasma insulin concentrations.

All of the PK models, with the exception of the peripheral-compartment model, incorporate the common assumption that the elimination of insulin from the plasma is a first-order process. This is a drastic assumption since true first-order elimination applies only to compounds that are eliminated exclusively by mechanisms that do not involve enzymatic or transport processes, i.e. processes that require energy. Another simplifying assumption is that the rate constant for elimination is a true constant and is independent of the drug concentration. The percentage of the plasma insulin that is eliminated pr. unit time is therefore constant and any saturable elimination kinetics are neglected. Nevertheless, the elimination of insulin seems to be adequately described by the first-order elimination rate constant k_e. The reason why the insulin exhibit apparent first-order elimination kinetics in most cases is that the plasma insulin concentrations are well below those required to saturate the processes involved.

To investigate if saturable elimination kinetics are present in the elimination of plasma insulin, the elimination of insulin is described in the form of Michaelis-Menten elimination kinetics in the peripheral-compartment model. Michaelis-Menten kinetics is a combination of zero- and first-order kinetics and is a generally accepted expression

for the elimination of drug from the organism. Furthermore, the plasma insulin equilibration with tissue is included in the peripheral-compartment model. This reduces the apparent volume of distribution dramatically for insulin A while the estimates for insulin B do not seem to have converged. Unfortunately, the number of parameters to be estimated in the peripheral-compartment model seem to exceed the number of parameters which can be identified from the experimental data since the correlation and uncertainty of the parameter estimates are quite high. For the peripheral-compartment model to work, information about the insulin equilibration with tissue or the Michaelis-Menten parameters must be specified thereby reducing the number of parameters to be estimated. The information about the Michaelis-Menten parameters can perhaps be obtained by performing different experiments where the insulin is administered in different doses while the insulin equilibration with tissue can be assessed by labelling the injected insulin which thereby acts as a tracer for the distribution.

The various PK models presented in this thesis produce rather similar predictions/simulations of the plasma insulin concentrations. The different expansions of the single-compartment model add valuable insights about the differences of the two types of insulin but are not considered for the PK/PD models since the parsimonious description of the single-compartment model is adequate at describing the PK of insulin which is needed to build a PK/PD model.

10.1.2 PK/PD Models and Assumptions

The primary objective of PK/PD modelling in this thesis is to identify key properties of insulin *in vivo* and thereby characterize and predict the insulin effect under physiologic conditions.

First of all, it is essential to identify the significance of the biological processes involved in eliciting the insulin-induced response. The delay between the plasma insulin concentration and the amount of

glucose needed to maintain a constant blood glucose concentration is illustrated through a counter-clockwise hysteresis loop in a phase-plot of GIR vs. C_I (see Figure 6.5). The delay for treatment with insulin B is significantly larger than for insulin A but the phase-plot cannot explain whether or not the delay is due to a distributional delay or an indirect response mechanism. These two possibilities are therefore tested in an attempt to determine which model is best at describing the delay.

The effect-compartment model, where the before mentioned delay is assumed to be distributional, has previously been applied with success to clamp studies of insulin. Instead of specifying the PD parameters using *in vitro* data, the approach is to investigate the possibility of estimating the PK and PD simultaneously. This approach seems more reasonable since the PK and PD of insulin are interdependent.

The obtained estimates of the three PD parameters are similar to those from *in vitro* studies which indicates that the simultaneous estimation of PK and PD parameters is successful. The estimate of the maximum effect E_{max} for treatment with insulin A is made difficult since the observed effect of insulin A only assumes values in the linear area between 20 % and 80 % effect. To circumvent these estimation problems, the maximum effects of insulin A and B are assumed to be identical for the same subject. Since the observed effects are well below the value of E_{max}, this assumption seems reasonable.

The parameter EC_{50}, which can be interpreted as the insulin concentration producing 50 % of the maximum effect, contributes with information about the concentration needed to produce a clinical observable effect. The sample means of EC_{50} for treatment with insulin A and B are almost equal which also is expected since the change in the primary structure of insulin B should not change the PD properties significantly but only the absorption kinetics of the molecule.

The final PD parameter which is estimated is the sigmoidicity factor

γ. The estimated value of $\gamma \approx 2$ for many of the subjects in the study is similar to the expected value from a theoretical point of view since the estimated value of γ can be interpreted as the number of insulin molecules it takes to elicit the transport of glucose into the cells.

The derived parameters of t_{max}, C_{max}, TR_{max}, and R_{max} are estimated using the simulated time series of plasma insulin and GIR, respectively. The uncertainties of the derived parameters in this thesis are therefore much lower compared with the procedures in previous insulin studies where the derived parameters are estimated using the sparse information of only a few measurements in the determination of the maximum concentration and effect.

The drawbacks of the effect-compartment model is that several different doses of insulin preferably should be used to validate the use of an indirect link model such as the 'black box' approach of the effect-compartment model. Since this information is not available for the current clamp study, the model cannot be further validated except by comparing the simulated and observed response GIR. Another problem with the effect-compartment model is that the estimated PD parameters are not reasonable for all the subjects in the study. The doubtful estimates are investigated further by changing the initial estimates but without success. The subjects with doubtful PD parameters are not removed from the study since the estimation procedure seems to have converged and the simulated time series of GIR are similar to the measurements.

Instead of ascribing the delay to be distributional in nature as in the effect-compartment model, an indirect response model where the delay is assumed to be caused by a delay downstream from the insulin receptor, is applied to the data from the clamp study. This approach is the physiological most likely but has not been used in previous clamp studies because of the experimental procedures. The variation of GIR is quite large since the amount of glucose infused is regulated by a nurse in the attempt to keep the blood glucose concentration at the clamped level. The nurse uses the values of the measured blood glucose concentration from the previous minute to determine

how much glucose should be infused. If the nurse infuses too much glucose, the glucose will rise above the clamped level and the nurse must wait until the glucose returns to the clamped level because the GIR only assume values larger than zero since glucose cannot be withdrawn from the plasma.

When comparing the ability of the effect-compartment model and the indirect response model to predict the response to the injected insulin, it seems like it is better to use the GIR as a measure of the utilized glucose rather than trying to add a compartment for the blood glucose concentration where GIR is used as an input. The effect-compartment model is therefore preferred compared to the indirect response model.

10.2 Glucose Tolerance Models

Glucose tolerance tests are a commonly used technic to determine metabolic indices of possible diabetics. Compared with the euglycaemic clamp study where the insulin production is suppressed and the blood glucose concentration is clamped manually by varying the glucose infusion, the glucose tolerance tests use an open-loop approach where no 'external' regulation is present. The feedback mechanisms of the insulin/glucose system therefore has to be included in mathematical models of the glucose tolerance tests.

10.2.1 IVGTT

The IVGTT is a reasonably simple experiment yielding an informative set of data about the glucose tolerance of a subject by estimating parameters referring both to insulin-dependent and insulin-independent glucose uptake in the MM proposed by Bergman *et al.* [7].

The estimation of 125 out of the 288 subjects in the IVGTT is successful and the glucose residuals are not far from being white noise.

The validity of the present MM analysis using grey-box modelling is somehow diminished by the many subjects for whom it is impossible to estimate a reasonable set of parameters. Since this is a known problem in previous MM analyses of IVGTT, it will not be discussed any further.

The simplifying assumption of the single-compartment glucose distribution in the MM was initially implemented by Bergman *et al.* [7] so that the MM parameters could be estimated from a single, relative simple experimental procedure. The consequences of the single-compartment glucose kinetics approximation are investigated using the estimated system noise parameter σ_G in the grey-box MM which indicates that the unmodelled dynamics of the system is considerable.

The effect of undermodelling the glucose kinetics seems to result in an overestimation of the glucose effectiveness S_G to fit the glucose data, especially for IGT subjects. The insulin action X is thereby underestimated until the glucose returns to the baseline and is overestimated thereafter. This structural bias introduced by glucose model simplifications also affects the estimation of the insulin sensitivity index since S_I can be expressed as the ratio between the AUC of insulin action and the insulin concentration above basal level. The insulin sensitivity index S_I is thereby underestimated. Furthermore, the occurrence of S_I values indistinguishable from zero for IGT subjects is not negligible in the MM and might be a consequence of overestimating S_G. The overestimation of the glucose effectiveness S_G might also be a result of combining the hepatic and peripheral components of S_G in a single parameter in the MM, i.e. parameter p_1.

In previous IVGTT studies, the overestimation of S_G in MinMod is also caused by the glucose concentration is specified in mM while the insulin concentration is in pM. The consequence is that the insulin measurements are weighted more in the calculation of the likelihood function. This numerical problem is avoided in this thesis by inserting the values of the glucose and insulin concentrations in mM and 10^{-1} μM, respectively.

The wide rage of insulin sensitivity, glucose effectiveness, and acute insulin response due to the inter-individual variability of these indices for NGT and IGT subjects makes it difficult to distinguish between NGT and IGT subjects since the thresholds between the two populations overlap each other. NGT and IGT subjects are often separated in a discriminant analysis using the disposition index $S_I \cdot AIR_{0-8}$. A discriminant analysis using only the values of S_I for NGT and IGT subjects results in a lower misclassification than when using the disposition index and the test for further information using the values of S_G and AIR_{0-8} along with S_I is rejected. The MM does therefore not seem adequate enough for providing metabolic indices other than the insulin sensitivity index S_I which can be used at separating NGT from IGT subjects.

From a dynamical point of view, it would be desirable to build a combined model of glucose and insulin kinetics but the coupling of the two parts of the MM has been shown not to be appropriate in a formal study of the MM [20]. In the search for more accurate predictions of possible diabetic patients, several new IVGTT models have been derived. They all include injection of labelled glucose which is why these models are not considered in this thesis.

10.2.2 OGTT

The best OGTT model for insulin sensitivity is the Matsuda index using fasting and mean values of the insulin and glucose concentration from the OGTT. The Matsuda index explains 45 % of the variance in the estimates of S_I from the MM of the IVGTT while the three other OGTT models explain from 17 % to 44 % of the variance. Compared with previous OGTT studies, the R^2 values in this thesis are somewhat lower. This is probably due to the OGTT regression models are derived to obtain the maximum correlation with the estimates of S_I from MinMod and not the estimates from CTSM which are slightly lower.

The OGTT models for the beta-cell function are compared with the estimates of the acute insulin response AIR_{0-8} from the IVGTT which is not estimated using the principles of grey-box modelling. The models are nevertheless included for the completion of the OGTT. The Stumvoll index for the beta-cell function explains 38 % of the variance in AIR_{0-8} from the IVGTT while the R^2 statistics for the HOMA index is 0.27. The accuracy of the OGTT models for the beta-cell function is highly doubtful and seem to be too simple at deriving indices which are correlated with those from an IVGTT.

The assessment of S_I and AIR_{0-8} from an IVGTT using the measurements from an OGTT along with different regression models do not seem overwhelmingly accurate. The OGTT models should preferably be revised before being used in large-scale epidemiological studies of NGT and IGT subjects.

10.3 Grey-box PK/PD Modelling of Insulin

The usefulness of grey-box PK/PD modelling of insulin is discussed in this section in the light of the obtained results from the two different insulin studies in this thesis.

The structural identifiability of the linear models is investigated since it is of key importance for well-posedness of the parameter estimation of physiological systems to ensure the uniqueness of the solution for the unknown model parameters. Unfortunately, the identifiability of the non-linear models is not investigated since it is far more complicated and outside the scope of this thesis. The correlation between model parameters though seem to indicate an over-parameterization in some of the non-linear models.

Another issue concerning identifiability has to do with the experimental data. The data from the clamp study does not seem to be persistently excited due to the experimental procedures of the study and the constraints in human clinical studies. All the dynamics of

the insulin/glucose system are therefore not represented in the measured data. The estimates of the noise term in the system equations are estimated to zero in most of the presented clamp models and it is difficult to determine whether the models capture all of the dynamics of the insulin/glucose system or if it is because the dynamics are not present in the measured data. To make full use of grey-box PK/PD modelling, the experimental data from clamp studies of insulin therefore needs to be more excited.

The experimental data from the glucose tolerance studies are much more excited than that of the clamp study and the estimated noise parameters in the system equations symbolizing disturbances and unmodelled dynamics indicate that the minimal model of glucose kinetics is too simple and should be revised.

10.4 Future Work

The reflections of the present work are summarized in the following section as a direction and perspective for future work.

10.4.1 Euglycaemic Clamp Study

The presented PK/PD models of the clamp study seem to be successful in capturing the dynamics of the insulin/glucose system. The next step in modelling the clamp study would be to use a population PK/PD approach instead of the individual approach applied in this thesis. Since the data from the clamp study is balanced, i.e. the insulin, GIR, and BG measurements are sampled at the same time points for all the subjects, it can easily be used in population modelling.

The estimation of population and individual parameters, one at a time, using MAP estimates for the population parameters would require some sort of recursive estimation scheme so that all the infor-

mation gathered after the twenty estimations would be used to estimate the parameters for the twenty subjects once again. At present, CTSM is not suitable for population PK/PD modelling since the recursive estimation scheme has not been implemented yet and it is therefore not possible to estimate population and individual parameters.

Instead of using CTSM for population modelling, the statistical program S-Plus could preferably be used since population modelling already is implemented using non-linear mixed-effect models. The estimation of parameters for the inter- and intravariability between subjects is performed using algebraic instead of differential equations. The Wiener process is therefore not applied to the state equations of the system. This can be justified since the noise parameters in the system equations are estimated to zero in CTSM. The non-linear mixed-effect model of the insulin concentration for individual i at time t_j can thereby be written as [43, pp. 273-287]:

$$C_{ij} = (\beta_1 + b_{1i}) \cdot e^{-(\beta_2+b_{2i})t_j} + (\beta_3 + b_{3i}) \cdot e^{-(\beta_4+b_{4i})t_j} + \epsilon_{ij} \quad (10.1)$$

where the fixed effect β_1, β_2, β_3, and β_4 represent the mean values of the parameters in the population of individuals and the individual deviations are represented by the random effect b_{1i}, b_{2i}, b_{3i}, and b_{4i} which are assumed to be distributed normally with mean 0 and variance-covariance matrix Ψ. The random effects corresponding to different individuals are assumed to be independent while the within-group errors ϵ_{ij} are assumed to be independently distributed as $N(0, \sigma^2)$ and to be independent of the random effects.

As a final suggestion for future work of modelling the PK/PD of the clamp study, it would be interesting to include pharmacological knowledge in the PK/PD models to make them more mechanistic instead of empirical along with a more physiological modelling approach where the body is divided into compartments based on true anatomical regions or volumes such as e.g. blood, heart, and liver. This approach seems very unlikely to succeed using the sparse information about the dynamics of the insulin/glucose system which

is represented in the present measurements since the system is not excited enough. It will perhaps be possible to build and estimate a physiological model of the insulin/glucose system if measurements of the renal and urine excretion are available and by distributing different doses of labelled and unlabelled insulin.

10.4.2 Glucose Tolerance Studies

From the present analysis of the MM using grey-box modelling, the model of glucose kinetics seems too simple to estimate metabolic indices which can be used to assess the differences of NGT and IGT subjects. Furthermore, the glucose and insulin kinetics are fitted separately in the MM. It would be desirable to have a model representing the whole dynamical system of insulin and glucose. By fitting the two parts simultaneously, a more coherent dynamical model is obtained using the entire set of observations.

IVGTT studies indicate that the MM of glucose kinetics needs to be expanded with an additional compartment for the glucose distribution to obtain a more reasonable model due to the limitations of the mono-compartmental representation of glucose kinetics at non steady-state. To estimate parameters in such models, it is necessary to use labelled glucose to investigate the distribution of glucose and to be able to separate the injected glucose from the hepatic glucose production.

A two-compartment minimal model has been presented in [10] which provides a physiologically plausible profile of endogenous glucose production during the IVGTT along with indices of the glucose effectiveness and insulin sensitivity. Furthermore, the estimates of the glucose effectiveness and the plasma clearance rate are singled out in the two-compartmental minimal model compared to the original minimal model which is unable to separate the two estimates.

The OGTT regression models which are used in this thesis are derived using the MinMod estimates. It would therefore be interesting

to build new OGTT regression models for the insulin sensitivity and beta-cell function using the grey-box estimates from CTSM to evaluate the possibility of getting better predictions of the metabolic indices from an IVGTT using OGTT measurements.

Chapter 11

Conclusion

The purpose of this thesis is to model the *in vivo* dynamical system of insulin and glucose using grey-box PK/PD modelling where a stochastic term is added to a derived PK/PD model to represent disturbances and unmodelled dynamics of the physiological system.

The grey-box PK/PD modelling method is applied to two insulin studies. All PK/PD models presented in this thesis are implemented in the program CTSM and the parameters are estimated using ML estimation.

Several different PK and PK/PD models are tested and compared for the euglycaemic clamp study to determine the characteristics of two types of insulin, i.e. insulin A and B. The single-compartment model presented in this thesis is the simplest and most parsimonious PK model consisting of a central compartment with first-order absorption of SC insulin and first-order elimination. This model is shown to be adequate at capturing the different PK of insulin A and B and the derived PK parameters show that insulin A is a slower and longer lasting insulin than insulin B.

The purpose of modelling the euglycaemic clamp study is also to investigate the possibility of estimating the PK and PD of insulin

simultaneously. The effect-compartment model where the apparent delay between the plasma insulin concentration and the observed response is assumed to be distributional, is suitable for predicting the PD response with the Hill response equation as the effect model. The estimated PD parameters of the effect-compartment model are similar to those estimated from *in vitro* studies which is why the simultaneous estimation of PK and PD parameters is concluded to be successful.

The estimates of the diffusion term in the stochastic differential equations representing disturbances and unmodelled dynamics of the insulin/glucose system are insignificant in most of the clamp models. The proposed models therefore seem to capture the dynamics of the *in vivo* insulin/glucose system but it is difficult to make any conclusions since the experimental data from the clamp study is not persistently excited.

The focus of the two glucose tolerance tests presented in this thesis is to compare the grey-box estimates with previously published results.

The minimal model of glucose kinetics is used to model the data from the IVGTT. Out of the three metabolic indices which are estimated from the minimal model, the insulin sensitivity index S_I, a measure of the insulin-dependent glucose elimination, is the only one which can be used to distinguish between normal and impaired glucose tolerant subjects.

The grey-box estimates of S_I are lower than previously published results using the program MinMod due to the added diffusion term in the system equations. The estimated noise parameters indicate that the minimal model of glucose kinetics is too simple and should preferably be revised.

The presented regression models for the OGTT are used to investigate the correlation with the estimates of the insulin sensitivity and beta-cell function from the IVGTT. The OGTT estimates are not very correlated with the indices from the IVGTT and it can therefore be concluded that the OGTT models are too simple and cannot

be used to make accurate predictions of the indices from an IVGTT.

Hopefully, this novel way of modelling the PK/PD of insulin will lead to a better understanding of the *in vivo* system of insulin and glucose and thereby come up with better ways to treat diabetes.

Bibliography

[1] Leon Aarons, Mats O. Karlsson, France Mentré, Ferdinand Rombout, Jean-Louis Steimer, and Achiel van Peer. Role of modelling and simulation in phase 1 drug development. *European Journal of Pharmaceutical Sciences*, 13:115–122, 2001.

[2] M. Albareda, J. Rodriguez-Espinosa, M. Murugo, A. de Leiva, and R. Corcoy. Assesment of insulin sensitivity and beta-cell function from measurements in the fasting state and during an oral glucose tolerance test. *Diabetologia*, 43:1507–1511, 2000.

[3] Kurt Munk Andersen. *Matematisk analyse i modeller for kemiske systemer*. Institut for Matematik, DTU, 2000.

[4] James Arima, Dale Chah, Timothy Ham, and Alvin Liem. Analysis of intravenous glucose tolerance. http://www.ugrad.cs.jhu.edu/ liemat/seminar1/outlinec.htm.

[5] American Diabetes Association. Consensus development conference on insulin resistance. *Diabetes Care*, 21(2):310–314, 1998.

[6] Stefania Audoly, Giuseppina Bellu, Leontina D'Angiò, Maria Pia Saccomani, and Claudio Cobelli. Global identifiability of nonlinear models of biological systems. *IEEE Transactions on Biomedical Engineering*, 48(1):55–65, 2001.

[7] Richard N. Bergman, Y. Ziya Ider, Charles R. Bowden, and Claudio Cobelli. Quantitative estimation of insulin sensitivity.

American Journal of Physiology, 236(6):E667–E677, 1979.

[8] Richard N. Bergman, Lawrence S. Phillips, and Claudio Cobelli. Physiologic evalution of factors controlling glucose tolerance in man. *Journal of Clinical Investigation*, 68:1456–1467, 1981.

[9] George E. P. Box and Gwilym M. Jenkins. *Time Series Analysis: Forecasting and Control*. Holden-Day, San Francisco, 1976.

[10] Andrea Caumo and Claudio Cobelli. Hepatic glucose production during the labelled ivgtt: Estimation by deconvolution with a new minimal model. *American Journal of Physiology*, 264:E829–E841, 1993.

[11] Andrea Caumo, Paolo Vicini, Jeffrey J. Zachwieja, Angelo Avogaro, Kevin Yarasheski, Dennis M. Bier, and Claudio Cobelli. Undermodelling affects minimal model indexes: Insights from a two-compartment model. *American Journal of Physiology*, 276:E1171–E1193, 1999.

[12] M. J. Chapman and K. R. Godfrey. Nonlinear compartmental model indistinguishability. *Automatica*, 32(3):419–422, 1996.

[13] M. J. Chappell, N. D. Evans, K. R. Godfrey, and M. J. Chapman. Structural identifiability of controlled state space systems: A quasi-automated methodology for generating identifiable reparameterisations of unidentifiable systems. In *Symbolic Computation for Control (Ref. No. 1999/088), IEE Colloquium*, pages 8/1–812, 1999.

[14] Knut Conradsen. *En Introduktion til Statistik, Bind 1*. Informatics and Mathematical Modelling (IMM), DTU, 1999.

[15] Knut Conradsen. *En Introduktion til Statistik, Bind 2*. Informatics and Mathematical Modelling (IMM), DTU, 2001.

[16] D. Z. D'Argenio and A. Schumitzky. *ADAPT II: Interactive Mathematical Software for Pharmacokinetic/Pharmacodynamic Systems Analysis. User's Guide*, 1990. http://bmsr.usc.edu/Software/Adapt/adptmenu.html.

[17] Hartmut Derendorf. Pharmacodynamic aspects of systemic drug delivery. *Drug Development and Industrial Pharmacy*, 20(4):485–502, 1994.

[18] Agamemnon Despopoulos and Stefan Silbernagl. *Color Atlas of Physiology*. Thieme Medical Publishers, Inc., New York, 4. edition, 1991.

[19] Aristides Dokoumetzidis and Panos Macheras. Investigation of absorption kinetics by the phase plane method. *Pharmaceutical Research*, 15(8):1262–1269, 1998.

[20] Andrea De Gaetano and Ovide Arino. Mathematical modelling of the intravenous glucose tolerance test. *Journal of Mathematical Biology*, 40:136–168, 2000.

[21] Jogarao V. S. Gobburu and William J. Jusko. Role of dosage regimen in controlling indirect pharmacodynamic responses. *Advanced Drug Delivery Reviews*, 46:45–47, 2001.

[22] Miriam Gutt, Catherine L. Davis, Susan B. Spitzer, Maria M. Llabre, Mahendra Kumar, Eileen M. Czarnecki, Neil Schneiderman, Jay S. Skyler, and Jennifer B. Marks. Validation of the insulin sensitivity index (isi): Comparison with other measures. *Diabetes Research and Clinical Practice*, 47:177–184, 2000.

[23] T. Hansen, T. Drivsholm, S. A. Urhammer, R. T. Palacios, A. Vølund, K. Borch-Johnsen, and Oluf Pedersen. Ogtt derived insulin sensitivity and beta-cell function. Novo Nordisk, 2000.

[24] http://www.blc.arizona.edu/courses/181gh/rick/expression2/translation.html.

[25] http://www.winsaam.com/minmod.htm.

[26] James R. Jacobs and Eric A. Williams. Algorithm to control "effect compartment" drug concentrations in pharmacokinetic model-driven drug delivery. *IEEE Transactions on Biomedical Engineering*, 40(10):993–999, 1993.

[27] Judith L. Jacobsen. Glucose infusion rate and insulin data for a randomised crossover trial to compare the pharmacodynamic response between a single dose of two different insulins in healthy volunteers during a euglycaemic clamp. Novo Nordisk, 2002.

[28] Steven Kang, Jens Brange, Anna Burch, Aage Vølund, and David R. Owens. Subcutaneous insulin absorption explained by insulin's physiochemical properties: Evidence from absorption studies of soluble human insulin and insulin analogues in humans. *Diabetes Care*, 14(11):942–948, 1991.

[29] Niels Rode Kristensen, Henrik Melgaard, and Henrik Madsen. *CTSM 2.0, User's Guide*, 2001.

[30] Wojciech Krzyzanski and William J. Jusko. Indirect pharmacodynamic models for responses with multicompartmental distribution or polyexponential disposition. *Journal of Pharmacokinetics and Pharmacodynamics*, 28(1):57–78, 2001.

[31] Julie Laurin, François Donati, Fahima Nekka, and France Varin. Peripheral link model as an alternative for pharmacokinetic-pharmacodynamic modeling of drugs having a very short eliminations half-life. *Journal of Pharmacokinetics and Pharmacodynamics*, 28(1):7–25, 2001.

[32] Eleanor Lawrence, editor. *Henderson's Dictionary of Biological Terms*. Prentice Hall, 2000.

[33] Henrik Madsen and Jan Holst. *Modelling Non-Linear and Non-Stationary Time Series*. Informatics and Mathematical Modelling (IMM), DTU, 2000.

[34] A. Mari. Assessment of insulin sensitivity and secretion with the labelled intravenous glucose tolerance test: Improved modelling analysis. *Diabetologia*, 41:1029–1039, 1998.

[35] Andrea Mari, Giovanni Pacini, Elaine Murphy Bernhard Ludvik, and John J. Nolan. A model-based method for assessing insulin sensitivity from the oral glucose tolerance test. *Diabetes Care*, 24(3):539–548, 2001.

[36] Masafumi Matsuda and Ralph A. DeFronzo. Insulin sensitivity indices obtained from oral glucose tolerance testing. *Diabetes Care*, 22(9):1462–1470, 1999.

[37] B. Meibohm and H. Derendorf. Basic concepts of pharmacokinetic/pharmacodynamic (pk/pd) modelling. *International Journal of Clinical Pharmacology and Therapeutics*, 35(10):401–413, 1997.

[38] Ta-Chen Ni, Marilyn Ader, and Richard N. Bergman. Reassessment of glucose effectiveness and insulin sensitivity from minimal model analysis: A theoretical evaluation of the single-compartment glucose distribution assumption. *Diabetes*, 46:1813–1821, 1997.

[39] Henrik Aalborg Nielsen and Henrik Madsen. A generalization of some classical time series tools. *Computational Statistics and Data Analysis*, 37:13–31, 2001.

[40] Patrice Nony, Michel Cucherat, and Jean-Pierre Boissel. Revisiting the effect compartment through timing errors in drug administration. *Trends in Pharmacological Sciences*, 19:49–54, 1998.

[41] Gianluca Nucci and Claudio Cobelli. Models of subcutaneous insulin kinetics. a critical review. *Computer Methods and Programs in Biomedicine*, 62:249–257, 2000.

[42] José Pérez-Urizar, Vinicio Granados-Soto, Francisco J. Flores-Murrieta, and Gilberto Casta neda Hernández. Review article: Pharmacokinetic-pharmacodynamic modeling: Why? *Archives of Medical Research*, 31:539–545, 2000.

[43] José C. Pinheiro and Douglas M. Bates. *Mixed-effects models in S and S-PLUS*. Springer-Verlag, New York, 2000.

[44] Søren Rasmussen. *Noter i farmakomatematik*. Forlaget ved Danmarks Farmaceutiske Højskole, 1985.

[45] Amarnath Sharma and William J. Jusko. Characterization of four basic models of indirect pharmacodynamic responses. *Journal of Pharmacokinetics and Biopharmaceutics*, 24(6):611–635, 1996.

[46] Lewis B. Sheiner. Commentary to pharmacokinetic/pharmacodynamic modeling: What it is! *Journal of Pharmacokinetics and Biopharmaceutics*, 15:553–555, 1987.

[47] Lewis B. Sheiner, D. R. Stanski, S. Vozeh, R. D. Miller, and J. Ham. Simultaneous modelling of pharmacokinetics and pharmacodynamics: Application to d-tubocurarine. *Clinical Pharmacology and Therapeutics*, 25:358–371, 1979.

[48] Giovanni Sparacino, Chiara Tombolato, and Claudio Cobelli. Maximum-likelihood versus maximum *a posteriori* parameter estimation of physiological system models: The c-peptide impulse response case study. *IEEE Transactions on Biomedical Engineering*, 47(6):801–811, 2000.

[49] Lubert Stryer. *Biochemistry*. W. H. Freeman and Company, New York, 4. edition, 1999.

[50] Michael Stumvoll, Asimina Mitrakou, Walkyria Pimenta, Trond Jensen, Hannele Yki-Jarvinen, Timon Van Haeften, Walter Renn, and John Gerich. Use of the oral glucose tolerance test to assess insulin release and insulin sensitivity. *Diabetes Care*, 23(3):295–301, 2000.

[51] Jeppe Sturis. *Possible Mechanisms Underlying Slow Oscillations of Human Insulin Secretion*. PhD thesis, The Technical University of Denmark, 1991.

[52] Peter Veng-Pedersen. An introduction to pharmacokinetics and pharmacodynamics in pharmaceutical r&d, 1st of May 2002. Presentation at half-day meeting about PK/PD at Novo Nordisk A/S.

[53] Paolo Vicini, Andrea Caumo, and Claudio Cobelli. Glucose effectiveness and insulin sensitivity from the minimal models:

Consequences of undermodeling assessed by monte carlo simulation. *IEEE Transactions on Biomedical Engineering*, 46(2):130–137, 1999.

[54] Aage Vølund. *Personal correspondance with Aage Vølund*, 23rd of April 2002. Novo Nordisk A/S.

[55] P. Wach, Z. Trajanoski, P. Kotanko, and F. Skrabal. Numerical approximation of mathematical model for absorption of subcutaneously injected insulin. *Medical & Biological Engineering & Computing*, 33:18–23, 1995.

[56] Jørgen Warberg. *Human Fysiologi*. Polyteknisk Forlag, 4. edition, 1998.

[57] Greg Welch and Gary Bishop. An introduction to the kalman filter. *Department of Computer Science, University of North Carolina at Chapel Hill*, 1997.

[58] Peter G. Welling. *Pharmacokinetics: Processes and Mathematics*. American Chemical Society, Washington, D.C., 1986.

[59] James R. Woodworth, Daniel C. Howey, and Ronald R. Bowsher. Establishment of time-action profiles for regular and nph insulin using pharmacodynamic modeling. *Diabetes Care*, 17(1):64–69, 1994.

[60] James R. Woodworth, Daniel C. Howey, Ronald R. Bowsher, Rocco L. Brunelle, Howard Rowe, Joyce Compton, and Benito Cerimele. Comparative pharmacokinetics and glucodynamics of two human insulin mixtures. *Diabetes Care*, 17(5):366–371, 1994.

Appendix A

Euglycaemic Clamp Study

This appendix deals with the clamp study. First, the anthropometric measurements of the twenty subjects in the study are shown in Table A.1. These measurements include the age, height, body weight (BW), and body mass index (BMI) of each subject. Next, the identifiability of the single-compartment model and the two-compartment SC uptake model are investigated. Finally, the equations for the effect-compartment model are derived and the input and output files from CTSM for the effect-compartment model are shown.

A.1 Anthropometric Measurements

Table A.1: Anthropometric measurements for the clamp study.

Subject	Age [years]	Height [cm]	BW [kg]	BMI [kg/m^2]
1	18.5	175	70.10	22.9
2	26.1	182	70.10	21.1
3	34.3	193	83.00	22.3
4	23.4	180	80.00	24.7
5	27.5	178	85.20	26.9
6	23.6	196	90.00	23.4
7	27.1	193	81.20	21.8
8	26.7	187	86.00	24.6
9	24.5	183	77.00	23.0
10	26.4	180	78.00	24.1
11	23.0	184	70.00	20.7
12	28.5	185	73.00	21.3
13	25.8	196	103.00	26.8
14	28.0	190	84.00	23.3
15	25.3	180	74.60	23.0
16	23.7	188	76.70	21.7
17	27.3	188	80.00	22.6
18	23.2	187	78.70	22.5
19	25.6	182	78.00	23.5
20	29.5	168	65.00	23.0

A.2 Identifiability of Single-Compartment Model

The second order linear differential equation for the single-compartment model mentioned in Section 6.1.1 is considered in the following. The state space model (without the noise model) written in matrix notation is:

$$\frac{d\boldsymbol{X}}{dt} = \boldsymbol{A}\boldsymbol{X} + \boldsymbol{B}\boldsymbol{U} \tag{A.1a}$$

$$\boldsymbol{Y} = \boldsymbol{C}\boldsymbol{X} \tag{A.1b}$$

translates into (A.2) for the single-compartment model:

$$\begin{bmatrix} dI_{sc} \\ dI_c \end{bmatrix} = \begin{bmatrix} -k_a & 0 \\ k_a F & -k_e \end{bmatrix} \begin{bmatrix} I_{sc} \\ I_c \end{bmatrix} dt + \begin{bmatrix} 1 & 0 \\ 0 & 1 \end{bmatrix} \begin{bmatrix} D \\ R_{in} \end{bmatrix} dt \tag{A.2a}$$

$$C_I = \begin{bmatrix} 0 & V_d^{-1} \end{bmatrix} \begin{bmatrix} I_{sc} \\ I_c \end{bmatrix} \tag{A.2b}$$

The transfer function $\boldsymbol{G}(s) = \boldsymbol{Y}(s)/\boldsymbol{U}(s)$ for the linear state space model is obtained by Laplace transformation of (A.2). The Laplace transform of (A.2a), using the notation in (A.1), is:

$$(s\boldsymbol{I} - \boldsymbol{A})\,\boldsymbol{X} = \boldsymbol{B}\boldsymbol{U} \tag{A.3}$$

and the transfer function can be found by combining (A.3) and (A.2b):

$$\begin{aligned} \boldsymbol{G}(s) &= \boldsymbol{C}\,(s\boldsymbol{I} - \boldsymbol{A})^{-1}\,\boldsymbol{B} \\ &= \begin{bmatrix} 0 & V_d^{-1} \end{bmatrix} \begin{bmatrix} s + k_a & 0 \\ -k_a F & s + k_e \end{bmatrix}^{-1} \begin{bmatrix} 1 & 0 \\ 0 & 1 \end{bmatrix} \\ &= \frac{\begin{bmatrix} k_a F & s + k_a \end{bmatrix}}{(s + k_e)\,(s + k_a)\,V_d} \end{aligned} \tag{A.4}$$

The expression for $\boldsymbol{G}(s)$ is then compared with what is possible to observe, namely:

$$G(s) = \frac{s + p_2}{q_0 s^2 + q_1 s + q_2} \tag{A.5}$$

The parameters in the numerator (p) and denominator (q) can then be found as:

$$\begin{aligned} p_2 &= k_a\,(F+1) \\ q_0 &= V_d \\ q_1 &= V_d\,(k_a + k_e) \\ q_2 &= V_d k_e k_a \end{aligned}$$

By comparing (A.4) with the parameters above it is clearly seen that the system is not structural identifiable since a second order equation is obtained for k_e or k_a which results in two solutions for k_e or k_a. The model can be made structural identifiable by eliminating F making the parameter $p_2 = 2k_a$, thereby making the parameters k_a, k_e and V_d uniquely identifiable.

A.3 Identifiability of Two-Compartment SC Uptake Model

The identifiability of the two-compartment SC uptake model is examined using the same procedure as in the single-compartment model (see Appendix A.2).

The transfer function for the two-compartment SC uptake model is:

$$\begin{aligned}\boldsymbol{G}(s) &= \boldsymbol{C}\left(s\boldsymbol{I}-\boldsymbol{A}\right)^{-1}\boldsymbol{B} \\ &= \begin{bmatrix}0 & 0 & V_d^{-1}\end{bmatrix}\begin{bmatrix}s+k_a & 0 & 0\\ -k_a & s+k_a-k_d & 0\\ 0 & -k_a & s+k_e\end{bmatrix}^{-1}\begin{bmatrix}1 & 0\\ 0 & 0\\ 0 & 1\end{bmatrix} \\ &= \frac{\begin{bmatrix}k_a^2 & (s+k_a)(s+k_a-k_d)\end{bmatrix}}{V_d\left(s+k_e\right)\left(s+k_a\right)\left(s+k_a-k_d\right)}\end{aligned} \tag{A.6}$$

Next, equal powers of s in the transfer function are combined:

$$G(s) = \frac{s^2+s(2k_a-k_d)+2k_a^2-k_ak_d}{V_d\left[s^3+s^2(2k_a+k_e-k_d)+s(k_a^2+2k_ak_e-k_ak_d-k_ek_d)+k_a^2k_e-k_ak_ek_d\right]} \tag{A.7}$$

The observable transfer function for the system is:

$$G(s) = \frac{s^2+p_2s+p_3}{q_0s^3+q_1s^2+q_2s+q_3} \tag{A.8}$$

The expression for the parameters in the numerator (p) and denominator (q) can be found by comparison with the coefficients in (A.7), i.e.:

$$\begin{aligned} p_2 &= 2k_a-k_d \\ p_3 &= 2k_a^2-k_ak_d \\ q_0 &= V_d \\ q_1 &= 2k_a+k_e-k_d \\ q_2 &= k_a^2+2k_ak_e-k_ak_d-k_ek_d \\ q_3 &= k_a^2k_e-k_ak_ek_d \end{aligned}$$

It is clearly seen that the two-compartment SC uptake model is *a priori* non-identifiable with the current parameters since there does

not exist a unique solution for the parameters. The identifiability of the model is obtained by fixing the rate constant k_d for insulin degradation in SC compartment II at $0.015\,\mathrm{min}^{-1}$ thereby reducing the equation for k_a to a simple first-order equation.

A.4 Equations for the Effect-Compartment Model

The following differential equations for the effect-compartment model describe the rate of change of SC, plasma, and effective insulin:

$$\frac{dI_{sc}}{dt} = D \cdot \delta(t) - k_a I_{sc} \tag{A.9a}$$

$$\frac{dI_c}{dt} = k_a I_{sc} + R_{in} - k_e I_c \tag{A.9b}$$

$$\frac{dI_e}{dt} = k_{ce} I_c - k_{e0} I_e \tag{A.9c}$$

The equation for the amount of insulin in the plasma is the same as for the single-compartment model since the effect compartment receives a negligible mass from the central compartment.

Using Laplace transformation, the following system of equations is obtained:

$$sI_{sc}(s) - I_{sc,0} = D - k_a I_{sc}(s) \tag{A.10a}$$

$$sI_c(s) - I_{c,0} = k_a I_{sc}(s) + \frac{R_{in}}{s} - k_e I_c(s) \tag{A.10b}$$

$$sI_e(s) - I_{e,0} = k_{ce} I_c(s) - k_{e0} I_e(s) \tag{A.10c}$$

since $\mathcal{L}\{\delta(t)\} = 1$.

The initial conditions at $\tau = t + 90 = 0$ in (A.10) are:

$$\begin{aligned} I_{sc} &= 0 \\ I_c &= I_{c,0} \\ I_e &= I_{e,0} \end{aligned}$$

First, $I_{sc}(s)$ is isolated in (A.10a). Next, $I_c(s)$ is isolated in (A.10b) using the expression for $I_{sc}(s)$:

$$I_{sc}(s) = \frac{D}{s+k_a} \tag{A.11a}$$

$$I_c(s) = \frac{k_a D}{(s+k_e)(s+k_a)} + \frac{R_{in}}{s(s+k_e)} + \frac{I_{c,0}}{s+k_e} \tag{A.11b}$$

The expression for $I_{sc}(s)$ and $I_c(s)$ are then substituted into (A.10c) and $I_e(s)$ is isolated:

$$\begin{aligned} I_e(s) = &\frac{k_{ce}k_a D}{(s+k_e)(s+k_a)(s+k_{e0})} + \frac{k_{ce}R_{in}}{s(s+k_e)(s+k_{e0})} \\ &+ \frac{k_{ce}I_{c,0}}{(s+k_e)(s+k_{e0})} + \frac{I_{e,0}}{s+k_{e0}} \end{aligned} \tag{A.12}$$

Since all the poles ($-k_e$, $-k_a$, $-k_{e0}$, and 0) and coefficients in (A.12) are real, equation (A.12) can be transformed back using the single-pole rule [3, p. 292] giving the following equation for the inverse Laplace transform of $I_e(s)$:

$$\begin{aligned} \mathcal{L}^{-1}\{I_e(s)\} = &\left.\frac{k_{ce}k_a D}{(s+k_a)(s+k_{e0})}\right|_{s=-k_e} \cdot e^{-k_e t} \\ &+ \left.\frac{k_{ce}k_a D}{(s+k_e)(s+k_{e0})}\right|_{s=-k_a} \cdot e^{-k_a t} + \left.\frac{k_{ce}k_a D}{(s+k_e)(s+k_a)}\right|_{s=-k_{e0}} \cdot e^{-k_{e0} t} \\ &+ \left.\frac{k_{ce}R_{in}}{(s+k_e)(s+k_{e0})}\right|_{s=0} \cdot e^{-0\tau} + \left.\frac{k_{ce}R_{in}}{s(s+k_{e0})}\right|_{s=-k_e} \cdot e^{-k_e \tau} \\ &+ \left.\frac{k_{ce}R_{in}}{s(s+k_e)}\right|_{s=-k_{e0}} \cdot e^{-k_{e0}\tau} + \left.\frac{k_{ce}I_{c,0}}{(s+k_{e0})}\right|_{s=-k_e} \cdot e^{-k_e \tau} \\ &+ \left.\frac{k_{ce}I_{c,0}}{(s+k_e)}\right|_{s=-k_{e0}} \cdot e^{-k_{e0}\tau} + I_{e,0} \cdot e^{-k_{e0}\tau} \end{aligned} \tag{A.13}$$

The analytical solution for the amount of insulin in the effect com-

partment I_e can thereby be written as:

$$I_e = k_{ce}k_aD\left(\frac{e^{-k_et}}{(k_a-k_e)(k_{e0}-k_e)} + \frac{e^{-k_at}}{(k_e-k_a)(k_{e0}-k_a)} + \frac{e^{-k_{e0}t}}{(k_e-k_{e0})(k_a-k_{e0})}\right) + k_{ce}R_{in}\left(\frac{1}{k_ek_{e0}} - \frac{e^{-k_e\tau}}{k_e(k_{e0}-k_e)} - \frac{e^{-k_{e0}\tau}}{k_{e0}(k_e-k_{e0})}\right) + k_{ce}I_{c,0}\left(\frac{e^{-k_e\tau}}{(k_{e0}-k_e)} + \frac{e^{-k_{e0}\tau}}{(k_e-k_{e0})}\right) + I_{e,0}\cdot e^{-k_{e0}\tau} \tag{A.14}$$

The insulin concentration in the effect compartment C_e is expressed as $C_e = I_e/V_e$, where V_e is the volume of the effect compartment. Since V_e cannot be measured, the insulin effect is related to the insulin concentration in the plasma under steady-state conditions where $C_{c,ss} = C_{e,ss}$. At steady-state, the following equation is therefore valid:

$$V_d \cdot k_{ce} \cdot C_{c,ss} = V_e \cdot k_{e0} \cdot C_{e,ss} \tag{A.15}$$

which solved for V_e gives:

$$V_e = \frac{V_dk_{ce}}{k_{e0}} \tag{A.16}$$

By using the expression for V_e, the equation for the insulin concentration in the effect compartment becomes:

$$C_e = \frac{I_ek_{e0}}{V_dk_{ce}} \tag{A.17}$$

Substituting (A.14) into (A.17) yields:

$$C_e = \frac{Dk_{e0}k_a}{V_d}\left(\frac{e^{-k_et}}{(k_a-k_e)(k_{e0}-k_e)} + \frac{e^{-k_at}}{(k_e-k_a)(k_{e0}-k_a)} + \frac{e^{-k_{e0}t}}{(k_e-k_{e0})(k_a-k_{e0})}\right) + \frac{R_{in}k_{e0}}{V_d}\left(\frac{1}{k_ek_{e0}} - \frac{e^{-k_e\tau}}{k_e(k_{e0}-k_e)} - \frac{e^{-k_{e0}\tau}}{k_{e0}(k_e-k_{e0})}\right) + \frac{I_{c,0}k_{e0}}{V_d}\left(\frac{e^{-k_e\tau}}{(k_{e0}-k_e)} + \frac{e^{-k_{e0}\tau}}{(k_e-k_{e0})}\right) + \frac{I_{e,0}k_{e0}}{V_dk_{ce}}\cdot e^{-k_{e0}\tau} \tag{A.18}$$

where the part with D is equal to zero for $t \in [-90, 0]$ since the SC insulin is injected at $t = 0$.

In the equation above, it is seen that the insulin concentration in the effect compartment is independent of k_{ce} except for the fraction with $I_{e,0}$ in the nominator thus not affecting the differential equations for the system since the initial amount of insulin in the effect compartment easily can be redefined as $I_{e,0}/k_{ce}$. Consequently, the time-dependent aspects of the equilibrium between the plasma and effect concentration are only controlled by the equilibrium constant K_{e0}.

The differential equations for the effect-compartment model can thereby be written as:

$$\frac{dI_{sc}}{dt} = D \cdot \delta(t) - k_a I_{sc} \tag{A.19a}$$

$$\frac{dI_c}{dt} = k_a I_{sc} + R_{in} - k_e I_c \tag{A.19b}$$

$$\frac{1}{V_e}\frac{dI_e}{dt} = K_{e0}\Big(\frac{I_c}{V_d} - \frac{I_e}{V_e}\Big) \tag{A.19c}$$

where K_{e0} is the equilibrium constant for equilibrium between the central and effect compartment.

A.5 CTSM Files

Input to CTSM

The input file used for estimation of the effect-compartment model is shown in Table A.2 for subject 3.

Table A.2: CTSM input file for the effect-compartment model.

Time [min]	D [nmol]	R_{in} [nmol]	C_I [nM]	GIR [10^{-2} mol/min]
-90	0.0	0.081672	0.055104	0.10491
-60	0.0	0.081672	0.10824	0.13877
-30	0.0	0.081672	0.093808	0.068274
0	108.896	0.081672	0.066256	0.061613
1	0.0	0.081672	$2.0E$+300	0.041076
10	0.0	0.081672	0.1417	0.13377
20	0.0	0.081672	0.39098	0.067164
30	0.0	0.081672	0.52611	0.26533
40	0.0	0.081672	0.42771	0.4757
50	0.0	0.081672	0.41656	0.57062
60	0.0	0.081672	0.4487	0.57561
75	0.0	0.081672	0.4041	0.59948
90	0.0	0.081672	0.46838	0.72493
105	0.0	0.081672	0.41197	0.54619
120	0.0	0.081672	0.36014	0.51067
150	0.0	0.081672	0.29651	0.67775
180	0.0	0.081672	0.25387	0.48958
210	0.0	0.081672	0.21058	0.43129
240	0.0	0.081672	0.16138	0.41298
270	0.0	0.081672	0.16203	0.41131
300	0.0	0.081672	0.1535	0.30141
330	0.0	0.081672	0.081344	0.056063
360	0.0	0.081672	0.10365	0.13766
390	0.0	0.081672	0.11414	0.19483
420	0.0	0.081672	0.11414	0.11101
450	0.0	0.081672	0.1043	0.11823
480	0.0	0.081672	0.097088	0.094918
510	0.0	0.081672	0.081344	0.14709
540	0.0	0.081672	0.089216	0.07438
570	0.0	0.081672	0.069536	0.079376
600	0.0	0.081672	0.09184	0.11601

Output from CTSM

The output from CTSM consists of some information about the optimization, the setup used for estimation along with the estimation results, and the estimated correlation matrix.

Table A.3: CTSM optimization results for the effect-compartment model.

Value of objective function	$-1.000963822904744E{+}02$
Value of penalty function	$5.663221463800949E{-}04$
Negative logarithm of determinant of Hessian	$-1.172734634881623E{+}02$
Number of iterations	119
Number of objective function evaluations	172

Table A.4: CTSM estimation results for the effect-compartment model.

Name		Min. value	Initial value	Max. value	Prior std. dev.	Estimate	Std. dev.	t-score	p($>\|t\|$)	dF/dPar	dPen/dPar
$I_{sc,0}$	Fix	N/A	0.0	N/A	N/A	0.0	N/A	N/A	N/A	N/A	N/A
$I_{c,0}$	ML	0.0	3.0	10.0	N/A	2.6384E+00	1.2955E+00	2.0366	0.0474	0.0000	0.0000
$C_{e,0}$	ML	0.0	0.1	1.0	N/A	1.0780E-01	3.1777E-02	3.3924	0.0014	0.0000	0.0000
k_a	ML	0.0	0.01	0.1	N/A	7.3497E-03	7.2944E-04	10.0759	0.0000	-0.0000	0.0000
F	Fix	N/A	1.0	N/A	N/A	1.0	N/A	N/A	N/A	N/A	N/A
k_e	ML	0.0	0.01	0.1	N/A	3.9059E-02	6.6901E-03	5.8383	0.0000	0.0000	0.0001
K_{e0}	ML	0.0	0.01	0.1	N/A	2.6053E-02	4.3714E-03	5.9598	0.0000	0.0000	0.0000
V_d	ML	0.0	30.0	100.0	N/A	3.4359E+01	6.3678E+00	5.3956	0.0000	0.0000	0.0001
σ_{sc}	ML	0.0	1.0	10.0	N/A	1.7460E-07	3.0731E-02	0.0000	1.0000	-0.0000	0.0000
σ_c	ML	0.0	1.0	10.0	N/A	7.2017E-09	1.4657E-03	0.0000	1.0000	-0.0000	0.0000
σ_e	ML	0.0	1.0	10.0	N/A	2.4896E-12	6.7938E-07	0.0000	1.0000	-0.0000	0.0000
E_{max}	ML	0.0	0.5	1.5	N/A	9.1570E-01	2.3371E-01	3.9181	0.0003	-0.0000	0.0004
γ	ML	1.0	2.0	5.0	N/A	2.0325E+00	4.3342E-01	4.6894	0.0000	-0.0000	-0.0001
EC_{50}	ML	0.0	0.2	1.0	N/A	2.6840E-01	7.7334E-02	3.4706	0.0012	0.0000	0.0001
S_c^2	ML	0.0	1.0	10.0	N/A	1.2529E-03	3.5428E-04	3.5365	0.0010	-0.0000	0.0000
S_{GIR}^2	ML	0.0	1.0	10.0	N/A	3.7529E-03	9.2274E-04	4.0672	0.0002	-0.0000	0.0000

Table A.5: CTSM estimation of correlation matrix for the effect-compartment model.

	$I_{c,0}$	$C_{e,0}$	k_a	k_e	K_{e0}	V_d	σ_{sc}	σ_c	σ_e	E_{max}	γ	EC_{50}	S_c^2	S_{GIR}^2
$I_{c,0}$	1													
$C_{e,0}$	-0.1578	1												
k_a	0.3538	-0.2777	1											
k_e	-0.4430	0.1856	-0.7273	1										
$K_{e,0}$	0.0527	-0.0681	-0.0811	-0.3472	1									
V_d	0.4518	-0.2309	0.8106	-0.9798	0.2733	1								
σ_{sc}	-0.0328	0.0406	-0.0274	0.0787	-0.0826	-0.0797	1							
σ_c	-0.0328	0.0405	-0.0274	0.0787	-0.0826	-0.0797	1.0000	1						
σ_e	-0.0328	0.0406	-0.0274	0.0787	-0.0826	-0.0797	1.0000	1.0000	1					
E_{max}	-0.1588	-0.1623	-0.1544	0.1821	0.0790	-0.1814	-0.0393	-0.0393	-0.0393	1				
γ	0.0744	0.3361	-0.1092	0.0614	-0.2132	-0.0794	0.0735	0.0735	0.0735	-0.8828	1			
EC_{50}	-0.1634	-0.1300	-0.1877	0.1768	0.1446	-0.1972	-0.0407	-0.0407	-0.0407	0.9853	-0.8783	1		
S_c^2	-0.0339	0.0271	-0.1037	0.1855	-0.1298	-0.1887	0.0845	0.0845	0.0845	0.0178	0.0379	0.0217	1	
S_{GIR}^2	-0.1066	0.0562	-0.0452	0.0581	-0.0615	-0.0645	0.0316	0.0316	0.0316	-0.0078	0.0192	-0.0104	-0.0606	1

Appendix B

Glucose Tolerance Studies

The sample mean and standard deviation of the anthropometric measurements from the glucose tolerance studies are shown in this appendix along with the MM parameter estimates. The MM equation for plasma glucose is derived and the input and output files from CTSM for the estimation of the parameters in the MM of glucose kinetics are shown at the end of this appendix.

B.1 Anthropometric Measurements

Table B.1: Anthropometric measurements for the glucose tolerance studies.

	Units	NGT	IGT	Type II diabetics	Total
N (men/women)	[-]	261 (112/149)	27 (10/17)	70 (38/32)	358 (160/198)
Age	[years]	42.0 (12.2)	46.4 (12.0)	62.8 (12.2)	46.4 (14.6)
Height	[cm]	172.2 (8.7)	168.6 (9.8)	168.7 (10.2)	171.3 (9.2)
Weight	[kg]	77.2 (14.5)	85.6 (17.8)	86.4 (17.6)	79.6 (15.9)
Waist	[cm]	85.7 (12.4)	94.0 (15.2)	99.2 (13.9)	88.8 (14.0)
Hip	[cm]	99.6 (9.0)	107.5 (8.8)	105.0 (11.0)	101.2 (9.7)
BMI	[kg/m^2]	26.0 (4.5)	30.0 (5.3)	30.3 (5.0)	27.1 (5.0)

The numbers are mean values with the standard deviation shown in brackets.

B.2 Derivation of MM Glucose Equation

The accumulation of plasma glucose can be written using equation (8.1) for the hepatic glucose production B and equation (8.2) for the utilization of glucose into the peripheral tissue U_p, i.e.:

$$\begin{aligned} \text{Accumulated} &= \text{In} - \text{Out} \\ &= \Big(B + D \cdot \delta(t)\Big) - U_p \\ \frac{dG}{dt} &= B_0 - (k_5 + k_6 I_r)G + D \cdot \delta(t) - (k_1 + k_4 I_r)G \end{aligned}$$

The equation for the accumulation of plasma glucose is next rear-

ranged to the following equation:

$$\frac{dG}{dt} = -\Big[\big(k_1 + k_5\big) + \big(k_4 + k_6\big)I_r\Big]G + \big(k_1 + k_5\big)G_b + D \cdot \delta(t) \quad \text{(B.1)}$$

where the extrapolated hepatic glucose production at zero glucose concentration B_0 is written as $\big(k_1{+}k_5\big)G_b$ to obtain the MM equation for plasma glucose. The insulin-independent glucose elimination is therefore only dependent on the glucose above the basal level of glucose G_b since the equation for the plasma glucose can be rewritten as:

$$\frac{dG}{dt} = -\big(k_1 + k_5\big)\big(G - G_b\big) + \big(k_4 + k_6\big)I_rG + D \cdot \delta(t) \quad \text{(B.2)}$$

B.3 Parameter Estimates from the MM

Table B.2: Sample mean and standard deviation of the MM parameter estimates.

		NGT		IGT	
Parameter	Unit	$\bar{\theta}$	$\bar{s}$	$\bar{\theta}$	$\bar{s}$
G_0	[mmol]	69.5577	17.9816	73.1372	18.2347
p_1	[min^{-1}]	0.0206	0.0095	0.0211	0.0102
p_2	[min^{-1}]	0.0804	0.0846	0.2778	0.3580
p_3	[$\text{min}^{-2}\text{pM}^{-1}$]	0.0008	0.0008	0.0004	0.0005
V	[L]	13.3401	3.1637	12.6624	2.7233
σ_G	[-]	0.1487	0.4219	0.1912	0.5555
σ_X	[-]	0.0079	0.0371	0.0221	0.0561
S^2	[-]	0.0630	0.0792	0.0296	0.0233
AIR_{0-8}	[pM min]	$2.3265E03$		$1.0320E03$	

B.4 CTSM Files

Input to CTSM

The input file used for estimation of the minimal model is shown in Table B.3 for a representative NGT patient in the study.

Table B.3: CTSM input file for the minimal model.

Time [min.]	D [mmol]	C_I [10^{-1} μM]	C_{G_b} [mM]	$C_{G,obs}$ [mM]
-10	0.0	0.49	3.6667	5.45
-5	0.0	0.45	3.6667	5.35
0	125.6558	0.49	3.6667	5.35
1	0.0	1.93	3.6667	$2.0E300$
2	0.0	4.35	3.6667	15.15
3	0.0	5.27	3.6667	15.25
4	0.0	4.47	3.6667	15.40
5	0.0	3.9	3.6667	14.20
6	0.0	3.09	3.6667	13.85
7	0.0	2.55	3.6667	13.00
8	0.0	2.1	3.6667	12.75
10	0.0	1.95	3.6667	12.35
12	0.0	1.71	3.6667	12.15
14	0.0	1.49	3.6667	11.60
16	0.0	1.31	3.6667	11.05
19	0.0	1.23	3.6667	10.65
22	0.0	4.15	3.6667	10.20
23	0.0	4.61	3.6667	10.30
24	0.0	4.38	3.6667	10.25
25	0.0	4.07	3.6667	9.90
27	0.0	3.43	3.6667	9.55
30	0.0	2.41	3.6667	9.00
35	0.0	1.97	3.6667	7.85
40	0.0	1.76	3.6667	6.95
50	0.0	1.16	3.6667	6.10
60	0.0	0.76	3.6667	5.10
70	0.0	0.65	3.6667	4.50
80	0.0	0.48	3.6667	4.35
90	0.0	0.31	3.6667	4.05
100	0.0	0.21	3.6667	3.75
120	0.0	0.12	3.6667	3.45
140	0.0	0.09	3.6667	3.50
160	0.0	-0.04	3.6667	3.45
180	0.0	-0.05	3.6667	4.05

Output from CTSM

The output from CTSM consists of some information about the optimization, the setup used for estimation along with the estimation results, and the estimated correlation matrix.

Table B.4: CTSM optimization results for the minimal model.

Value of objective function	$3.557747789279118E{+}00$
Value of penalty function	$2.726449889477113E{-}04$
Negative logarithm of determinant of Hessian	$-5.715943569711322E{+}01$
Number of iterations	48
Number of objective function evaluations	75

Table B.5: CTSM estimation setup and results for the minimal model.

Name		Min. value	Initial value	Max. value	Prior std. dev.	Estimate	Std. dev.
G_0	ML	0.0	1.0	100.0	N/A	6.5504E+01	3.5506E+00
X_0	Fix	N/A	0.0	N/A	N/A	0.0	N/A
p_1	ML	1.0E-5	0.03	0.1	N/A	2.0097E-02	4.8879E-03
V	ML	0.0	40.0	50.0	N/A	1.2610E+01	3.9444E-01
p_3	ML	1.0E-5	1.0E-4	0.1	N/A	6.9959E-04	1.7469E-04
p_2	ML	1.0E-5	0.5	2.0	N/A	5.7490E-02	1.7436E-02
σ_G	ML	0.0	0.1	2.0	N/A	9.8176E-01	3.4316E-01
σ_X	ML	0.0	0.1	1.0	N/A	7.9394E-09	5.3310E-06
S_G^2	ML	0.0	0.1	1.0	N/A	7.3042E-02	2.5261E-02
Name	t-score	p($>\|t\|$)	dF/dPar	dPen/dPar			
G_0	18.4487	0.0000	0.0000	0.0006			
X_0	N/A	N/A	N/A	N/A			
p_1	4.1117	0.0004	-0.0000	0.0000			
V	31.9691	0.0000	-0.0000	0.0000			
p_3	4.0048	0.0006	-0.0000	-0.0000			
p_2	3.2973	0.0031	0.0000	0.0000			
σ_G	2.8609	0.0087	0.0000	0.0002			
σ_X	0.0015	0.9988	-0.0000	0.0000			
S_G^2	2.8914	0.0081	-0.0000	0.0000			

Table B.6: CTSM estimation of correlation matrix for the minimal model.

	G_0	p_1	V	p_3	p_2	σ_G	σ_X	S_G^2
G_0	1							
p_1	-0.3951	1						
V	0.7979	-0.5535	1					
p_3	0.2891	-0.8071	0.3883	1				
p_2	0.2436	-0.7177	0.3338	0.9289	1			
σ_G	-0.0593	0.2933	-0.1937	-0.2725	-0.2870	1		
σ_X	-0.2860	0.7411	-0.3507	-0.8562	-0.8877	-0.0749	1	
S_G^2	0.0942	-0.1600	0.2102	0.1320	0.1356	-0.4035	-0.0004	1

List of Figures

List of Tables

Index